University of Alberta

Coupled Supercritical CO_2 – Membrane Technology for Lipid Separations

by

Oguz Akin

A thesis submitted to the Faculty of Graduate Studies and Research
in partial fulfillment of the requirements for the degree of

Doctor of Philosophy
in
Bioresource and Food Engineering

Department of Agricultural, Food and Nutritional Science

Fall 2011
Edmonton, Alberta

This thesis is dedicated to my parents, Abdullah and Ayten Akin

Abstract

Coupling supercritical CO_2 extraction with membrane separation leads to energy savings by recycling CO_2 at supercritical state while separating extract components. Commercially available polyamide-based membranes are commonly used with coupled systems due to their availability and robust structures. However, high pressure operating conditions may cause physicochemical and morphological changes in polymer membranes, which in turn can adversely affect membrane performance.

Since most of the information on commercial reverse osmosis membranes is proprietary, further investigation on their structure would be beneficial for selection of the proper membranes, especially for processes involving various solvents such as supercritical CO_2. Therefore, detailed characterization of four polyamide membranes was performed using advanced instrumental techniques for better understanding of their physicochemical and morphological properties. Findings suggest that AK and AG membranes had excess of intermolecular hydrogen bonds, while SG and SE had modified covalently cross-linked structure.

Temperature, pressure and CO_2 flux were the major processing parameters investigated to assess the interactions between the polyamide membranes and CO_2. The observed interactions between the polymer and CO_2 were attributed to Lewis acid and base interactions and hydrogen bonding. The change in surface hydrophobicity and drop in absorbance of particular functional groups were determined as indicator of physicochemical changes in the structure.

Morphological changes were also observed upon processing with supercritical CO_2 up to 24 h.

Performance of the membranes was tested using pure oleic acid retention and separation of a triacylglycerol/oleic acid mixture. Covalently cross-linked membrane structures were found to be more resistant to supercritical conditions. Reorganization of the polymer network due to interactions during CO_2 exposure affected the membrane performance dramatically.

Investigation of performance and stability of polyamide membranes clarified the major factors responsible for adverse effects on their structures such as swelling and plasticization during processing. Results obtained in this thesis research contribute both to the fundamental understanding of polymer membrane behaviour under supercritical conditions and to the type of membrane materials needed for such novel process development without sacrificing membrane performance.

Acknowledgments

First and foremost, I would like to thank Dr. Feral Temelli for her constant encouragement, support, and guidance during my entire course of study. This research and thesis would not have been possible without her great support. Her dedication and her enthusiasm towards research has been a great inspiration to me. She is a great mentor who considers student's growth as the topmost priority and I am very fortunate to have her as an advisor.

Thanks to Dr. Thava Vasanthan and Dr. David Bressler for being in my supervisory committee and giving great support, valuable guidance and feedback making this work a success. Many thanks to Dr. William McCaffrey from the Department of Chemical and Materials Engineering for being on my examining committee and providing great support. Thanks to Dr. Jonathan Curtis for providing helpful feedback and valuable guidance in my research.

I would like to thank to Dr. Sefa Koseoglu for his incredible support and encouragement. He has been one of the most important reasons for me to pursue a career as a membrane technologist.

Special thanks to Dr. Levente Diosady from the Department of Chemical Engineering and Applied Chemistry at the University of Toronto for being my external examiner.

Furthermore, I am grateful to NSERC (Natural Sciences and Engineering Research Council of Canada) for financial support.

I would like to thank to my labmates and friends Paul Moquin, Bernhard Seifried, Lauren Comin, Ehsan Jenab and Ozan Ciftci. I also would like to thank to Jody Forslund who assisted me with administrative work throughout my PhD program. Thanks a lot to Jamie, Mei Sun and Jean Bourgois for always being there giving a hand when I need it. Also, I am grateful to Dr. Tony Yeung for providing equipment for my contact angle study. Special thanks to Dimitre

Karpuzov, Shihong Xu and Anquang He for all the help and valuable discussions on the surface analysis. Thanks to George and De-ann in the SEM lab who contributed to my work.

Finally, I would like to thank to my dear Anum for her support and love. She has always been there for me from beginning to the end. Many thanks for making my priorities her priorities whenever I need an extra hand throughout this thesis.

Table of Contents

List of Tables

List of Figures

List of abbreviations

ACSES	Alberta Centre for Surface Engineering and Science
AFM	Atomic Force Microscopy
ATR-FTIR	Attenuated Total Reflection - Fourier Transform Infrared Spectroscopy
b	Hole affinity constant
C_H	Hole saturation constant
C_i	Penetrant concentration in polymer
D	Diffusivity
DOD	Deodorizer Distillate
FAME	Fatty Acid Methyl Ester
FFA	Free Fatty Acids
FE-SEM	Field Emission - Scanning Electron Microscopy
GRAS	Generally Regarded As Safe
MF	Microfiltration
m-PDA	m-Phenyl diamine
MUFA	Monounsaturated Fatty Acids
MW	molecular weight
MWCO	molecular weight cut-off
NF	nanofiltration
P	permeability
p	pressure
PA	polyamide
PL	Phospholipid
PUFA	Polyunsaturated Fatty Acids
PVA	polyvinyl alcohol
RO	reverse osmosis
RPME	Red Palm Methyl Ester
S	Solubility
SC-CO_2	Supercritical Carbon Dioxide
S_i	Henry dissolution constant
TAG	Triacylglycerol
T_G	glass-rubber transition
T_M	crystalline melting point
TMC	Trimesoyl chloride
UF	ultrafiltration
VCR	volume concentration ratio
XDF	explosive decompression failure
XPS	X-ray photoelectron spectroscopy

1. Introduction and Thesis Objectives

Carbon dioxide is at supercritical state above its critical point (74 bar and 31^{o}C). Supercritical carbon dioxide (SC-CO_2) is an environmentally friendly solvent and a great alternative to replace organic solvents. Its low viscosity and high diffusivity make it a promising solvent for the extraction of high-value components. Besides, tunable solvent properties provide selective extraction of the components in a mixture.

Membrane technology is a relatively mature process compared to SC-CO_2 extraction. Many different aqueous and non-aqueous solutions have been purified using this technology. In addition, supercritical fluid systems have been integrated with membrane systems in terms of coupled processes for over 20 years. Applications of membrane separations where SC-CO_2 was used as a solvent have been increasing over the last decade [1-7]. Such integration provides major advantages compared to individual applications of each system. Integrated SC-CO_2 extraction + membrane system results in substantial processing advantages.

Compared to the other solvents used with membrane systems, SC-CO_2 has higher penetration power. Depending on the solute, SC-CO_2 provides higher selectivity compared to other aqueous and non-aqueous solvent extractions from the matrix of the target compound. In addition, lower viscosity and higher diffusivity properties of SC-CO_2 may help to decrease the level of concentration polarization together with fouling effect, which will result in longer term usage of the membrane with higher flux. Membrane permeate can be recycled in the supercritical phase so that regeneration of supercritical fluids will require much lower pumping costs. These state-of-the-art systems have great potential for application in a wide range of natural products; however, different membrane types suitable for supercritical fluid solvents and better understanding of the fundamentals of separation under these conditions are needed.

Generally, polymer membranes, including polyamide membranes, are economically more feasible than inorganic membranes. However, there is no polymer membrane commercially produced targeting SC-CO_2 applications. On the other hand, superior mechanical and thermal properties of the polyamide structure result in high performance separations over long term processing with aqueous solutions. Membranes produced by interfacial polymerization without sacrificing performance would give rise to the application of these membranes in many different areas other than aqueous solutions. Therefore, it is essential to know the possible modifications made during the polymerization reaction towards the formation of relatively hydrophobic polyamide membranes to better understand their chemical structure and assess their potential use in novel processes such as processing with SC-CO_2.

In order to assess the effect of CO_2 on polymer membranes, the physicochemical properties of the membrane and plasticization phenomena should be well understood [8-12]. Plasticization can be explained as the weakening effect on the polymer structure due to swelling via reduction of interactions between neighbouring polymer chains [13]. The solubility of CO_2 in polymers depends on the specific interactions between CO_2 and the polymer. CO_2 has a quadrupole moment accommodating both acid and base cites. Lewis acid and base interactions were shown to be the most important interactions between various polymers and CO_2 [14]. Different physicochemical properties such as polymer chain mobility, steric hinderance (accessability), pendant group member or backbone member, aliphatic or aromaticity, hydrocarbon tail, molecular weight, side chain size and free volume can affect molecular interactions. Even for the case of well-known polymer structures, there are no methods available to fully predict whether the polymer will be plasticized by CO_2. In order to assess the efficiency of the separation using coupled technology, characterization of membrane behaviour under supercritical conditions must be a priority to ensure the stability of the membranes throughout processing.

The interactions of CO_2 with different moieties in polymers have been studied extensively [15-21]. These interactions are the major reason for the morphological and chemical changes on the polymer membrane structures and the determining factor for the efficiency of processes involving CO_2 as a solvent. Polyamide membranes have not been used commonly for gas separations mainly due to excess intermolecular hydrogen bonding resulting in high cohesive energy density in the polymer network [22]. Moreover, processing conditions, such as temperature and pressure have been found to have an impact on the strength of hydrogen bonds, resulting in potential physicochemical and morphological changes in the structure [23].

Extraction of lipid components from various plant materials is one of the main applications of the SC-CO_2 technology, which is growing rapidly due to the numerous advantages over organic solvents as mentioned above. On the other hand, fractionation of dissolved components may not be always efficient if the targeted lipid components have similar solubility behaviour in SC-CO_2. Therefore, integrating a membrane separation system may target further separation of the extract, taking advantage of size and shape differences between those lipid components and thus increasing the overall separation efficiency while providing the opportunity to recycle SC-CO_2 without depressurization.

In the coupled system, the interactions between the polymer membrane, solute and solvent should be well understood to maintain the highest efficiency throughout separation for a particular process, which includes a membrane system and SC-CO_2 as solvent. In particular, tunable properties of SC-CO_2 will most likely result in potential changes among these interactions depending on the processing conditions. However, the literature lacks information in this regard. Therefore, the main objective of this thesis research was to investigate the potential of using SC-CO_2 extraction-membrane separation coupled technology by evaluating the membrane performance, assessing the stability throughout

processing and determining the effect of processing parameters on overall separation efficiency for a model lipid mixture. The specific objectives were:

- To characterize four relatively hydrophobic commercial RO membranes by using advanced techniques, including contact angle, X-ray photoelectron spectroscopy (XPS), attenuated total reflection - Fourier transform infrared spectroscopy (ATR-FTIR), field emission - scanning electron microscopy (FE-SEM) and atomic force microscopy (AFM) measurements to provide insight into their unusual hydrophobicity and their physicochemical structures, considering their current and potential application areas (Chapter 3),

- To investigate the effect of temperature and flux of pure SC-CO_2 at constant pressure over processing times of 0–8 h on the physicochemical and morphological properties of the most commonly used commercial polyamide membranes by using contact angle, ATR-FTIR and FE-SEM (Chapter 4),

- To evaluate the changes in physicochemical and morphological properties of two commercial reverse osmosis membranes (AK and SG) under different pressure, temperature, flux and processing time conditions by using contact angle, ATR-FTIR and FE-SEM analysis and to assess the effect of SC-CO_2 processing on membrane performance by determining CO_2 flux and oleic acid retention (Chapter 5),

- To determine the effects of different temperature, transmembrane pressure, processing time and depressurization rate on the performance of two commercial polyamide membranes (AK and SG) in terms of CO_2 flux and oleic acid retention (Chapter 6),

- To investigate the performance of various polymer membranes during oleic acid (OA) and triacylglycerol (TAG) separation by evaluating the effect of processing time on CO_2 flux and oleic acid retention as well as total lipid yield and TAG separation factors (Chapter 7), and

- To investigate the effect of pressure during the separation of oleic acid from a model mixture of OA+TAG using commercially available polymer membranes in terms of CO_2 flux, OA retention, TAG and OA separation factors and total lipid yield in the permeate stream (Chapter 8).

1.1. References

[1] W. Artz, T. Kinyanjui, M. Cheryan, Deacidification of soybean oil using supercritical fluid and membrane technology, Journal of the American Oil Chemists' Society, 82 (2005) 803-808.

[2] L.H.C. Carlson, A. Bolzan, R.A.F. Machado, Separation of d-limonene from supercritical CO_2 by means of membranes, The Journal of Supercritical Fluids, 34 (2005) 143-147.

[3] J.M.L.N. de Moura, L.A.G. Gonçalves, L.A.V. Sarmento, J.C.C. Petrus, Purification of structured lipids using $SCCO_2$ and membrane process, Journal of Membrane Science, 299 (2007) 138-145.

[4] L.A.V. Sarmento, R.A.F. Machado, J.C.C. Petrus, T.R. Tamanini, A. Bolzan, Extraction of polyphenols from cocoa seeds and concentration through polymeric membranes, The Journal of Supercritical Fluids, 45 (2008) 64-69.

[5] L.A.V. Sarmento, C.B. Spricigo, J.C.C. Petrus, L.H.C. Carlson, R.A.F. Machado, Performance of reverse osmosis membranes in the separation of supercritical CO_2 and essential oils, Journal of Membrane Science, 237 (2004) 71-76.

[6] S. Sarrade, C. Guizard, G.M. Rios, New applications of supercritical fluids and supercritical fluids processes in separation, Separation and Purification Technology, 32 (2003) 57-63.

[7] C.B. Spricigo, A. Bolzan, R.A.F. Machado, L.H.C. Carlson, J.C.C. Petrus, Separation of nutmeg essential oil and dense CO_2 with a cellulose acetate reverse osmosis membrane, Journal of Membrane Science, 188 (2001) 173-179.

[8] S. Kanehashi, T. Nakagawa, K. Nagai, X. Duthie, S. Kentish, G. Stevens, Effects of carbon dioxide-induced plasticization on the gas transport properties of glassy polyimide membranes, Journal of Membrane Science, 298 (2007) 147-155.

[9] A. Bos, I.G.M. Pünt, M. Wessling, H. Strathmann, CO_2-induced plasticization phenomena in glassy polymers, Journal of Membrane Science, 155 (1999) 67-78.

[10] A. Bos, I.G.M. Pünt, M. Wessling, H. Strathmann, Plasticization-resistant glassy polyimide membranes for CO_2/CO_4 separations, Separation and Purification Technology, 14 (1998) 27-39.

[11] J.H. Petropoulos, Plasticization effects on the gas permeability and permselectivity of polymer membranes, Journal of Membrane Science, 75 (1992) 47-59.

[12] S.R. Reijerkerk, K. Nijmeijer, C.P. Ribeiro Jr, B.D. Freeman, M. Wessling, On the effects of plasticization in CO_2/light gas separation using polymeric solubility selective membranes, Journal of Membrane Science, 367 (2011) 33-44.

[13] A.F. Ismail, W. Lorna, Penetrant-induced plasticization phenomenon in glassy polymers for gas separation membrane, Separation and Purification Technology, 27 (2002) 173-194.

[14] S.P. Nalawade, F. Picchioni, J.H. Marsman, L.P.B.M. Janssen, The FT-IR studies of the interactions of CO_2 and polymers having different chain groups, The Journal of Supercritical Fluids, 36 (2006) 236-244.

[15] Z. Shen, M.A. McHugh, J. Xu, J. Belardi, S. Kilic, A. Mesiano, S. Bane, C. Karnikas, E. Beckman, R. Enick, CO_2-solubility of oligomers and polymers that contain the carbonyl group, Polymer, 44 (2003) 1491-1498.

[16] S. Kilic, Y. Wang, J.K. Johnson, E.J. Beckman, R.M. Enick, Influence of tert-amine groups on the solubility of polymers in CO_2, Polymer, 50 (2009) 2436-2444.

[17] I. Kikic, Polymer-supercritical fluid interactions, The Journal of Supercritical Fluids, 47 (2009) 458-465.

[18] H. Lin, B.D. Freeman, Materials selection guidelines for membranes that remove CO_2 from gas mixtures, Journal of Molecular Structure, 739 (2005) 57-74.

[19] L. Hong, M.C. Thies, R.M. Enick, Global phase behavior for CO_2-philic solids: the CO_2 + [beta]-d-maltose octaacetate system, The Journal of Supercritical Fluids, 34 (2005) 11-16.

[20] P. Raveendran, S.L. Wallen, Cooperative C–H···O Hydrogen bonding in CO_2−Lewis base complexes: Implications for solvation in supercritical CO_2, Journal of the American Chemical Society, 124 (2002) 12590-12599.

[21] P. Raveendran, S.L. Wallen, Sugar Acetates as Novel, Renewable CO_2-philes, Journal of the American Chemical Society, 124 (2002) 7274-7275.

[22] J.M. García, F.C. García, F. Serna, J.L. de la Peña, High-performance aromatic polyamides, Progress in Polymer Science, 35 (2010) 623-686.

[23] Y. He, B. Zhu, Y. Inoue, Hydrogen bonds in polymer blends, Progress in Polymer Science, 29 (2004) 1021-1051.

2. Literature review

Very few substances in nature are found in pure form. Most require some type of separation before the resulting form can be consumed directly. Separation processes are an integral part of today's agricultural, food and bioproduct industries. One of the key problems in the processing of biomaterials and foods, and indeed in all chemical processes is the purification of specific components by separating them from a complex, multi-component matrix. This may be as simple as clarifying a functional beverage by removing small suspended solid impurities, and/or precipitated impurities or as complex as the fractionation of proteins from liquid extracts of oilseed flours. The cost of these separation and purification steps often determines the economic viability of a product or process. Effective separation of bioactive components from biomaterials requires a good understanding of the mechanisms of bioactivity loss due to processing, storage, decomposition or reactions with other components.

Separations are based on physical properties such as particle/molecular size, molecular structure, physico-chemical characteristics, such as boiling point differences or surface charges, or on chemical properties including solubility, polarity and specific chemical affinity. Ability to separate efficiently without losing activity of the bioactive compounds, and at low energy, capital and labor costs has been the deciding factor in the production of products/ingredients. Separation and purification techniques can be quite costly. For example, in the pharmaceutical industry, it is common for the downstream processing, including separation and purification operations, to cost 5 to 6 times more than production of the crude product by synthesis or fermentation. In addition, the problems associated with the cost of handling the residual by-products, which are typically larger in volume than the components extracted, should not be overlooked. Despite such limitations, various techniques have been successful in increasing

the concentrations of valuable components in crops by 10 to 100 fold. Separations based on supercritical fluid and industrial membrane technologies are different approaches for the concentration and purification of bioactives from various feed streams, which will be discussed in detail with a focus on lipid applications.

2.1. SC-CO_2 technology

2.1.1. Principles

When a component is pressurized over its critical pressure and heated over its critical temperature it gets into the supercritical phase. In the supercritical region, there is no phase boundary between the gas and the liquid phases and a single phase is formed. Above the critical temperature, a pure gas cannot be liquefied even at very high pressures. CO_2 has liquid like density and gas like diffusivity at supercritical conditions. The change in CO_2 density with temperature and pressure is presented in Fig. 2-1.

Supercritical carbon dioxide (SC-CO_2) is the most widely used supercritical fluid due to its moderate critical pressure and temperature. It is a solvent with physical properties in between those of a gas and a liquid that is environmentally benign, and is generally regarded as safe (GRAS). It is easily removable upon depressurization, recyclable and readily available.

In addition to SC-CO_2, some other supercritical fluids, such as ethane [1] and propane [2], have also been tested for their performance during extraction of fats and oils due to their relatively higher solubility power on lipids. However, their flammable nature limits their use. CO_2 is a safe solvent with moderate critical temperature (31 ^{o}C) and pressure (74 bar). Also, it is not flammable and it is cheap and abundant. All these properties provide the basis for SC-CO_2 to be used as the solvent of choice for fats and oils processing.

In order to make efficient use of SC-CO_2, understanding some of the fundamentals associated with its physicochemical properties are essential. These properties include phase behaviour, solubility, density and interfacial tension as

well as transport properties, such as viscosity, thermal conductivity and diffusion coefficients. As it was presented in Fig. 2-1, density of CO_2 increases with increasing pressure while decreases with increasing temperature at supercritical state.

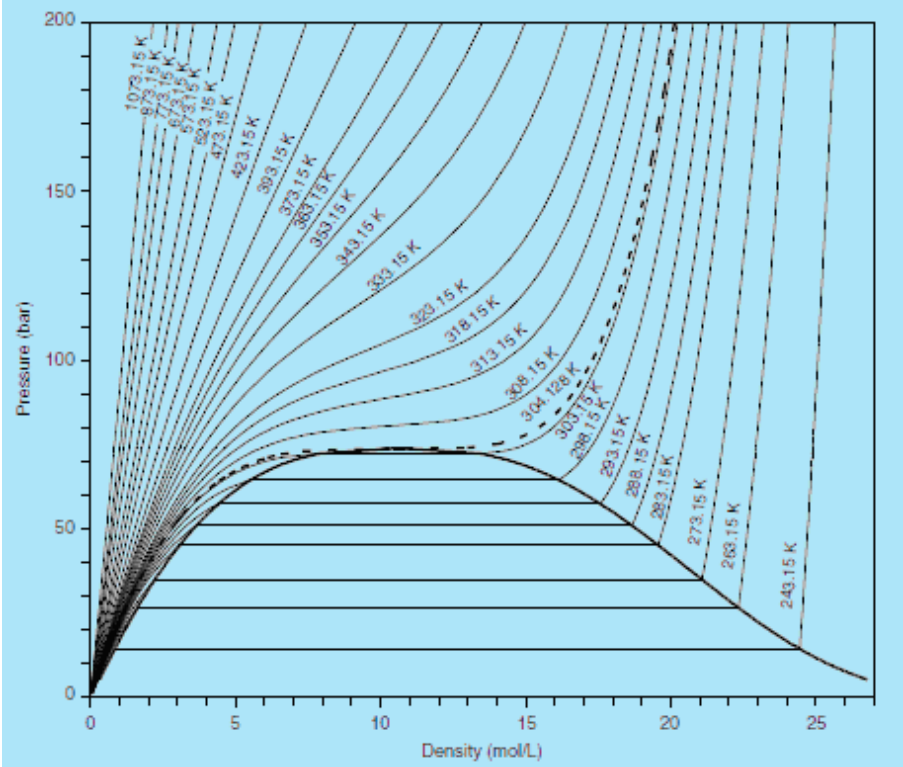

Figure 2-1. Density variation of CO_2 with temperature and pressure. Data taken from National Institute of Standards and Technology, Gaithersburg, MD, http://webbok.nist.gov

Guclu-Ustundag and Temelli [3-5] compiled literature data and conducted a critical evaluation of the solubility behavior of different lipid classes in supercritical CO_2 for binary, ternary and higher level systems using Chrastil's equation, which is a simple empirical model correlating solute solubility with CO_2 density. Fig. 2-2 shows the solubility isotherms for representatives of some of the major lipid classes and minor components of interest, reflecting the impact of solute properties on solubility.

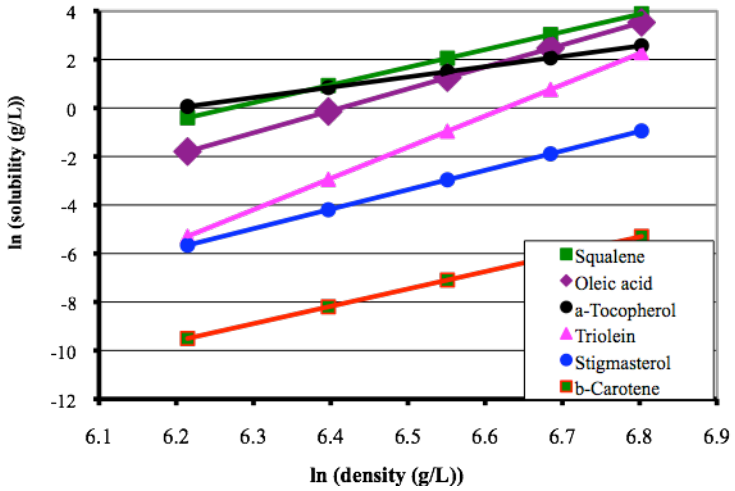

Figure 2-2. Solubility isotherms of lipid components at 50 °C (Reprinted with permission from Elsevier [4]).

Use of co-solvents, especially ethanol, has been studied extensively in terms of its impact on the solubility behaviour of lipids. Solubility enhancement is a result of an increase in the density of the SC-CO_2 and co-solvent mixture or intermolecular interactions between the co-solvent and a particular solute. Solubility enhancement as high as 63 fold was reported for some fatty acids using ethanol as a co-solvent, mainly due to H-bonding interactions [6]. Information on phase behaviour under supercritical conditions is also essential for optimal processing. During separation of oil components, operation takes place in the two phase region and the properties of both phases are important to know to achieve separation of the targeted lipid components.

2.1.2. Lipid applications

Applications of SC-CO_2 for fats and oils processing mainly started in the 1980s, focusing on the extraction of oilseeds [7-9]. In the following years, its applications expanded to separation and conversion processes for the purposes of extraction of oil products, isolation and enriching certain components in the mixtures and conversion of lipids to many other high-value products via reactions.

Hexane has been the most commonly used solvent in commercial operations for the extraction of oils from various plant materials. Due to environmental and health regulations, hexane use is facing stricter limitations especially in food processing. As an alternative to the use of organic solvents, cold pressing has been introduced as a non-solvent technique. However, the amount of oil left in the meal after cold pressing is the major disadvantage resulting in inefficient processing. All these shortcomings have made SC-CO_2 a strong alternative to replace organic solvents like hexane.

SC-CO_2 has many applications in fats and oils processing due to the relatively hydrophobic structure of those components. Triglycerides, mono- and diglycerides, free fatty acids, phospholipids, glycolipids, sterols, as well as other fat-soluble components such as tocopherols, tocotrienols, carotenoids and squalene are all included in the lipids family. All these lipid components have great use not only in the food industry but also in the cosmetic, pharmaceutical, oleochemical and other industries due to their physical, chemical and physiological properties.

Extraction of oils using SC-CO_2 has been studied extensively since the early 1980s. Studies focused on the impact of extraction variables such as temperature, pressure, particle size and moisture content of feed material, extraction time, CO_2 flow rate and solvent-to-feed ratio. Their effect on the yield, recovery, and composition of the extracted oils from various sources has been of major interest. In general, optimization of extraction variables provided the first fundamental knowledge on the feasibility of the use of SC-CO_2 for such separations. Due to the increase in density and thus lipid solubility in SC-CO_2 with increasing pressure, extraction yield increases with pressure. The effect of temperature also depends on other parameters: the CO_2 density decreases with temperature while the vapor pressure of solutes increases. This leads to the well known cross-over phenomenon for solubility isotherms. In addition, increasing

temperature increases the diffusivity and thus enhances mass transfer kinetics during extraction.

Specialty oils are also of great interest due to their high concentrations of bioactive lipid components, such as polyunsaturated fatty acids, phytosterols, tocopherols, tocotrienols, carotenoids and squalene. Nut oils (almond, hazelnut, peanut, pecan, pistachio, and walnut), seed oils (apricot, borage, cherry, evening primrose, flax, grape, hiprose, pumpkin, sea buckthorn, sesame, etc.), cereal oils (amaranth, oat, rice bran, and wheat germ), and oils of fruits and vegetables (buriti fruit, carrot, cloudberry, olive husk, and tomato) are classified under specialty oils [10], which are high value, small volume oils as opposed to the commodity oils (soybean, canola, corn, sunflower, etc.) of low value and high volume.

In order to increase the recovery of more polar components, co-solvents are introduced during SC-CO_2 extraction of oils. Ethanol has been mainly used as the co-solvent of choice for food applications since it is generally recognized as safe (GRAS). Relatively polar components, such as phospholipids, were recovered from oil seeds with the introduction of ethanol, which is not possible with neat SC-CO_2 [11]. Although the extraction yield can be dramatically increased with increasing solvation power, co-solvent use diminishes the biggest advantage of SC-CO_2, which is the ease of solvent removal. Thus, another approach based on the use of vegetable oil as a co-solvent was introduced for the recovery of fat-soluble carotenoids such as carotene [12] and lycopene [13, 14]. This approach provided higher extraction yield of total carotenoids compared to neat SC-CO_2 extraction without or with ethanol as a co-solvent.

It is possible to further fractionate a crude lipid extract and increase the concentration of the targeted component in the mixture for the purpose of refining. Fractionation of lipid mixtures can be achieved using different approaches. Fractions can be collected throughout an extraction period as a function of time by changing the extraction temperature and/or pressure over time. In another approach, fractional separation can be achieved by using several

separators in series. In this case, the extraction temperature and pressure can be set to achieve as high a CO_2 density as possible to extract the maximum amount of solutes. Then, CO_2 density is decreased in the separators to collect fractions of high, medium and low molecular weight corresponding to low, medium and high volatility compounds, respectively [10]. Thirdly, a fractionation column can be used for the separation of liquid feed mixtures. Applications include the fractionation of deodorizer distillates [15-19], vegetable and fish oils [20-24], and milk fat [25].

2.2. Membrane technology

2.2.1. Principles

Over the years, many industries have come to accept cross-flow filtration, such as microfiltration (MF), ultrafitration (UF), nanofiltration (NF) and reverse osmosis (RO), as standard technologies for clarification or concentration. In some instances, more than one type of membrane process may be used in series to achieve the desired performance. These membrane filtration processes are carried out using the concept of cross-flow, in the sense that the solution to be filtered is flowing parallel to the membrane surface at a certain velocity while the filtrate is going through the membrane. The cross-flow technique is used in order to increase the rate of mass transfer on the membrane surface and thus ensure reasonable filtration conditions at the membrane surface, contrary to conventional dead-end filtration.

One of the main advantages of membrane technology is the elimination of the energy-intensive evaporation process, generally used for solvent removal that can damage the product. Other advantages of membrane technology include: 1) reduced fresh water requirements due to re-utilization of waste water, 2) potential increased profit margins from creation of new products, 3) reduced waste treatment volume and costs, and 4) relatively low floor space and capital requirements when establishment of steam generation facilities can otherwise be avoided. On the other hand, disadvantages include: 1) expenses and time required to document product

safety and obtain approval from the regulatory agencies for use of new membrane materials in food processing, 2) uncertainty about membrane durability, effective operating life, and replacement costs, 3) concerns about chemical inertness and pH sensitivities, 4) operating pressure limitations in certain designs, and 5) fouling problems with certain feedstocks.

Although membrane pore size is an important parameter dictating which molecules can permeate, pore size might change depending on the conditions applied during processing. Therefore, it is important to measure the pore size under applied pressure and in the presence of the solvent to be used during separation. All separation processes should be evaluated individually for each solute, solvent and membrane material as well as processing parameters and membrane types. Studies conducted with model mixtures provide valuable insight to better understand these complex interactions prior to dealing with real multi-component mixtures of natural products.

Because of the low molecular size of free fatty acids relative to other major lipid and protein components, smaller pore size or denser (non-porous) membranes are preferred for separation. The mechanism of separation changes from convection to solution-diffusion theory during applications from large pore size to small pore size and denser membranes. The smaller the pore size the higher the solution-diffusion effects on separation.

In a non-porous membrane, pores are between the polymer chains on a molecular level. These molecular pores can be described in terms of free volume. Solution diffusion mechanism is the main transport mechanism of gas, vapor, and liquid through polymers and it consists of three major steps. In the first step, penetrant is sorbed into the polymer. In the case of gas transport, gases get condensed at the upstream surface before getting dissolved. In the second step, penetrant diffuses through the polymer matrix, and in the last step the penetrant desorbs at the downstream side.

One of the most commonly used models explaining transport in membranes is the dual-mode sorption model. This model consists of two distinct molecular populations [26]: Ordinary dissolution of the molecules in the polymer described by Henry's law and dissolution of the molecules in a limited number of fixed sites and microcavities in the polymer matrix described by Langmuir sorption.

2.2.2. Lipid applications

Polyunsaturated fatty acids (PUFA) and the lipid-soluble minor components such as carotenoids, tocopherols and phytosterols have become the focus of lipid-based products. The main source of PUFA is fish oils whereas the main source of phospholipids (PL), carotenoids, tocopherols and phytosterols is vegetable oils and other plant materials.

Vegetable oil processing is one of the major applications of membrane operations in food processing. Conceptually, membranes can be used in almost all stages of oil production and purification provided that the membranes are stable in solvent and oil mixtures [27]. As new membranes became available, various applications in fats and oils processing, including deacidification, degumming, clarification, decolorization and solvent removal have emerged recently.

Molecular weight (MW) of triacylglycerols (TAG), PL, tocopherols, sterols and other lipid compounds can range from 400 to 1,050 Da, which are too close to be differentiated by MF, UF and even NF membranes. However, PLs are surfactants, with both hydrophilic and hydrophobic groups, and can form reverse micelles in non-aqueous environments with a globular structure that can have a molecular weight of 20,000 Da or more. Accordingly, in this form PL now have a sufficient size difference compared to other compounds that will allow them to be rejected by an appropriate membrane. This membrane-based crude oil degumming procedure yields permeate and retentate fractions containing TAG and PL, respectively. The majority of the coloring matter and some of the free

fatty acids (FFA) and other impurities can interact with the PL micelles and are removed as well.

PUFA play an important role in human health especially in reducing the risk of cardiovascular heart disease [28]. Thus, there is growing demand from pharmaceutical and nutraceutical industries for purified PUFA products. Linder *et al.* [29] investigated restructuring and enrichment of PUFA in salmon oil. It was a two-step hydrolysis and re-esterification reaction with enrichment of PUFA in between the two reaction steps. A regenerated cellulose membrane was used between the two reaction steps to retain most of the saturated fatty acids and to concentrate monounsaturated fatty acids (MUFA) and PUFA in the permeate. Membrane separation was carried out at 4 $^{\circ}$C with the aim of crystallizing most of the saturated fatty acids including C14:0, C16:0, C18:0, which resulted in a decrease in the saturated fatty acid content from 29.5 mol% in the hydrolyzed oil to 22.9 mol% in the permeate. Also, PUFA and MUFA concentrations in thepermeate increased by 8 mol% each. Total PUFA increased from 39.2 mol% in the crude oil to 43.3 mol% in the re-esterified permeate [29].

Tocopherols (vitamin E) are lipid soluble components and are widely used as ingredients in various food products as antioxidants [30]. In addition to being potent antioxidants, they also have non-antioxidant functions such as inhibition of protein kinase activity and vascular smooth cell growth [31]. Carotenoids are primarily used as food colorants. Some carotenoids also have pro-vitamin A activity. The benefits of carotenoids to human health, such as reducing the risk of cancer, cardiovascular disease, osteoporosis and diabetes have been reported [32]. Some of the vegetable oils like palm oil and soy oil contain high concentrations of tocopherols and carotenoids, respectively. These minor components are removed during the conventional oil refining process. However, there is growing interest in the recovery of these high-value bioactive components from various natural sources.

Deodorizer distillate (DOD), a by-product of the vegetable oil refining process, is a rich source of tocopherols and membrane processing has been applied for the recovery of tocopherols from DOD. Nagesha *et al*. [33] processed a model mixture, representing soy DOD, to show that tocopherols permeated preferentially over oleic acid and other oil components through a non-porous (denser) polymeric composite membrane. Solubility and diffusivity of solute components were calculated based on the solution diffusion theory and oleic acid gave higher values compared to tocopherols. Also, MW of oleic acid is 282 Da and that of tocopherol is 417 and 431 Da for gamma and alpha isomers, respectively. Even though fatty acids were expected to permeate over tocopherols, that was not the case because polarity had a greater influence on the permeation rate through denser membranes. Since tocopherols are less polar molecules compared to fatty acids and the membrane material was hydrophobic, tocopherols permeated selectively over fatty acids. It was also found that when esterified soy DOD was used both rejection of fatty acids and flux increased [33]. The increase in flux can be explained with the much lower viscosity of the esterified oils. In addition, esterification increased the MW of fatty acids, leading to higher selectivity for tocopherol in the permeate of the hydrophobic membrane. Compared to FFA, the less polar fatty acid methyl esters (FAME) had greater interaction with less polar tocopherol and such coupling resulted in a positive effect in terms of their transport through the membrane. Dilution with hexane also increased the selectivity together with permeate flux since hexane is known to have higher permeability than any of the oil components through the membrane due to its high solubility in the membrane material [33].

Darnoko and Cheryan [34] studied the recovery of carotenes from red palm methyl esters (RPME). They carried out transesterification of red palm oil, and then used NF to separate carotenes from the methyl esters. They evaluated the results with their model system, which was prepared by adding carotenes to RPME. Of the three different membranes tested, DS7, a flat sheet membrane provided the highest flux with the lowest rejection rate of 63.5% and it was

selected for further experiments based on the calculations that showed high flux and moderate rejection to be more advantageous than high rejection and very low flux. The rejection rate was increased up to 80% with a volume concentration ratio (VCR) of 10. Based on these results, a multistage membrane system design was suggested by Darnoko and Cheryan [34] with a process feed rate of 11,111 L/h containing 0.45 g/L carotenes. The retentate flow rate was 3,611 L/h with a carotene concentration of 1.19 g/L after multistage membrane separation.

Tsui and Cheryan [35] investigated the recovery of xanthophylls such as lutein and zeaxanthin from ethanol extracts of corn using a UF-NF membrane system. They aimed to separate ethanol-soluble proteins in the UF step followed by carotenoid recovery in the NF step. They tested several UF and NF membranes and the three best in terms of flux and selectivity were selected for further experiments. Membranes with an estimated molecular weight cut-off (MWCO) of 1,000-2,000 Da gave the best results in terms of protein concentration in the UF retentate. Then, membranes with a molecular weight cut off (MWCO) of 300 Da performed best with the highest flux, rejection and stability at the end of a VCR of 7.6 for the NF step.

2.3. Supercritical extraction – membrane separation coupled technology

Considering all the latest developments in the use of SC-CO_2 technology for the extraction and fractionation of the lipids and lipid-based nutraceuticals as described above, there is potential for coupling of membrane separation and supercritical technologies. Such an approach would lead to novel technology development combining the advantages offered by both techniques.

2.3.1. Equipment

Even though the following discussion focuses on lab-scale equipment, because such coupled systems are not available at commercial scale at this point, the basic principles would also apply to commercial scale.

High pressure equipment is needed for the coupled SC-CO_2 extraction – membrane separation system both at laboratory and commercial scale. The type of pumps, membrane modules, valves, regulators and o-rings all must be well designed and properly placed in the system due to the high pressures applied. The main difference in the coupled system compared to conventional membrane processing is the fact that downstream pressure in the permeate stream of the membrane module is much higher than ambient pressure. This requires an appropriate design to be able to build up transmembrane pressure properly without causing any compaction or damage in the membrane structure.

Another important factor to maintain a proper operation is to avoid any potential leakage likely to happen throughout processing. Since CO_2 is a very small molecule, high pressure processing increases the possibility of its escape out of the system through any cracks, blisters or connections. Thus, all equipment and parts including the valves, nuts and o-rings should be carefully checked prior to pressurization of the system.

High pressure pumps used in such systems can be of various types. Compressors and pressure booster pumps use gas phase CO_2 in the feed tank whereas syringe pumps use CO_2 tanks with liquid withdrawal. The main disadvantage arising from the use of booster pumps and the compressors is that compressed air pressure and feed pressure should be well adjusted to be able to achieve constant set pressure. Because of the strong pulsation associated with booster pumps and compressors, system pressure may not be controlled easily to achieve a smooth increase during pressurization. That may possibly lead to a reversible compaction in the polymer membrane and delay the start up of the separation process. In order to prevent this effect, a vessel of large volume can be placed at the inlet of the system after the pump/compressor to dampen the degree of pulsation and to increase the control during pressurization.

Most commonly used pumps during high pressure CO_2 applications are syringe pumps. The main advantage of this pump is the accurate control of

pressure during processing by minimizing any possible fluctuations in pressure. The system can be easily pressurized at a specified rate, which prevents any potential damage on membrane structure.

Use of different valves and regulators is associated with the different types of modules used throughout processing. In the case of cross-flow modules, pressure of CO_2 at the upstream can be adjusted by using front pressure regulators at the inlet of the module. During processing with dead-end modules, there is no need for an additional regulator.

One of the most important issues to be considered prior to the start up of the system is the type of o-rings used in the membrane modules and regulators. Thermophysical properties of those materials should be carefully checked prior to their use in such a process. Some of the materials used in such systems are not entirely impermeable and can undergo sorption/diffusion phenomena resulting in rupture after a sharp pressure drop due to depressurization. This can cause irreversible explosive deterioration of the structures, resulting in blisters, cracks and microstructure formations described as 'explosive decompression failure' (XDF).

It is essential that the material o-rings are made of can resist XDF. There are different types of o-rings available, targeting high temperature and high pressure applications. Although the cost of an o-ring is reasonably cheap, utmost care is needed for their selection and use. Although polymer membranes used during separations have similar risks upon depressurization of the system, their relatively stronger thin film structures minimize the possibility of XDF.

2.3.2. CO_2 - membrane interactions

Temperature and pressure conditions employed during supercritical processing may lead to physicochemical and morphological changes in polymer materials used to make the membranes. Temperature of a coupled system must be well adjusted to efficiently run both extraction and membrane separation units together. High temperatures can directly affect the physicochemical properties of

a polymer membrane. Structures of polymer materials change at certain transition temperatures, which are specific for each polymer material. The main transition points can be described as glass-rubber transition (T_g) and the crystalline melting point (T_m).

When the temperature of the system exceeds the glass transition temperature, T_g, of the polymer material, free volume begins to increase with temperature. Mulder [36] reported that thermal energy is sufficient to overcome the restrictions in chain mobility and/or to overcome the interactions between the polymer chains. When interacting penetrants such as CO_2 is used mobility of the polymer chains are mainly a function of penetrant concentration.

Solute, solvent and polymer material interactions during membrane processes play an important role for the performance of separation. Those interactions are strongly related to the process conditions. When CO_2 is used as the solvent, pressure of the system is maintained above its critical pressure to be able to dissolve solute components. Increasing pressure increases the solubility of those components via increasing CO_2 density. High pressure applications of CO_2 result in swelling, leading to plasticization of the polymer network during processing. In order to clarify the plasticization phenomenon and its effects on membrane performance, CO_2 - polymer interactions must be well understood for a given polymer material.

2.3.2.1. CO_2 - polymer interactions

Major factors affecting polymer plasticization during CO_2 processing can be listed as: polymer chain mobility, steric hinderance (accessability), pendant group member or backbone member, aliphatic, aromaticity, hydrocarbon tail, molecular weight, side chain size and free volume.

Nalawade *et al.* [37] emphasized that specific interactions between CO_2 and a polymer material are the major factors determining the solubility in polymers. The most important interactions between polymer and CO_2 are due to Lewis acid and base interactions, resulting in the quadrupole moment of CO_2

accommodating both acid and base sites. Accordingly, carbonyl groups were found to have specific interactions with CO_2 where the carbonyl group acts as a Lewis acid and CO_2 as a Lewis base. Also, O of CO_2 has cooperative interaction with H of carbonyl C or α-C [37].

Since sp3 oxygen atoms are generally better electron donors than sp2 oxygen atoms, ether and alcohol oxygen atoms are expected to have Lewis acid and base interactions with CO_2 similarly to carbonyl groups. Kilic *et al.* [38] reported that tertiary amine groups increase the CO_2-philicity of a carbonyl group via strengthening the Lewis basicity. According to Shen *et al.* [39], ether oxygen in addition to carbonyl group of esters results in an increase in CO_2 – polymer interactions in a cumulative manner. Nalawade *et al.* [38] also reported that CO_2 - ether interactions were greater than the interactions between an ester and CO_2.

According to Koros [40], carbonyl groups and their amount were one of the most important factors affecting plasticization of a polymer network. These interactions were also found to dictate the selectivity during CO_2 – CH_4 separations [40]. Kilic *et al.* [38] also exhibited that the loss of rotational motion of the side chain due to the lack of oxygen atom between the backbone and the carbonyl group caused a decrease in interactions between CO_2 and the polymer network. Staudt-Bickel and Koros [42] demonstrated that when cross-linking was achieved between carboxyl groups, the plasticization effect was reduced due to the decrease in the amount of carboxyl groups, which were replaced by ester linkages.

According to Ravendraan *et al.* [41], CO_2 can solubilize several dipolar and nondipolar molecular systems due to site-specific solute solvent interactions. Those effects were attributed to the CO_2 - polar group interactions.

Kazarian *et al.* [43] emphasized the advantage of SC-CO_2 processing of polymers over various other methods. Since CO_2 has weak interactions with basic cites of macromolecular chains, CO_2 can be used as a plasticizer to process the polymers via increasing the inter-chain distances and chain segmental mobility.

Glass transition temperature and melting point are decreased in the case of crystalline polymers. Polymer plasticization can be achieved by heat treatment or through the use of some organic solvents. Heat intensive processes can result in difficulties in handling of polymer materials at high temperatures. Also, organic solvent treatment to achieve plasticization can cause contamination of the polymer material with residual solvent in the network. Therefore, the use of supercritical CO_2 seems promising for polymer plasticization especially targeting pharmaceutical, food and biotechnological applications.

2.3.2.2. Impact of CO_2 on membranes

To select the proper membrane for a targeted separation, three important factors should be considered; permeability, selectivity and stability. Most of the published work focuses on the permeability and the selectivity of the membranes. As a primary screening tool, if the membranes do not exhibit efficient performance, stability would not be a concern for further investigations. As such, stability is one of the most important considerations during membrane selection at a more advanced level. Interaction of membrane material with solvent and solute material is of particular importance affecting separation performance of membranes.

Although aromatic polyamides have been known as strong and efficient barrier materials due to their high selectivity for gas separations, high cohesive energy density of the polymer chains of the traditional aramids lead to very low gas permeabilities. Further research is focused on the reduction of cohesive energy density in terms of reducing the effectiveness of the interchain hydrogen bonds and increasing the free volume to increase gas permeability.

Wholly aromatic polyamide materials are used extensively for the production of nanofiltration and reverse osmosis membranes targeting water treatment. Garcia *et al.* [44] postulated that the common use of these materials is due to their outstanding thermal and mechanical resistance. Aromatic and amide linkages in the polymer network provide rod-like macromolecular chains, which

also are further strengthened by strong and highly directional hydrogen bonds. Effective selectivity of polyamide - based membranes arises from high-level intermolecular packing and cohesive energy.

Vitoux *et al.* [45] reported that although free volume and chain flexibility had an important effect on the solubility of CO_2 in corresponding polymers, interactions between CO_2 and the polymer had the strongest effect on CO_2 solubility resulting in a higher amount of CO_2 in the polymer network. Similarly, swelling of the polymer was found to be strongly correlated with CO_2 pressure. However, for a given polymer swelling phenomena was found to depend mostly on the nature of the polymer. Swelling was not only controlled by CO_2 – polymer interactions but also other properties such as viscosity, cohesivity and chain flexibility played an important role.

Sanders [46] indicated that permeability of CO_2 increased with increasing CO_2 pressure. It is most probably due to the higher increase in diffusivity coefficient with concentration than the decrease of solubility coefficient. It was suggested that polymer concentration further increases chain mobility whereby the diffusivity of the penetrant increases. Since the diffusion coefficient increases more rapidly with sorbed gas concentration, the permeability increases with increasing pressure.

On the other hand, for the polymers where permeability decreases with pressure, solubility coefficient decreases more rapidly than the increase of diffusion coefficient with pressure. Since the pressure dependence of solubility coefficient is comparable for different polymers, permeability depends more on the effect of pressure and thus concentration of CO_2 in the polymer, on the diffusivity coefficient.

Sanders [46] also reported that CO_2 was a strong plasticizer for polyethersulphone material. During the plasticization studies it was hypothesized that plasticization of the material must not be the only factor determining the permeation behaviour. Molecular motions responsible for plasticization of the

bulk physical and mechanical properties of the polymer could be different than those that control the diffusion of small molecules through the polymer. Sanders [46] also postulated that movement of the side groups in a polymer may either affect the local packing of the polymer upon swelling, resulting in easy passage of the small penetrant molecule or provide kinetic openings, which allow the solvent to perform a diffusional jump. Therefore, Sanders [46] argued that side groups were responsible for the diffusion of the solvent whereas the main chain was responsible for providing physical and mechanical properties to the membrane network.

Wonders and Paul [47] suggested that an increase in sorption and specific volume upon CO_2 exposure was due to the sample remaining in slightly dilated state following CO_2 removal. The sites giving rise to Langmuir sorption increase with an increase in the number of these sites or the enlargement of the existing ones. Since glassy polymers relax slowly, some level of increased microvoid volume remains after CO_2 removal.

Covalent bonds are more robust than ionic bonds. CO_2 cannot break or weaken covalent bonds. In addition, uniform distribution of covalent cross-links provides better control of segmental mobility upon applications of high feed pressures and preserves the selectivity of the membranes. Kratochvil and Koros [48] reported that CO_2 concentration in a cross-linked polymer can be as high as 80 cm^3 (STP)/(cm^3 of polymer) without plasticizing the polymer. Interchain rigidity is an essential factor to preserve diffusion selectivity of a polymer. Sorption levels are strongly related with segmental packing whereas segmental mobility and the resistance to plasticization depends on the segmental mobility.

Kratochvil and Koros [48] also exhibited that cross linking reduced the Henry's law constant. He suggested that Henry's law mechanism was the dominant factor affecting sorption at high pressures where plasticization occurs because Langmuir sorption sites are ideally at saturated state at these pressures. Cross-linking reduces the mobility of the polymer chains by reducing the Henry's

law mechanism via reducing the sorption. That is due to the rigid polymer structure formed by covalent bonds where the chains cannot have the mobility to accommodate excess amounts of CO_2 in their structure. Covalent cross linking can be used to suppress the effect of swelling and control the swelling behaviour.

There is no method to fully predict if a given polymer will be plasticized by a penetrant. In addition, it is not known if it is the plasticization that affects the selectivity of a particular membrane. Thus, it is essential to test each and every polymer material individually to be able to clarify the potential plasticization of the structure upon processing with SC-CO_2.

2.3.3. Applications of coupled systems

2.3.3.1. Food related applications

Applications of coupled systems to food related components mainly focused on lipids, essential oils and caffeine. These studies mainly emphasized the performance of membranes in terms of rejection, CO_2 flux, selectivity and yield under supercritical conditions. Membranes used were mostly commercially available polymer membranes whereas some inorganic custom made membranes were also tested during applications.

Artz *et al.* [49] used a custom made dead-end module during separation of free fatty acids from sunflower oil triglycerides. Four polymer membranes were tested during processing under supercritical conditions. All membranes showed a decrease in flux throughout processing with time due to reasons such as compaction, fouling or formation of a concentration gradient. Decrease in flux increased with increasing transmembrane pressure applied during processing because of compaction. Flux of DK and NF90 membranes were found to be higher with SC-CO_2 than that with hexane, which was attributed to the much lower viscosity of SC-CO_2. Sequential processing of TAG/FFA mixture resulted in an efficient separation using the BW30 membrane. Adding hexane as a co-solvent did not enhance selectivity but the amount of oil dissolved in CO_2 was increased. Results indicated that deacidification of sunflower oil was promising

but removal of carotenoids from the lipid mixture was not performed efficiently via the coupled SC-CO_2 – membrane separation system using NF90 and BW30 membranes.

Lai *et al.* [50] also tested the deacidification of soybean oil under subcritical CO_2 conditions using the same membranes, NF90 and BW30. The amount of dissolved lipids was about one order of magnitude less than that under supercritical conditions due to the lower pressures applied at subcritical conditions. CO_2 flux of NF90 was significantly higher than that of BW30 membrane whereas oleic acid selectivity was much higher for BW30. Although the results demonstrated the feasibility of subcritical CO_2 – membrane separation coupled system, deacidification of soybean oil, CO_2 flux and the amount of lipids dissolved were found to be substantially higher under supercritical conditions.

deMoura *et al.* [51] used the coupled system to remove the by-products from structured lipids formed during interesterification between medium chain triacylglycerols and ethyl esters of long chain fatty acids. Two nanofiltration (DL-4040 and HL-4040) and one reverse osmosis (BW30) membranes were used. Highest TAG retention was achieved with BW30 membrane. There was a decrease in CO_2 flux with time during processing due to the blockage of the membrane pores when BW30 membranes were used. Also, processing at very high transmembrane pressure (40 bar) increased the TAG retention because of the possible compaction in the membrane structure. The feed pressure affected the CO_2 flux and lipid in the permeate stream. Increasing feed pressure increased lipid permeation whereas decreased CO_2 flux. On the other hand, increase in the feed pressure caused a decrease in extraction selectivity due to the increasing solubility of TAG. This study was unique in terms of optimization of processing conditions during a reaction to increase the purity of the product in the retentate with the use of a coupled system. Low transmembrane pressure (7 bar) and a low feed pressure (90 bar) resulted in the highest retention of structured lipids. In addition, low temperature processing (40 °C) was found to be ideal for the extraction and

purification of structured lipids, especially for the protection of polyunsaturated fatty acids against oxidation and acyl migration.

Sarrade was one of the pioneers of the use of coupled SC-CO_2 – membrane separation systems. One of his studies [52] focused on the fractionation of TAGs from fish oil and purification of carotenoids from carrot oil and seeds. Custom made inorganic membranes where one of them had a nafion selective layer were used. TAGs having 36 to 52 carbon atoms were significantly enriched in the permeate stream. On other hand, TAGs with 44 and 46 carbon atoms were in higher concentration than TAGs with 42 carbon atoms in the permeate. This was attributed to the different steric conformation of TAG molecules at different carbon numbers affecting their transfer through the membrane. Membranes having nafion top layer were more selective towards TAGs during separations.

Sarrede *et al.* [52] also showed that using membranes without a nafion selective layer resulted in an increase in the carotenoid concentration of more than two fold in the permeate stream compared to their initial value in the feed streams. When carrot seeds were tested, main purification was obtained during the SC-CO_2 extraction step. However, membranes with nafion selective layer exhibited a 30% increase in carotenoid concentration in the permeate stream.

Due to the high solubility of essential oils in SC-CO_2, there are many applications of essential oils with coupled systems. Sarmento *et al.* [53] studied the separation of lemongrass, orange and nutmeg essential oils from SC-CO_2 by using three commercially available reverse osmosis membranes. All membranes had a linear increase in CO_2 flux with increasing transmembrane pressure, exhibiting a negligible effect on compaction of their structures. Different feed oil concentrations were tested along with different transmembrane pressures during separations. Except for the AG membrane, there was no significant change in CO_2 flux and permeability due to the change in essential oil feed concentration. Results indicated that lemongrass essential oil retention of SG membrane was the highest

among three membranes [53]. The change in CO_2 flux with transmembrane pressure was tested after the membranes were processed during lemongrass essential oil separation for three membranes. Although CO_2 flux increased with increasing transmembrane pressure as expected, that increase was much less than that for previously unprocessed membranes. That was the indication of fouling on membrane surface due to the use of a dead-end module resulting in accumulation of essential oil components.

Carlson *et al.* [54] studied the separation of d-limonene from SC-CO_2 using four commercial reverse osmosis and nanofiltration membranes. HL membrane exhibited the highest flux among all membranes. SG membrane was the only membrane giving stable d-limonene retentions throughout processing, whereas retentions of AK and HL membranes showed a substantial decrease with processing time. On the other hand, SG membrane had the highest decrease in CO_2 flux while HL membrane showed a slight decrease followed by almost a linear increase during processing [54]. Periodical addition of pure CO_2 to the system delayed the decrease in CO_2 flux for SG membrane.

Another essential oil application using nutmeg was performed by Spricigo *et al.* [55] by testing a commercially available cellulose acetate membrane. It was shown that CO_2 flux increased with processing time during nutmeg oil separation whereas retention rates did not show a substantial change. On the other hand, when the feed concentration was increased the effect of transmembrane pressure on CO_2 was less at all three temperatures tested (40, 50 and 60 °C). It was also reported that CO_2 permeability decreased with increasing concentration of oil in the feed stream. In order to investigate the effect of processing on CO_2 flux after the separation was completed, pure SC-CO_2 was passed through the membrane. It was emphasized that reduction in CO_2 flux due to concentration polarization during processing might be a reversible fouling phenomenon. Spricigo *et al.* [55] concluded that at feed pressure of 120 bar and transmembrane pressure of 40 bar, high retention of essential oils can be achieved with high CO_2 flux without

causing any compaction in the membrane structure. These operating conditions were found to be the best without having a phase change in the permeate stream while reducing the recompression work considerably.

Other than the lipid and essential oil applications summarized above, the use of coupled systems for caffeine separation was also investigated. One of the first applications was by Tokunaga *et al.* [56]. They used silica and zeolite membranes unlike polymers for rejection of caffeine. Due to the pore size difference, the silica membrane provided a much higher CO_2 flux. However, 10 min after caffeine was introduced into the system, CO_2 flux substantially decreased with silica membrane due to the adsorption layer forming in the pores whereas the flux remained constant for zeolite membranes. These results showed that caffeine was not adsorbed on zeolite membranes to any appreciable extent, making it possible to use for caffeine separations [56]. It was suggested that if the pore size of zeolite membranes could be controlled at subnanometer scale, zeolite membranes had huge potential for use in separation of solute components from SC-CO_2. Tan *et al.* [57] synthesized tubular filters coated with mesoporous silica and microporous silicalite for caffeine rejection. Other than their performance, membranes were characterized for their physical and chemical properties.

Mesoporous silica membranes exhibited rejections of up to 98% in the first 6 h and then dropped slightly. It was proposed that the major mechanism during separation of caffeine was the adsorption in mesoporous silica layer. Thus, steady state regeneration did not look promising because the adsorption equilibrium was approached. Microporous silicalite membranes also showed high caffeine rejections [57]. The separation mechanism was based on molecular sieving and adsorption mechanism depending on pressure due to the existence of defects on the surface of the membranes. It was emphasized that a thin microporous membrane filter could be used to regenerate pure SC-CO_2 at pressures where decaffeination process was normally achieved when the defects at the surface were removed.

Pietsch *et al.* [58] studied the pressure, temperature and caffeine concentration effect on the retentate. Separation of caffeine from aqueous solutions was investigated while recycling the industrial wash water stream. It was suggested that the use of FT30SW reverse osmosis membrane was efficient without having high amounts of CO_2 dissolved at moderate pressures and temperatures of up to 60 °C.

Chiou and Paul [59] used different membranes with various pore sizes to regenerate supercritical CO_2 from a mixture containing caffeine. Maximum size of caffeine clusters was estimated to be 3 nm and a membrane (N5) with an average pore size of 3 nm was tested. Rejection rates of 100% were achieved with CO_2 flux values of up to 0.024 mol/s m^2. Due to a decrease in cluster size when the system was operated over critical pressure, both CO_2 flux and caffeine rejection were reduced. Those results were verified when polycarbonate membranes with an average pore size of 10 nm was used. Since the system pressure was always higher than the critical pressure during extraction, pressure was reduced with regeneration of CO_2 during the process.

Sarmento *et al.* [60] also studied the extraction and separation of polyphenols from cocoa seeds and their separation using nanofiltration membranes. As expected, SC-CO_2 was not an efficient solvent for extraction of polyphenol due to their relatively hydrophilic nature. On the other hand, with a transmembrane pressure of 10 bar, DL, HL, NF90 and BW30 membranes exhibited promising results with polyphenol rejections of over 90%. Among all the membranes investigated, HL gave the best results especially with long chain polyphenols with rejections reaching up to 100%.

2.3.3.2. Non-food related applications

Coupled systems have been employed for many other applications other than food components. Filtration of highly viscous liquids such as motor oils was assisted by using pressurized CO_2. The permeate flux increased by 5 fold for

mineral oils and 3 fold for used motor oil [61]. Sarrade *et al.* [62] reported the use of a coupled system to reduce the viscosity of used oils during their processing. Hsu and Tan [63] studied a method to separate ethanol from water-ethanol mixture using SC-CO_2 and reverse osmosis membranes. This method gave promising results depending on the introduction of SC-CO_2 in the reverse osmosis operation. Similarly, Semenova *et al.* [64] investigated the separation of SC-CO_2 and ethanol by using asymmetric polyimide membranes.

Ohya *et al.* [65] reported the use of asymmetric polyimide membranes for the separation of SC-CO_2 iso-octane mixtures. Kosuri and Koros [66] used the asymmetric hollow fiber membranes and employed Torlon, which had resistance against plasticization caused by the strong interactions of CO_2 with polymer material for the separation of CO_2 from hydrocarbons.

Another study was performed regarding microemulsions and dispersions using an inorganic membrane with the coupled process [67]. The permeation was analyzed regarding material, pore size, and geometry. This technology was targeted for the recovery of a wide range of polar solute molecules from supercritical fluids. Yonker *et al.* [68] also investigated a membrane process using near-critical and supercritical fluids for the separation of polar, water-soluble macro-molecules. The technique was targeted for the use of reverse micelles in the fluid solvents to extend the capabilities of membrane separations in supercritical fluids to include both nonpolar and polar molecules.

There are also a few studies focusing on applications of contactors and reactors where SC-CO_2 is used as a solvent. Bothun *et al.* [69] investigated the advantages of tunability of compressed solvents and the high efficiency of hollow fibre contactors on the economical replacement of hexane for the extraction of a variety of natural products, including essential oils. Goetheer *et al.* [70] emphasized that when membranes with pore sizes smaller than the size of the catalyst, but larger than the diameter of the products were used, it would lead to various new opportunities of homogeneous catalysis in supercritical fluids.

2.4. References

[1] G. Brunner, S. Peter, On the solubility of glycerides and fatty acids incompressed gases in the presence of an entrainer, Separation and Purification Technology 17 (1982) 199–214.

[2] E.J.M. Straver, J.L. de Roo, C.J. Peters, J. de Swaan Arons, Phase behavior of the binary system propane and tristearin, Journal of Supercritical Fluids 11 (1998) 139–150.

[3] O. Güclü-Üstündağ, F. Temelli, Correlating the solubility behavior of fatty acids, mono-, di- and triglycerides, and fatty acid esters in supercritical carbon dioxide, Industrial & Engineering Chemistry Research 39 (2000) 4756–4766.

[4] Reprinted from Journal of Supercritical Fluids, 31, O. Güclü-Üstündağ, F. Temelli, Solubility of minor lipid components in supercritical CO_2, 235-253, 2004 with permission from Elsevier.

[5] O. Güclü-Üstündağ, F. Temelli, Solubility behaviour of ternary systems of lipids in supercritical carbon dioxide: a review, Journal of Supercritical Fluids 38 (2006) 275–288.

[6] O. Güclü-Üstündağ, F. Temelli, Solubility behavior of ternary systems of lipids, cosolvents and supercritical carbon dioxide, Journal of Supercritical Fluids 36 (2005) 1–15.

[7] E. Stahl, E. Schutz, H.K. Mangold, Extraction of seed oils with liquid and supercritical carbon dioxide, J. Agric. Food Chem. 28 (1980) 1153–1157.

[8] R. Eggers, U. Sievers, W. Stein, High pressure extraction of oilseed, Journal of American Oil Chemists' Society 62 (1985) 1222–1230.

[9] J.P. Friedrich, G.R. List, A.J. Heakin, Petroleum-free extraction of oil from soybeans with supercritical CO_2, Journal of American Oil Chemists' Society 59 (1982) 288–292.

[10] F. Temelli, M.D.A. Saldana, P.H.L. Moquin, M. Sun, Supercritical fluid extraction of specialty oils, in (Chapter 3): J.L. Martinez (Ed.), Supercritical Fluid Extraction of Nutraceuticals and Bioactive Compounds, CRC Press, Taylor & Francis Group, Boca Raton, FL, 2008, pp. 51–101.

[11] N. Dunford, F. Temelli, Extraction of phospholipids from canola with supercritical carbon dioxide and ethanol, Journal of American Oil Chemists' Society 72 (1995) 1009–1015.

[12] M. Sun, F. Temelli, Supercritical carbon dioxide extraction of carotenoids from carrot using canola oil as a continuous co-solvent, Journal of Supercritical Fluids 37 (2006) 397–408.

[13] M.D.A. Saldana, F. Temelli, B. Tomberli, S.E. Guigard, C.G. Gray, Solubility of lycopene in supercritical CO_2, CO_2 + ethanol and CO_2 + canola oil using dynamic extraction of tomato, Journal of Food Engineering 99 (2010) 1-8.

[14] G. Vasapollo, L. Longo, L. Rescio, L. Ciurlia, Innovative supercritical CO_2 extraction of lycopene from tomato in the presence of vegetable oil as cosolvent, Journal of Supercritical Fluids 29 (2004) 87–96.

[15] G. Brunner, Th. Malchow, K. Sturken, Th. Gottschau, Separation of tocopherols from deodorizer condensates by countercurrent extraction with carbon dioxide, Journal of Supercritical Fluids 4 (1991) 72–80.

[16] P. Bondioli, C. Mariani, A. Lanzani, E. Fedeli, A. Muller, Squalene recovery from olive oil deodorizer distillates, Journal of American Oil Chemists' Society 70 (1993) 763–766.

[17] J.W. King, N.T. Dunford, Phytosterol-enriched triglyceride fractions from vegetable oil deodorizer distillates utilizing supercritical fluid fractionation technology, Separation and Purification Technology 37 (2002) 451– 462.

[18] O. Güclü-Üstündağ, F. Temelli, Column fractionation of canola oil deodorizer distillate using supercritical carbon dioxide, Journal of American Oil Chemists' Society 84 (2007) 953–961.

[19] T. Fang, M. Goto, M. Sakaki, D. Yang, Extraction and purification of natural tocopherols by supercritical CO_2, (Chapter 4) in: J.L. Martinez (Ed.), Supercritical Fluid Extraction of Nutraceuticals and Bioactive Compounds, CRC Press, Taylor & Francis Group, Boca Raton, FL, 2008, pp. 103–140.

[20] U. Fleck, C. Tiegs, G. Brunner, Fractionation of fatty acid ethyl esters by supercritical CO_2: high separation efficiency using an automated countercurrent column, Journal of Supercritical Fluids 14 (1998) 67–74.

[21] E. Reverchon, M. Poletto, L.S. Osseo, M. Somma, Hexane elimination from soybean oil by continuous packed tower processing with supercritical CO2, Journal of American Oil Chemists' Society 77 (2000) 9–14.

[22] E. Ibanez, A.M.H. Benavides, F.J. Senorans, G. Reglero, Concentration of sterols and tocopherols from olive oil with supercritical carbon dioxide, Journal of American Oil Chemists' Society 79 (2002) 1255–1260.

[23] W.B. Nilsson, E.J. Gauglitz Jr., J.K. Hudson, Supercritical fluid fractionation of fish oil esters using incremental pressure programming and a temperaturegradient, Journal of American Oil Chemists' Society 66 (1989) 1596–1600.

[24] O.J. Catchpole, J.B. Grey, K.A. Noemark, Fractionation of fish oils using supercritical CO_2 and CO_2 plus ethanol mixtures, Journal of Supercritical Fluids 19 (2000) 25–37.

[25] A.R. Bhaskar, S.S.H. Rizvi, J.W. Sherbon, Anhydrous milk fat fractionation with continuous countercurrent supercritical carbon dioxide, Journal of Food Science 58 (1993) 748.

[26] Stern, S. A., Trohalaki, S., Fundamentals of gas diffusion in rubbery and glassy polymers, in Barrier polymers and structures, Ed. Koros, W., J.; ACS Symposium Series 423; American Chemical Society, Washington, DC, USA, 1990

[27] S.S. Koseoglu, Membrane technology for edible oil refining, Oils & Fats International 5 (1991) 16-21.

[28] W. Kolanowski, F. Swiderski, S. Berger, Possibilities of fish oil application for food products enrichment with ω-3 PUFA, Int. Journal of Food Science and Nutrition 50 (1999) 39-49.

[29] M. Linder, E. Matouba, J. Fanni, M. Parmentier, Enrichment of salmon oil with n-3 PUFA by lipolysis, filtration and enzymatic re-esterification, European.Journal of Lipid Science and Technology 104 (2002) 455-462.

[30] Y. Shimada, S. Nakai, M. Suenaga, A. Sugihara, M. Kitano and Y. Tominaga, Facile purification of tocopherols from soybean oil deodorizer distillate in high yield using lipase, Journal of American Oil Chemists' Society 77 (2000) 1009-1013.

[31] A. Azzi, R. Ricciarelli, J. M. Zingg, Non-antioxidant molecular functions of alpha-tocopherol (vitamin E), FEBS Letters 519 (2002) 4-10

[32] A. V. Rao, L. G. Rao, Invited review: Carotenoids and human health, Pharmacology Research 55 (2007) 207-216.

[33] G. K. Nagesha, R. Subramanian, U. K. Sankar, Processing of tocopherol and FA systems using a nonporous denser polymeric membrane., Journal of American Oil Chemists' Society 80 (2003) 397-402.

[34] D. Darnoko, M. Cheryan, Carotenoids from red palm methyl esters by nanofiltration, Journal of American Oil Chemists' Society, 83 (2006) 365-370.

[35] E. M. Tsui, M. Cheryan, Membrane processing of xanthophylls in ethanol extracts of corn, Journal of Food Engineering 83 (2007) 590-595.

[36] M. Mulder, Basic Principles of Membrane Technology, Kluwer Academic Publishers, Dordrecht, NL, 1996.

[37] P. Nalawade, F. Picchioni, H. Marsman, L.P.B.M. Janssen, The FT-IR studies of the interactions of CO_2 and polymers having different chain groups, Journal of Supercritical Fluids 36 (2006) 236–244.

[38] S. Kilic, Y. Wang, J.K. Johnson, E.J. Beckman, R.M. Enick, Influence of tert-amine groups on the solubility of polymers in CO_2, Polymer, 50 (2009) 2436-2444.

[39] Z. Shen, M.A. McHugh, J. Xu, J. Belardi, S. Kilic, A. Mesiano, S. Bane, C. Karnikas, E. Beckman, R. Enick, CO_2-solubility of oligomers and polymers that contain the carbonyl group, Polymer, 44 (2003) 1491-1498.

[40] W.J. Koros, Simplified analysis of gas/polymer selective solubility behavior, J. Polym. Sci., Polym. Phys. Ed. 23 (1985) 1611-1628.

[41] P. Raveendran, R. Ikushima, L. Wallen, Polar attributes of supercritical carbon dioxide, Accounts of Chemical Research, 38 (2005) 478-485.

[42] C. Staudt-Bickel; W. J. Koros, Improvement of CO_2/CH_4 separation characteristics of polyimides by chemical crosslinking, Journal of Membrane Science 155, (1999) 145-164.

[43] S. G. Kazarian, M. F. Vincent, F.V. Bright, C. L. Liotta, and C. A. Eckert, Specific intermolecular interaction of carbon dioxide with polymers, Journal of American Chemical Society 118 (1996) 1729-1736.

[44] J.M. García, F.C. García, F. Serna, J.L. de la Peña, High-performance aromatic polyamides, Progress in Polymer Science, 35 (2010) 623-686.

[45] P. Vitoux,T. Tassaing, F. Cansell, S. Marre, and C. Aymonier, In situ IR spectroscopy and ab initio calculations to study polymer swelling by supercritical CO_2, Journal of Physical Chemistry B 113 (2009) 897–905.

[46] E. S. Sanders, Penetrant induced plasticization and gas permeation in glassy polymers, Journal of Membrane Science 37 (1988) 63-80.

[47] A.G. Wonders, D.R. Paul, Effective of CO_2 exposure history on sorption and transport in polycarbonate, Journal of Membrane Science 5 (1979) 63.

[48]A. M. Kratochvil and W. J. Koros, Effects of supercritical CO_2 conditioning on cross-linked polyimide membranes, Macromolecules, 43, (2010) 4679–4687

[49] W.E. Artz, T. Kinyanjui, and M. Cheryan, Deacidification of soybean oil using supercritical fluid and membrane technology, Journal of American Oil Chemists' Society 82, (2005) 803–808.

[50] L. L. Lai, K. C. Soheili, W. E. Artz, Deacidification of soybean oil using membrane processing and subcritical carbon dioxide, Journal of American Oil Chemists' Society, 85 (2008) 189–196.

[51] J.M.L.N. de Moura, L.A.G. Gonçalves, L.A.V. Sarmento, J.C.C. Petrus, Purification of structured lipids using $SCCO_2$ and membrane process, Journal of Membrane Science, 299 (2007) 138-145.

[52] S.J. Sarrade, G.M. Rios, M. Carlès, Supercritical CO_2 extraction coupled with nanofiltration separation: Applications to natural products, Separation and Purification Technology 14 (1998) 19-25.

[53] L.A.V. Sarmento, C.B. Spricigo, J.C.C. Petrus, L.H.C. Carlson, R.A.F. Machado, Performance of reverse osmosis membranes in the separation of

supercritical CO_2 and essential oils, Journal of Membrane Science 237 (2004) 71-76.

[54] L.H.C. Carlson, A. Bolzan, R.A.F. Machado, Separation of d-limonene from supercritical CO_2 by means of membranes, The Journal of Supercritical Fluids, 34 (2005) 143-147.

[55] C.B. Spricigo, A. Bolzan, R.A.F. Machado, L.H.C. Carlson, J.C.C. Petrus, Separation of nutmeg essential oil and dense CO_2 with a cellulose acetate reverse osmosis membrane, Journal of Membrane Science 188 (2001) 173-179.

[56] Y. Tokunaga, T. Fujii, K. Nakamura, Separation of caffeine from supercritical CO_2 with a zeolite membrane, Bioscience Biotechnology Biochemistry 61 (1997) 1024-1026.

[57] C.-S. Tan, H.-C. Lien, S.-R. Lin, H.-L. Cheng, K.-J. Chao, Separation of supercritical carbon dioxide and caffeine with mesoporous silica and microporous silicalite membranes, Journal of Supercritical Fluids 26 (2003) 55-62.

[58] A. Pietsch, W. Hilgendorff, O. Thom, R. Eggers, Basic investigation of integrating a membrane unit into high-pressure decaffeination processing, Separation and Purification Technology 14 (1998) 107-115.

[59] J.S. Chiou, D.R. Paul, Effects of CO_2 exposure on gas transport properties of glassy polymers, Journal of Membrane Science 32 (1987) 195-205.

[60] L.A.V. Sarmento, R.A.F. Machado, J.C.C. Petrus, T.R. Tamanini, A. Bolzan, Extraction of polyphenols from cocoa seeds and concentration through polymeric membranes, The Journal of Supercritical Fluids, 45 (2008) 64-69.

[61] D. Gourgouillon, L. Schrive, S. Sarrade, G. Rios, An environmentally friendly process for the regeneration of used oils, Environmental Science and Technology 34 (2000) 3469-3473.

[62] S. Sarrade, C. Guizard, G.M. Rios, New applications of supercritical fluids and supercritical fluids processes in separation, Separation and Purification Technology 32 (2003) 57-63.

[63] J.-H. Hsu and C.-S. Tan, Separation of ethanol from aqueous solution by a method incorporating supercritical CO_2 with reverse osmosis, Journal of Membrane Science 81 (1993) 273-285.

[64] S.I. Semenova, H. Ohya, T. Higashijima, Y. Negishi, Separation of supercritical CO_2 and ethanol mixtures with an asymmetric polyimide membrane, Journal of Membrane Science 74 (1992) 131-139.

[65] H. Ohya, T. Higashijima, Y. Tsuchiya, H. Tokunaga and Y. Negishi, Separation of supercritical CO_2, and iso-octane mixtures with an asymmetric polyimide membrane, Journal of Membrane Science 84 (1993) 185-189.

[66] M. R. Kosuri and W. J. Koros, Asymmetric hollow fiber membranes for separation of CO_2 from hydrocarbons and fluorocarbons at high-pressure

conditions relevant to C2F4 polymerization, Industrial & Engineering Chemistry Research, 48 (2009) 10577–10583.

[67] M. Koh, B. Fournel, S. Sarrade, L. Schrive, and I. Stoychev, Continuous supercritical CO_2 process using nanofiltration by inorganic membrane, Industrial & Engineering Chemistry Research 48 (2009) 5406-5414.

[68] C. R. Yonker, J. L. Fulton , M. R. Phelps , L. E. Bowman, Membrane separations using reverse micelles in nearcritical and supercritical fluid solvents, Journal of Supercritical Fluids 25 (2003) 225-231.

[69] G. D. Bothun, B. L. Knutson, H. J. Strobel, S. E. Nokes, E. A. Brignole, S. Diaz, Compressed solvents for the extraction of fermentation products within a hollow fiber membrane contactor, Journal of Supercritical Fluids 25 (2003) 119-134.

[70] E. L.V. Goetheer, A. W. Verkerk, B.-J. Deelman, L.J.P. van den Broeke, G. van Koten, Jos, T. F. Keurentjes, Membrane reactor for homogeneous catalysis in supercritical carbon dioxide, Journal of Catalysis 219 (2003) 126–133.

3. Probing the hydrophobicity of commercial reverse osmosis membranes produced by interfacial polymerization using contact angle, XPS, FTIR, FE-SEM and AFM[1]

3.1. Introduction

Reverse osmosis (RO) membranes have been widely used in separation processes in different industries, including water treatment and seawater desalination. Most of the commercially available RO membranes are made of cellulose acetate and aromatic polyamides [1]. In general, polyamide-based RO membranes formed by interfacial polymerization exhibit better performance than cellulose acetate-based membranes due to higher water flux, enhanced physical and chemical resistance and wider range of processing pH and temperature conditions [2]. Thus, interfacial polymerization has been the most commonly used technique for the preparation of thin film composite RO membranes.

The polymerization reaction involves two immiscible solvents; aqueous solvent containing the amine monomer and the organic phase containing acyl chloride. Polymerization reaction takes place on a porous ultrafiltration (UF) sublayer, usually a polysulfone, which is saturated with the aqueous amine solution. Thin film is formed immediately in between the two phases when they are brought together [3]. Membrane properties can be tuned by changing the reaction conditions such as the monomer concentration, type of organic solvent, curing time and temperature [3, 4]. Molecular structures of the amine and acyl chloride monomers are also very important for the final membrane properties. Recently, many different combinations of amines and acyl chlorides have been studied [5-7]. m-Phenyl diamine (m-PDA)-based polyamide (PA) membranes had higher salt rejection but lower flux compared to other PA membranes made of

[1] A version of this chapter has been published. Akin and Temelli 2011. Desalination, 278:387-396.

different amine monomers [7-9]. Trimesoyl chloride (TMC) is the generally preferred acyl chloride monomer during polymerization because of its ability to form a three-dimensional cross-linked structure [7]. Fig. 3-1 shows the most commonly used reactants and the structures of the thin films formed.

Superior mechanical and thermal properties of the polyamide structure result in high performance separations over long term processing with aqueous solutions. Hydrophilic properties contributed by the monomers used during polymerization prevent accommodation of processes involving non-aqueous solvents. Fabrication of the polyamide membranes by the same method without sacrificing performance would give rise to the application of these membranes in many different areas other than aqueous solutions. Therefore, it is essential to know the possible modifications made during the polymerization reaction towards the formation of relatively hydrophobic polyamide membranes to better understand their chemical structure and assess their potential use in novel processes, including those involving supercritical fluids.

Generally, permeability, salt rejection rate, temperature and pH processing range of the RO membranes are reported by the membrane manufacturers. With such limited information, it is difficult to characterize the commercial membranes since the chemistry and the reaction conditions are not accessible to the end users. A limited number of studies have reported detailed characterization of commercial membranes using advanced spectroscopic and microscopic techniques [10-14]. Studies involving characterization of relatively hydrophobic PA membranes have been scarce possibly due to the challenges associated with their unexpected surface properties caused by the commonly used reactants and/or unusual modifications influencing their hydrophobicity. Recent studies involving extensive characterization on many commercial membranes also concluded that relatively hydrophobic membranes require further investigation to be clearly identified [10, 11].

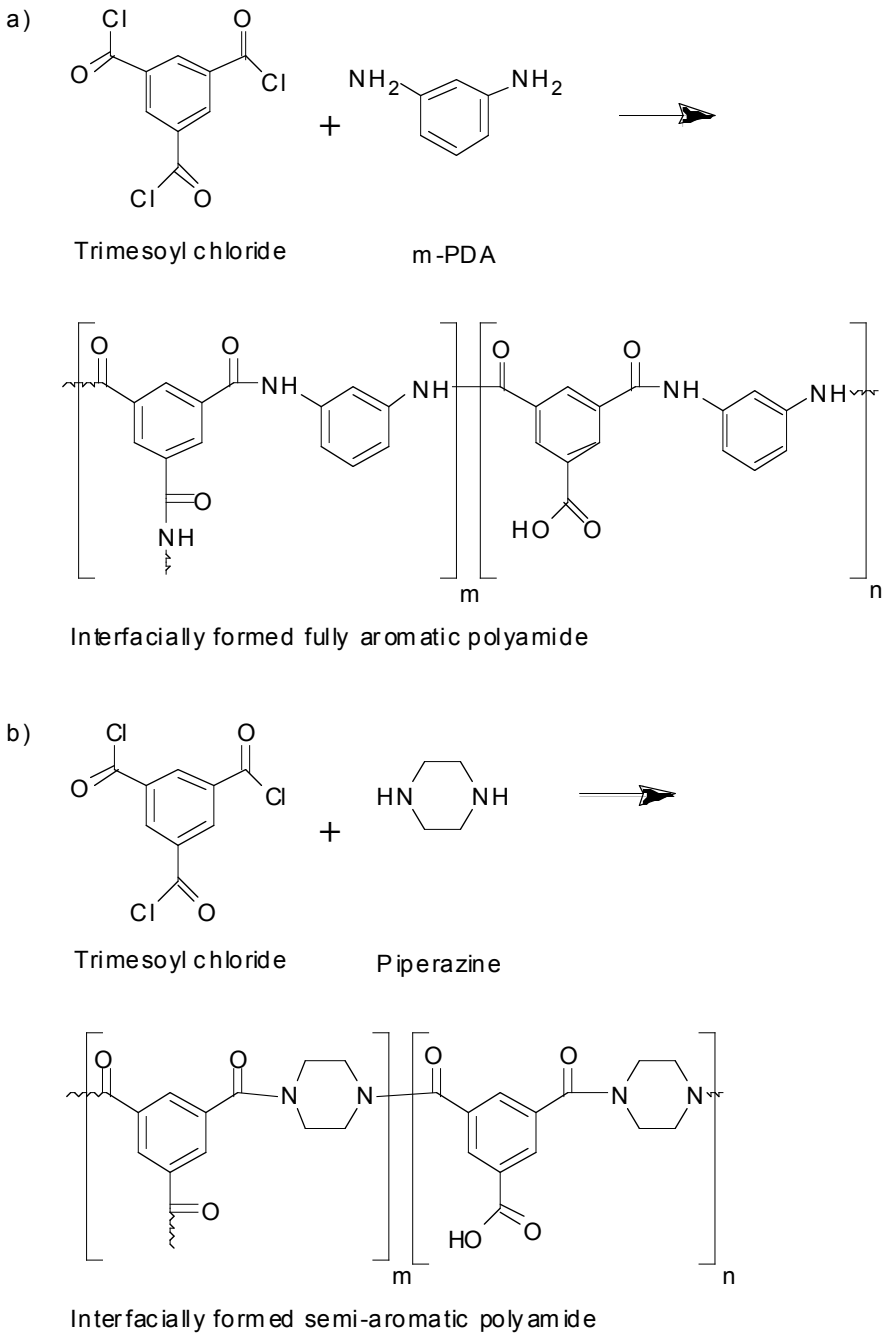

Figure 3-1. Most commonly used (a) aromatic (m-PDA) and (b) cycloaliphatic (piperazine) amine monomers undergoing interfacial polymerization reaction with TMC (m has value in between 0–1; m = 1 for fully cross-linked polyamide and n = 1 for fully linear one). O/N=1, fully cross-linked structure (all carbonyl groups formed amide linkages), O/N=2, fully linear structure (one carbonyl group formed carboxylic acid)(reprinted with permission from Elsevier [11]).

Therefore, the purpose of this study was to characterize four hydrophobic commercial RO membranes by using advanced techniques, including contact angle, X-ray photoelectron spectroscopy (XPS), attenuated total reflection - Fourier transform infrared spectroscopy (ATR-FTIR), atomic force microscopy (AFM), field emission – scanning electron microscopy (FE-SEM) measurements to provide insight into their unusual hydrophobicity and their physicochemical structures, considering their current and potential application areas.

3.2. Materials and methods

3.2.1. Materials and sample preparation

Four RO membranes (AK, AG, SE and SG) were kindly provided by GE Osmonics (Minnetonka, MN, USA). The virgin membranes were cleaned by soaking them in water for 24 h and then dried in a dryer at 45°C for 12 hr. After drying, they were placed in a desiccator for a minimum of 24 h. Based on trials of different protocols and initial FTIR and contact angle evaluations, this protocol was found to be sufficient for removal of water from the membranes.

3.2.2. Contact angle by sessile drop method

Contact angles of the dry membranes were measured using FTA 200 contact angle analyzer (Ten Angstroms, Folio Instruments, Kitchener, ON, Canada) located at the Department of Chemical and Materials Engineering, University of Alberta using the sessile drop method. A droplet of ultrapure water obtained from a MilliQ water system (Millipore, Billerica, MA, USA) was delivered onto the dry membrane surface and a static image of the droplet was taken immediately after contact with the surface. Contact angle measurements were performed using the FTA software for 2 replicates of each membrane and at a minimum of 10 different locations for each replicate.

3.2.3. Permeability and salt rejection

Performances of the membranes were determined by using a stainless steel dead-end filtration system located at the Department of Civil and Environmental

Engineering, University of Alberta, having a membrane area of 13.8 cm^2 at the operating pressure of 14 bar. NaCl solution (10 mM) was prepared for salt rejection analysis. Membrane permeability was determined as the stable flux at 24 h before NaCl addition and normalized by transmembrane pressure. Salt concentration in the permeate was determined by measuring the electrical conductivity of salt solution and using the calibration curve established between salt concentration and conductivity. NaCl rejection was calculated by using Eq. (3-1):

$$\text{Salt rejection (R\%)} = \left(1 - \frac{C_p}{C_f}\right) \times 100 \quad (3\text{-}1)$$

where C_p and C_f are NaCl concentrations (g/ml) of the feed and permeate streams, respectively.

3.2.4. X-Ray Photoelectron Spectroscopy (XPS)

The XPS measurements were performed using an AXIS 165 spectrometer (Kratos Analytical, Manchester, UK) at the Alberta Centre for Surface Engineering and Science (ACSES), University of Alberta. The base pressure in the analytical chamber was lower than 2×10^{-8} Pa. Monochromatic Al Kα source ($h\nu$ = 1486.6 eV) was used at a power of 210 W. The analysis spot was 400 x 700 µm. The resolution of the instrument is 0.55 eV for Ag 3d and 0.70 eV for Au 4f peaks. The survey scans were collected for binding energy spanning from 1100 eV to 0 with analyzer pass energy of 160 eV and a step of 0.35 eV. For the high-resolution spectra the pass-energy was 20 eV with a step of 0.1 eV. Since the samples were charging, electron flood neutralization was applied to compensate for the photoelectrons leaving the surface. XPS measurements were performed for 2 replicates of each membrane and at a minimum of 2 different locations for each replicate. Deconvolution of high resolution spectra was achieved by using CasaXPS software.

3.2.5. Attenuated Total Reflection - Fourier Transform Infrared Spectroscopy (ATR-FTIR)

ATR-FTIR spectra were obtained using a Nicolet 8700 FTIR spectrometer coupled to a germanium crystal operated at 45° using OMNIC 6.2 software (Thermo Electron Corp., Hampton, NH, USA) also located at ACSES, University of Alberta. Active layers of the dry membranes were pressed tightly against the crystal plate. CO_2 and water vapour were continuously purged out during the measurements. At least two replicates from each membrane sample were measured and 5 readings were taken from different points for each replicate. Each spectrum represents an average of 64 scans collected from 650 to 4000 cm^{-1} at 2 cm^{-1} resolution. No baseline or ATR corrections were applied.

3.2.6. Field Emission - Scanning Electron Microscopy (FE-SEM)

FE-SEM images of the cross-section and top layer of AK and SG membranes were taken by using JEOL 6301F field emission scanning electron microscope (Jeol, Tokyo, Japan) with Si diode detector located at the Department of Earth and Atmospheric Sciences, University of Alberta. Membranes were submerged in liquid nitrogen and cut by a sharp blade for cross-section analysis. AK and AG membranes were carbon coated by using a Leice SCD 005 (Analytical Technologies Group, Groton, CT, USA) with carbon evaporation attachment with 0.8 mm carbon thread. Carbon coating did not result in clear images for membranes with low roughness. Thus, SG and SE membranes were coated with chromium with an Edwards Xenosput XE 200 coater (Edwards High Vacuum International, Cambridge, UK).

3.2.7. Atomic Force Microscopy (AFM)

The experiments were performed using a atomic force microscope (Model MFP-3D, Asylum, Santa Barbara, CA, USA) operated in tapping mode using commercially available Si cantilevers (300 kHz frequency, Olympus, Tokyo,

Japan) located in ACSES, University of Alberta. The force constant of the cantilevers was 42 N/m. The oscillation frequency used for tapping mode was 310 ± 5 kHz. Scan rate of 1.0 Hz used with a scan size of 5 by 5 microns. At least 8 replicates were analyzed for each type of membrane.

3.3. Results and discussion

Four commercial RO membranes, AK, AG, SE and SG were characterized in depth. Within the two groups, AK and AG as well as SE and SG showed similar morphological and chemical properties according to the XPS, FTIR, FE-SEM and AFM analysis, in parallel to the manufacturer data, except for the fact that AG and SE were the tighter ones in each group as indicated in Table 3-1. Since FE-SEM and AFM analysis of AG and SE did not exhibit any difference from their counterparts (AK and SG, respectively) and were not useful to explain any structural differences, FE-SEM and AFM images of AG and SE were not presented in this discussion. The different methods possibly applied to produce the tighter AG and SE membranes were suggested based on XPS survey scans and ATR-FTIR analysis. Therefore, in the following discussion, AK and SG membranes, which were both looser than their counterparts, are presented in detail for ease of comparison and characterization followed by a brief comparison with the tighter counterparts, AG and SE membranes.

3.3.1. Surface hydrophilicity and membrane performance

Surface hydrophilicity is mostly tuned during fabrication of the membranes mainly to increase permeability and decrease fouling during aqueous separations. Prevention of fouling relies on the strategy to enhance the electrostatic repulsion between the foulants and the membrane surface. If the foulant is relatively hydrophobic, having a hydrophilic surface on the membrane would be desirable. Contact angle measurement is an important tool to assess the extent of hydrophilicity of a membrane surface. A few studies presented the contact angles of commercial RO membranes with values mostly in the range of 25-60 degrees [10, 15, 16]. The contact angles of the four commercial RO

membranes investigated in this study were between 60-70 degrees (Table 3-2). Relatively more hydrophobic surfaces indicate that these membranes would show less affinity towards hydrophilic compounds and create an interface, which is poor in polar solutes. Thus, these membranes would have higher selectivity against polar components compared to those membranes with lower contact angles reported previously [10, 15, 16].

Table 3-1. Properties of AK, AG, SE and SG membranes

Product[a]	**Structure**[a]	**Application**[a]	**Permeability**[b]	**Salt Rejection (%)**[c]	**pH range**[a]
AK	TF	Brackish water, Reactive silica	5.72 ± 0.62	97.1 ± 0.5	4 – 11
AG	TF	Brackish water, Reactive silica	2.88 ± 0.32	98.3 ± 0.6	4 – 11
SG	TF	Acid concentration	2.46 ± 0.15	94.4 ± 0.4	2 – 11
SE	TF	Acid concentration	1.21 ± 0.18	95.2 ± 0.3	2 – 11

TF: Thin film composite
[a] Manufacturer data
[b] L/m^2.h.bar based on duplicate measurements performed in this study.
[c] Salt rejection was performed in duplicate for 10 mM NaCl solution at pH 7 in this study.

Table 3-2. Contact angles of the four commercial membranes investigated

	AK	**AG**	**SG**	**SE**
Contact angle[a]	64.8 ± 2.3	63.5 ± 1.7	69.3 ± 2	69.9 ± 2.1

[a] Mean ± standard deviation based on 10 determinations

The relatively high hydrophobic surface properties of these membranes suggest that their surface could have been modified and the reasons for such modifications may be: 1) targeting hydrophilic contaminant removal to prevent fouling, and 2) focusing on a specific separation application. Table 3-1 presents the data regarding the performance of these membranes as determined in this study as well as the data obtained from the manufacturer. According to the manufacturer, AK and AG membranes were produced for reactive silica removal in addition to brackish water desalination. Since reactive silica is a hydrophilic material, AK and AG membranes satisfy the first reason for modification [17]. On the other hand, SG and SE membranes were reported to work under more acidic conditions (pH 2-11) compared to AK and AG (Table 3-1). Therefore, the physicochemical properties would have been modified to produce a stronger structure to accommodate acidic separation processes, which satisfies the second reason for surface modification.

Permeabilities of AK and AG membranes were found to be higher than those for SE and SG, despite the higher NaCl rejection of AK and AG (Table 3-1). These results were most probably due to the modifications made on the polyamide selective layer of SE and SG membranes to increase their stability against acidic conditions. Permeability was most likely affected by the decrease in hydrophilic sites, resulting in lower permeabilities as discussed later.

3.3.2. XPS

With an analysis depth of up to 10 nm depending on the electron energy, elemental composition and chemical binding information can be obtained using XPS from survey and high resolution scans, respectively.

3.3.2.1. Survey scans

The C, O and N concentrations of AK and SG membranes were determined using survey scans and the results are presented in Table 3-3.

Different PA membrane structures involving m-PDA and piperazine as amine monomers undergoing an interfacial reaction with TMC were presented in Fig. 3-1 where the variables m and n represent cross-linked and linear structures, respectively. The fully cross-linked structure implies that each carboxyl group of TMC is bonded to an amine monomer forming an amide linkage, thus three oxygen atoms correspond to three nitrogen atoms. However, the fully linear structure leaves one carboxyl group without bonding to an amine monomer forming a carboxylic acid. This structure has two nitrogen atoms corresponding to four oxygen atoms. Therefore, the fully linear structure theoretically has O/N ratio of 2 whereas the fully cross-linked structure has O/N of 1. This fact is only valid when there is no additional coating layer on top of the PA layer. The total number of theoretical oxygen and nitrogen atoms corresponding to different O/N ratios was calculated according to their existence in the cross-linked (m) and linear (n) portions of the polymer using Eq. (3-2).

$$\frac{O}{N} = \frac{(3m + 4n)}{(3m + 2n)} \qquad (3-2)$$

For the O/N ratio of 1.5, the C/O and C/N ratios were found to be lower than those obtained experimentally for the AK membrane (Table 3-4). Since many different reagents could have been utilized during the polymerization reaction, it is not possible to predict the exact nature of the reaction. However, this result showed that membrane hydrophobicity could also be related to the presence of additional alkyl groups other than the effect of intermolecular hydrogen bonds. Two different possibilities were taken into account during chemical structure analysis due to the potential presence of additional alkyl groups: 1) A different type of amine monomer (such as methyl substituted) other than m-PDA or together with m-PDA could be undergoing the polymerization reaction to produce the relatively hydrophobic surface, and 2) Other additives involving alkyl groups could have been used to increase the hydrophobicity of m-PDA and TMC based PA structure.

Table 3-3. Elemental composition of AK and SG membranes *

	C (%)	O (%)	N (%)	C/O	C/N	O/N
AK	73.39 ± 0.5	15.95 ± 0.5	10.66 ± 0.6	4.60	6.88	1.50
SG	74.82 ± 0.8	16.75 ± 0.4	8.43 ± 0.2	4.47	8.88	1.99

* Mean ± standard deviation based on 3 determinations

Table 3-4. Theoretical elemental composition and their ratios corresponding to different O/N ratios in comparison to experimental values obtained for the AK membrane

O/N	C (%)	O (%)	N (%)	C/O	C/N
1	71.4	14.3	14.3	4.99	4.99
1.5	71.4	17.1	11.4	4.18	6.26
1.5*	**73.39 ± 0.5**	**15.95 ± 0.5**	**10.66 ± 0.6**	**4.60**	**6.88**
2	71.4	19.0	9.5	3.76	7.52

* Mean ± standard deviation based on 3 determinations

To assess the first possibility, Table 3-5 shows the theoretical elemental ratios corresponding to potential methyl addition on the benzene rings of AK membrane. m-PDA monomer having methyl group substitutions on the benzene ring would provide a close configuration to the experimental results. It also should be noted that it is not always possible to reach the exact elemental concentrations even if the suggested chemical structure were similar to the original. The potential existence of methyl group substitution is further discussed with the FTIR results below. The presence of an additional amine monomer, preferably a linear alkyl diamine, could also explain the excess carbon in the structure and the high hydrophobicity but the manufacturer reported those types separately as "composite PA membranes," which was not the case with AK and AG (Table 3-1). Furthermore, the use of an additive containing alkyl groups could also be plausible to tune the surface hydrophobicity. It was previously shown that even the use of very low concentrations of additives resulted in more compact

structures partially covering the top surface [18]. As discussed later with FE-SEM results, this was not consistent with the open surface structure and cross section FE-SEM images of AK exhibiting no coating layer on top. Therefore, the possibility of the use of additives as coating was ruled out.

Table 3-5. Elemental composition and ratios as affected by possible methyl substitution for the AK membrane

Methyl substitution	C (%)	O (%)	N (%)	C/O	C/N
0	71.4	17.1	11.4	4.18	6.26
1	72.7	16.4	10.9	4.44	6.67
2	73.9	15.65	10.43	4.72	7.09
Experimental*	**73.39 ± 0.5**	**15.95 ± 0.5**	**10.66 ± 0.6**	**4.60**	**6.88**

* Mean ± standard deviation based on 3 determinations

SG membrane showed an O/N ratio of 2 (Table 3-3), which was assigned to fully linear PA structures with no esterification occurring during interfacial polymerization (Fig. 3-1b). One of the important commercial applications of piperazine monomer is its cross-linking with polyvinyl alcohol (PVA) during interfacial polymerization where the aqueous solution contains both the PVA polymer and piperazine [19]. Thus, a high O/N ratio was probably the result of cross-linking achieved between OH groups of PVA and carboxyl groups of the PA structure, which provided one additional oxygen atom for each cross-linking as exhibited in the suggested structure depicted in Fig. 3-2. In the fully linear structure, a high O/N ratio was due to the oxygen atoms related to the uncross-linked carboxylic acid. High amount of carbon content in the experimental results were probably due to the alkyl groups of PVA cross-linking the amine monomers. Theoretical C/O and C/N ratios regarding the fully linear piperazine structure, the suggested composite membrane structure as depicted in Fig. 3-2 and the experimental results were presented in Table 3-6.

Table 3-6. Elemental composition and their ratios as affected by esterification for SG

	C (%)	O (%)	N (%)	C/O	C/N	O/N
Theoretical [s]	72.72	18.18	9.09	4.00	8.00	2.00
Theoretical [l]	68.42	21.05	10.52	3.25	6.5	2.00
Experimental*	**74.82 ± 0.8**	**16.75 ± 0.4**	**8.43 ± 0.2**	**4.47**	**8.88**	**1.99**

s: suggested

l: fully linear

* Mean ± standard deviation based on 3 determinations

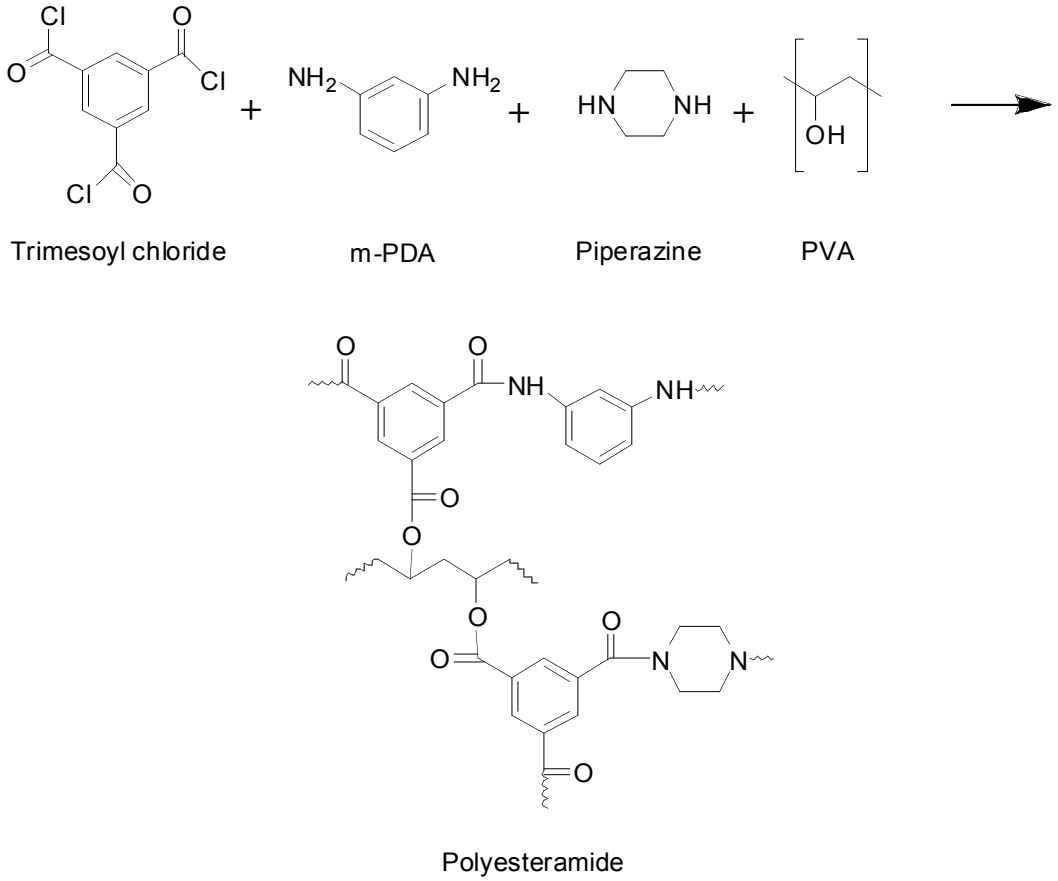

Figure 3-2. Suggested reaction route and chemistry of SG membrane.

In the case of AK and AG membranes, the degree of cross-linking was theoretically calculated using the data from the XPS survey scans of both membranes. Depending on the existence of the cross-linked (m) and linear (n) structures, the degree of cross-linking was calculated as:

$$(\%)\ cross-linking = \frac{m}{(m+n)} x100 \qquad (3-3)$$

To match the experimentally determined O/N of 1.5, the percentage of cross-linking of AK should be 40%, which means that 3 out of every 5 carboxyl groups remained free without participating in an amide bond for cross-linking. On the other hand, the O/N ratio for AG membrane was 1.22, corresponding to 70% of cross-linking. Decreasing the O/N ratio resulted in a tighter network for the AG membrane. Higher degree of cross-linking increased the rejection rate from 97.1% for AK to 98.3% for AG as shown in Table 3-1. The properties, including cross-linking, were reported to change mainly due to the relative solubility and diffusivity of m-PDA monomer in the solvents used during polymerization [4]. Altering the reaction conditions, such as monomer concentration, temperature or curing time in order to increase the diffusivity of m-PDA while decreasing its solubility could be suggested as the modification made to produce the tighter AG membrane.

Since carboxyl and N-H groups were one of the main reasons for the high hydrophilicity of the PA membranes, AK was expected to have much lower contact angle results compared to AG due to the excess amount of free carboxyl groups accommodated in its structure; however, this was not the case (Table 3-2). Contact angle results indicated that intermolecular hydrogen bonds formed between carbonyl groups and hydrogen of amide and carboxyl groups decreased the interaction between the polymer network and water.

When SG and SE were compared, XPS survey scans exhibited that SE membrane had C/N and O/N of 7.83 and 1.59, respectively. Increased amount of

nitrogen relative to carbon in comparison to that of SG indicated that the amine monomer amount was relatively increased in the thin layer.

3.3.2.2. High resolution scans

XPS spectra of C(1s) was deconvoluted to investigate the corresponding binding energies of carbon atoms in the polyamide structure. The spectra of both membranes were composed of one major (weak electron withdrawing environment) and one minor peak (strong electron withdrawing environment) centered at 285 and 288.3, respectively (Figs. 3-3 and 3-4). The major and minor peaks were formed by the corresponding deconvoluted peaks (Dc).

The major peaks of AK and SG membranes included two peaks underneath (Dc1 and Dc2). The first peak (Dc1) was at 285 and assigned to C-C and C-H of aliphatic and aromatic bonds [13]. The second one (Dc2) was associated with carbons in a relatively higher electron withdrawing environment (C-O and C-N). The minor peak of AK membrane represented the carbonyl groups (Dc3) of carboxylic acid and amides. The binding energy shift between the major and minor peaks was 3.3 eV for the AK membrane, which was consistent with the fully aromatic PA [11]. Two peaks were deconvoluted under the minor peak of carbons at strong electron withdrawing environment for the SG membrane. The first peak (Dc3) was assigned to carbonyl groups, similar to the AK membrane. The second peak (Dc4) could be assigned to the higher electron withdrawing environment caused by esters. The electron binding shift between the major and minor peaks was similarly found to be 3.3 eV for SG. Since SG was mostly a piperazine-based PA membrane, the binding shift was expected to be smaller due to less electron sharing by the piperazine monomer as suggested by Tang *et al*. [11]. The reason behind the similar binding energy shifts could be explained as follows: 1) SG could be a mixture of piperazine and m-PDA as suggested in Fig. 3-2, which involved diamine benzene ring with more electron drawing environment, and 2) SG had ester groups due to esterification with PVA, resulting in a relatively stronger electron withdrawing environment than AK.

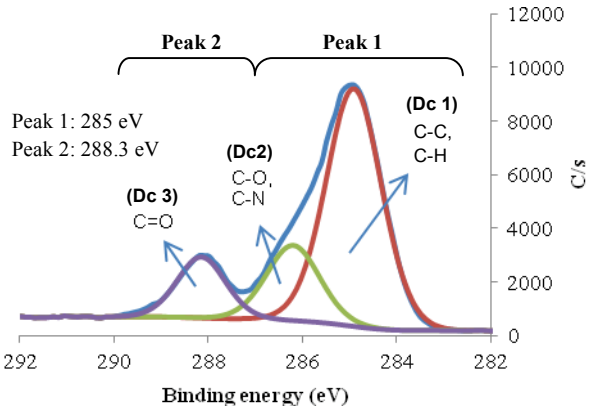

Figure 3-3. High-resolution XPS spectra for AK membrane (C1s).

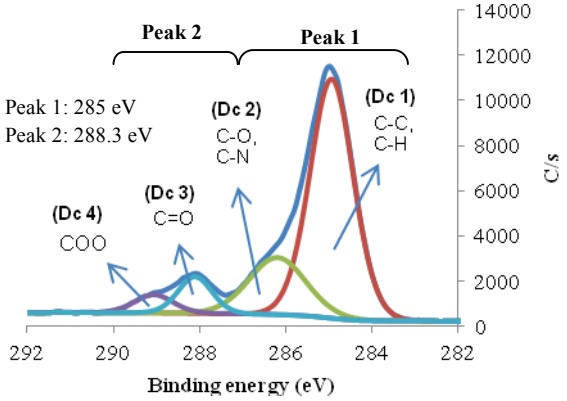

Figure 3-4. High-resolution XPS spectra for SG membrane (C1s).

3.3.3. ATR-FTIR

ATR-FTIR spectra were presented in two ranges. The first range covered wave numbers between 800-1800 cm^{-1} where relatively deep penetration depths (>300 nm) were reached. The peaks assigned to the polysulfone sublayer and the polyamide layer could be both identified in this region. The fingerprint region between 1500-1800 cm^{-1} involved carbonyl groups and amide bands where the polyamide thin film membranes presented their own characteristic peaks. The

second range evaluated was between 2700-3700 cm^{-1}, which focused on the chemical characteristics of the top layer (<200 nm).

3.3.3.1. Range 1 (800-1800 cm^{-1})

Recently, Tang *et al.* [11] presented a detailed characterization of RO membranes using FTIR spectra, including the SG membrane. The peaks in the region of 800-1500 cm^{-1} were reported to be at similar wave numbers for the commercial RO and NF membranes made of PA thin films on top of polysulfone sublayers. AK and SG membranes also fall into this category. In this study, some additional peaks were detected at ~1040 cm^{-1} for both membranes when the membranes were analyzed as received but they all disappeared after the membranes were washed with water. This indicated the existence of a trace amount of contaminants left from the manufacturing process (Fig. 3-5).

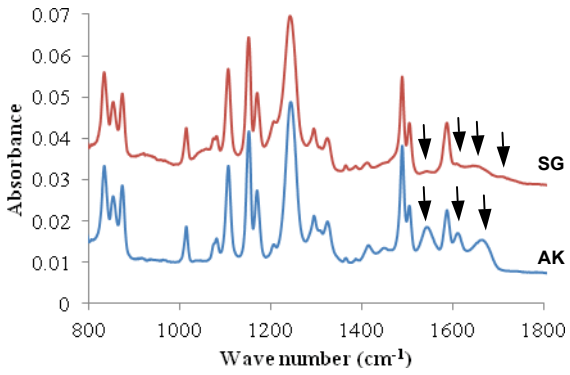

Figure 3-5. Spectra of AK and SG membranes in the range of 800-1800 cm^{-1}

The main difference between these membranes appeared to be in the fingerprint region (1500-1800 cm^{-1}). AK membrane exhibited peaks at 1541, 1609 and 1663 cm^{-1} assigned to amide 2 band, aromatic amide and amide 1 band, respectively [11]. The spectra presented the characteristics of fully aromatic polyamide membranes formed by the interfacial reaction of an aromatic amine monomer, m-PDA, and TMC, which was consistent with the FE-SEM and AFM images presented later. SG membrane had weaker peaks at 1541 cm^{-1} and 1609

cm^{-1} due to the weak N-H vibrations. In addition, unlike the peaks of piperazine-based PA membranes, due to C=O stretching at 1630 cm^{-1}, this peak was shifted to 1653 cm^{-1} for SG [11]. These findings indicated that a small amount of m-PDA was blended with piperazine during the polymerization reaction. SG membrane spectra also had a peak at 1730 cm^{-1}, which was assignable to C=O stretching observed in esters. This peak confirmed the possibility of esterification reaction, which occurred in the existence of PVA during interfacial polymerization. Esterification between the OH groups of carboxyl moiety and PVA, resulted in a highly hydrophobic surface structure, which was consistent with the contact angle measurements.

3.3.3.2. Range 2 (2700-3700 cm^{-1})

SG membrane exhibited a large prominent peak centered at 3405 cm^{-1} (Fig. 3-6), which was normally observed at 3330 cm^{-1} and 3440 cm^{-1} for m-PDA and piperazine-based membranes, respectively, as reported by Tang *et al*. [11]. This was another indication of the peak shift due to the additional N-H functional groups of m-PDA.

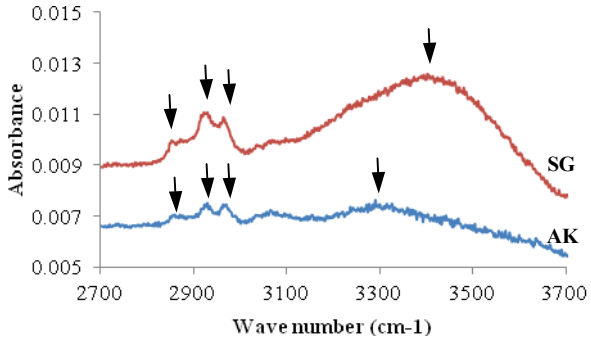

Figure 3-6. FTIR spectra of AK and SG membranes in the range of 2700-3700 cm^{-1}

The peaks between 2850-3000 cm^{-1} were assignable to C-H stretching. The wide and intense peaks in this region were associated with the alkyl groups of PVA underneath the PA layer. The PA layer acted as a coating on top as seen in

the FE-SEM images presented later. The peaks associated with aromatic C-H stretching at 3000-3100 cm^{-1} were hidden by the prominent peaks assigned to the OH group of PVA layer. A metal tool was used to gently scratch the surface in two steps to investigate the structure underneath the PA layer. Fig. 3-7 shows the spectra associated with the scratched surfaces of both membranes. The intensity of the peaks increased with each scratching step for the SG membrane. These results were consistent with the FE-SEM images exhibiting gradually expanding sponge-like structure as shown later. This structure was mainly due to the decrease of cross-linking density in highly PVA concentrated region at high penetration depths.

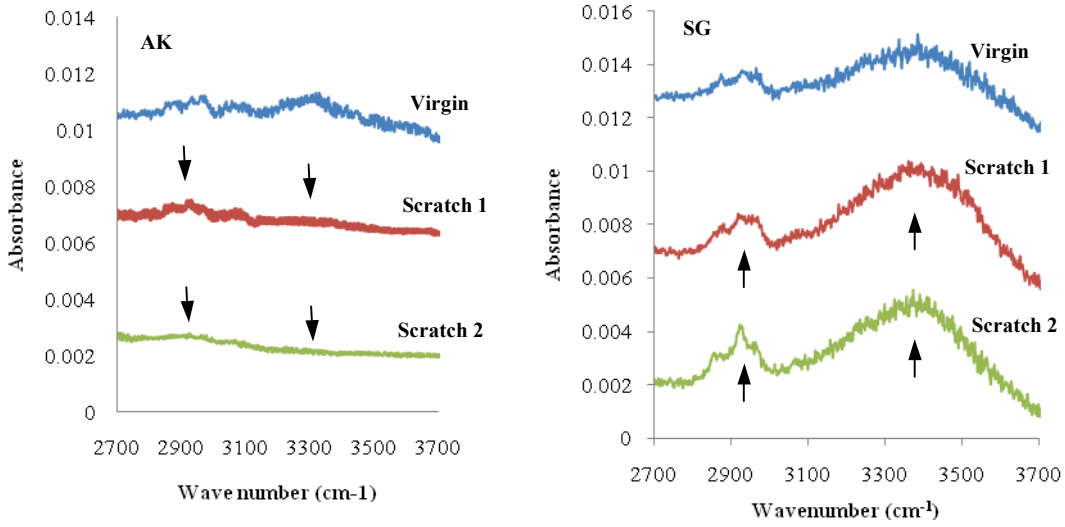

Figure 3-7. FTIR spectra in the range of 2700-3700 cm^{-1} for (a) AK and (b) SG membranes scratched on the top surface in two steps (Direction of arrows represent the change at the corresponding wave number).

On the other hand, the scratched surface of the AK membrane represented the polysulfone sublayer spectra [20]. This showed that the peaks between 2700-3700 cm^{-1} mostly belonged to the PA top layer unlike SG. The peaks of AK membrane spectra in the range of 2900-3000 cm^{-1} and 3000-3100 cm^{-1} were

assigned to aliphatic CH stretching and aromatic CH stretching, respectively [16]. C/O and O/N ratios obtained from XPS analysis generated a possibility that the reason behind the hydrophobicity of this membrane could be due to methyl substitution on m-PDA. Similarly, it was reported that methyl substitution on the benzene ring increased the hydrophobicity of m-PDA-based PA membranes. However, the substitution of methyl groups on the amino groups of benzene would not be feasible since that would correspond to a lack of N-H vibrations at 1541 and 1609 cm^{-1} due to CH_3 bonds, resulting in a tertiary amide configuration and that is not the case here (Fig. 3-5). Another alternative approach to increase C content via methyl substitution would be accommodating the methyl groups around the benzene ring. This was not likely since there would be a peak at 1370 cm^{-1} due to CH deformation vibration of CH_3 group bonded to an amide group [21]. These findings confirmed that the AK membrane was produced by the polymerization reaction of TMC and m-PDA.

When SG and SE were compared, FTIR spectra of SG and SE membranes exhibited peaks at different wave numbers at 3405 cm^{-1} and 3367 cm^{-1}, respectively (Fig. 3-8). This major peak shifted to a lower wave number for the SE membrane, indicating the possible use of higher concentration of m-PDA monomer, which tops at 3330 cm^{-1} when existed alone. The addition of m-PDA during the polymerization of another amine monomer was found to increase the performance by increasing the rejection rate [8]. This was also reflected in the SE membrane since it was reported to be tighter with higher salt rejection compared to the SG membrane (Table 3-1).

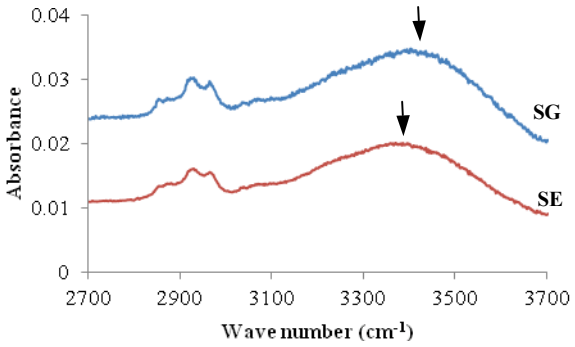

Figure 3-8. ATR-FTIR spectra of SE and SG membranes in the range of 2700-3700 cm^{-1}

3.3.4. FE-SEM

FE-SEM was employed to investigate both the top surface and cross-section morphologies of the membranes with its sharp imaging capabilities compared to conventional SEM (Fig. 3-9). Cross-section images were taken to demonstrate the possibility of having a coating layer on top as well as the morphology of the thin film and polysulfone support layers of the composite membranes. Cross-section images (Fig. 3-9a and d), which focused on the polysulfone layer, showed similar results for both membranes having a film of approximately 60 μm thickness sitting on a non-woven fabric.

Images representing the cross-section of the top layer (Fig. 3-9b and e) showed different morphologies for each membrane. AK membrane had a thicker and more rough top layer of about 200-300 nm while the SG membrane's top layer was relatively thinner at about 100-150 nm laying on polysulfone support. In fact, the top layer of SG membrane consisted of two thin layers. Both layers seemed to have similar structures, but the color of the top layer was relatively lighter than the bottom and their thickness was ~50 nm and ~70 nm, respectively. Overall, the SG membrane was light brown in color whereas the AK was white.

The macrovoid structure of the polysulfone sublayer of the AK membrane appeared to begin right underneath the thin top layer where the interfacial reaction

probably occurred. However, in the case of SG membrane, the macrovoid structure was relatively tighter underneath the top layer, resulting in a gradually expanding sponge-like structure. This structure was the continuation of the smooth darker region right underneath the lighter and thinner layer, which gradually increased with depth under the dense thin layer. SG membrane was classified as a thin film composite membrane by the manufacturer (Table 3-1) most probably due to the presence of additives other than amidic components. Gradually expanding sponge-like structure has been previously associated with the presence of polymer additives in the polyamide-based membranes [20]. In general, during the polymerization reaction with TMC, PVA cannot easily diffuse into the interfacial layer. As a result, piperazine monomer deposits on the top surface forming a very thin polyesteramide layer above the cross-linked PVA [19]. However, it seems like the biselective layer of the SG membrane evaluated in this study included a small amount of m-PDA monomer as well as piperazine as discussed with the FTIR results above during the formation of the polyesteramide layer on top, which was thinner and lighter in color. Relatively darker smooth part represented the dense, cross-linked PVA with gradually expanding macrovoid structure on top of the polysulfone support.

This hyphothesis, which was developed based on the microscopy analysis and an extensive literature review was consistent with the chemical structure analysis by XPS and ATR-FTIR as discussed above.

Images of the top surfaces of the membranes showed a substantial difference (Fig. 3-9c and f). AK and SG membrane surfaces exhibited structures consisting of a network of polymer strands and packed globules, respectively. These features were consistent with the cross-linked polyamide structure formed with TMC during interfacial reaction. On the other hand, acyl chlorides with only two COCl groups were reported to form linear polyamides resulting in different globular structures. Such morphological differences were clearly identified with FE-SEM images in a previous report [22]. AK membrane had a relatively open

surface and a tighter network at higher penetration depths, which made it possible to see a couple hundred nanometres of depth through the surface. This structure was characteristic of the open and rough surface structure of m-PDA-based PA membranes interfacially polymerized by TMC [3, 4, 22].

3.3.5. AFM

The atomic force microscopy was a useful technique to analyze the surface morphology of AK and SG membranes. Surface properties of thin film PA membranes formed by different monomer types were reported previously [10, 22] and it was shown that the different morphological properties of the RO membranes are mainly the result of reactions involving different monomer types, having different configurations (ortho-, meta-, or para-).

AK membrane showed a higher level of roughness compared to SG (Fig. 3-10). In general, the reason for that was the longer inter-chain distance for the meta-oriented amine monomer, m-PDA, which resulted in the lack of hydrogen bonding and formation of polymer strands with high roughness on the top surface compared to piperazine-based PA membranes [22]. These results were consistent with those of Tang *et al*. [10], who also demonstrated that m-PDA-based membranes showed higher roughness compared to piperazine-based membranes. Relatively much lower roughness of AK compared to other m-PDA based membranes listed by Tang *et al*. [10] could be the closer inter-chain distance provided by a high packing density due to the excess of intermolecular hydrogen bonds.

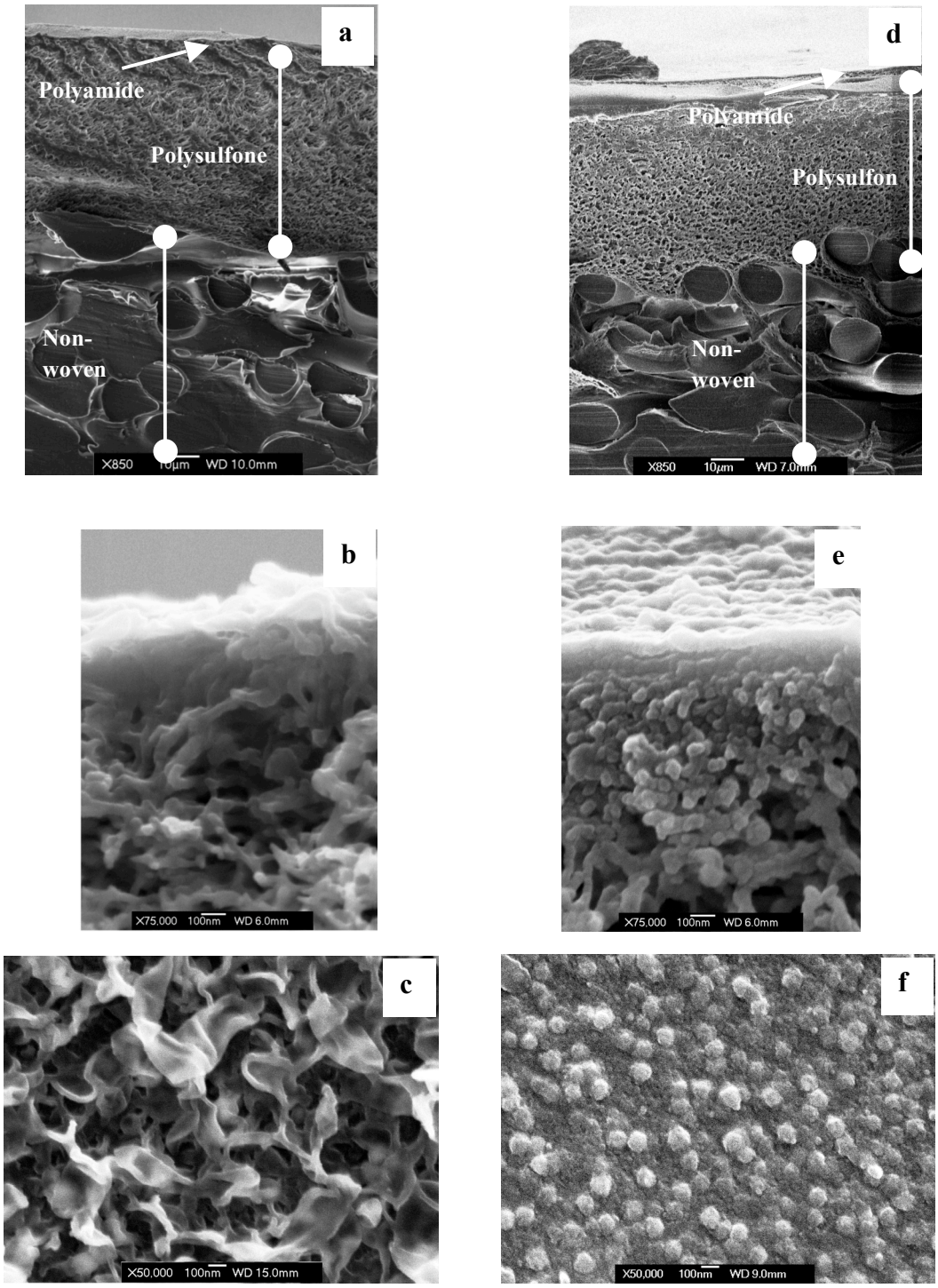

Figure 3-9 FE-SEM images of AK membranes (a) whole cross section (x850 magnification), (b) top cross section (x75,000 magnification), (c) top surface (x50,000 magnification) and SG membranes; (d) whole cross section (x850

magnification), (e) top cross section (x75,000 magnification), (f) top surface (x50,000 magnification).

Although there is no correlation known between hydrophilicity and surface roughness, one of the reasons for relatively high hydrophobicity of the structure of AK could be the strong self interactions by hydrogen bonding among the polymer molecules reducing the availability of hydrophilic functional groups to interact with water molecules [23]. Needless to say, additional evidence is needed to relate the surface hydrophobicity to roughness.

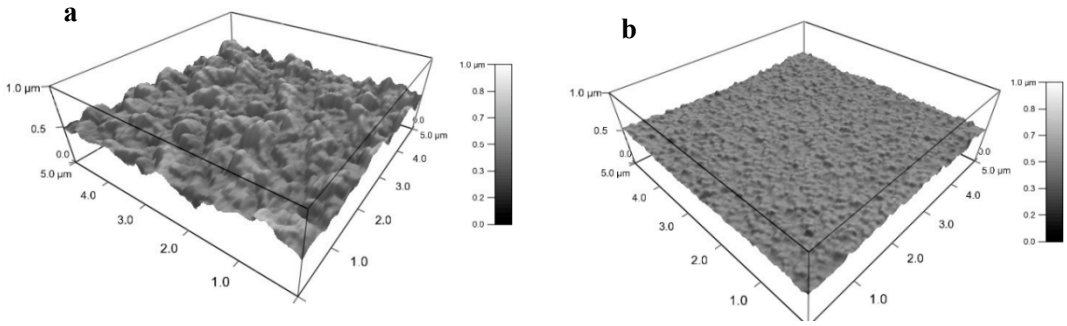

Figure 3-10. Atomic force microscopy images of (a) AK (roughness 54.2 nm) and (b) SG (roughness 15.3 nm) membranes.

3.4. Conclusions

Advanced analysis techniques were used to characterize four commercial hydrophobic polyamide membranes. Since the reaction media may include many additives and reagents, it is almost impossible to fully estimate the exact physicochemical structure of the commercial membranes investigated. However, the analysis results suggest that the surface properties and physicochemical structure of AK and AG membranes exhibited the characteristic properties of

polyamide membranes formed via interfacial polymerization of m-PDA and TMC monomers. Tighter structure of AG membrane was due to higher cross-linking of its structure. For the SG and SE membranes, piperazine and m-PDA blend was probably used as amine monomers, which underwent esterification with PVA during thin film formation. PVA would contribute to polyesteramide formation resulting in the strongly cross-linked structures in the selective layer. PVA polymer underneath the polyesteramide layer would provide extra physical support together with retention. SE membrane had a higher rejection rate probably due to the higher content of amine monomers used during polymerization, most likely m-PDA concentration being increased relatively more than piperazine.

The relatively hydrophobic nature of AK and AG membranes could be due to high intermolecular hydrogen bonds as a result of close chain distances. Since hydrogen bonds also contribute to the mechanical rigidity of the structure, it is promising to produce the membrane with high packing density and high rejection rates. SE and SG membranes were lacking most of the amide hydrogen and carboxyl groups due to the probable use of piperazine as one of the monomers and esterification reaction taking place during their fabrication. Although hydrophobic structure of both membranes compromises flux during aqueous separations, it provides new opportunities for the use of other classes of solvents such as supercritical CO_2.

3.5. References

[1] R.J. Petersen, Composite reverse osmosis and nanofiltration membranes, Journal of Membrane Science, 83 (1993) 81-150.

[2] M. Liu, S. Yu, J. Tao, C. Gao, Preparation, structure characteristics and separation properties of thin-film composite polyamide-urethane seawater reverse osmosis membrane, Journal of Membrane Science, 325 (2008) 947-956.

[3] Y. Jin, Z. Su, Effects of polymerization conditions on hydrophilic groups in aromatic polyamide thin films, Journal of Membrane Science, 330 (2009) 175-179.

[4] A.K. Ghosh, B.-H. Jeong, X. Huang, E.M.V. Hoek, Impacts of reaction and curing conditions on polyamide composite reverse osmosis membrane properties, Journal of Membrane Science, 311 (2008) 34-45.

[5] L. Li, S. Zhang, X. Zhang, G. Zheng, Polyamide thin film composite membranes prepared from isomeric biphenyl tetraacyl chloride and m-phenylenediamine, Journal of Membrane Science, 315 (2008) 20-27.

[6] L. Li, S. Zhang, X. Zhang, G. Zheng, Polyamide thin film composite membranes prepared from 3,4',5-biphenyl triacyl chloride, 3,3',5,5'-biphenyl tetraacyl chloride and m-phenylenediamine, Journal of Membrane Science, 289 (2007) 258-267.

[7] N.K. Saha, S.V. Joshi, Performance evaluation of thin film composite polyamide nanofiltration membrane with variation in monomer type, Journal of Membrane Science, 342 (2009) 60-69.

[8] C.K. Kim, J.H. Kim, I.J. Roh, J.J. Kim, The changes of membrane performance with polyamide molecular structure in the reverse osmosis process, Journal of Membrane Science, 165 (2000) 189-199.

[9] J.H. Kim, E.J. Moon, C.K. Kim, Composite membranes prepared from poly(m-animostyrene-co-vinyl alcohol) copolymers for the reverse osmosis process, Journal of Membrane Science, 216 (2003) 107-120.

[10] C.Y. Tang, Y.-N. Kwon, J.O. Leckie, Effect of membrane chemistry and coating layer on physiochemical properties of thin film composite polyamide RO and NF membranes: II. Membrane physiochemical properties and their dependence on polyamide and coating layers, Desalination, 242 (2009) 168-182.

[11] C.Y. Tang, Y.-N. Kwon, J.O. Leckie, Effect of membrane chemistry and coating layer on physiochemical properties of thin film composite polyamide RO and NF membranes: I. FTIR and XPS characterization of polyamide and coating layer chemistry, Desalination, 242 (2009) 149-167.

[12] C.Y. Tang, Y.-N. Kwon, J.O. Leckie, Probing the nano- and micro-scales of reverse osmosis membranes--A comprehensive characterization of physiochemical properties of uncoated and coated membranes by XPS, TEM, ATR-FTIR, and streaming potential measurements, Journal of Membrane Science, 287 (2007) 146-156.

[13] K. Boussu, J. De Baerdemaeker, C. Dauwe, M. Weber, K.G. Lynn, D. Depla, S. Aldea, I.F.J. Vankelecom, C. Vandecasteele, B. Van der Bruggen, Physico-Chemical Characterization of Nanofiltration Membranes, ChemPhysChem, 8 (2007) 370-379.

[14] A. Cañas, M.J. Ariza, J. Benavente, Characterization of active and porous sublayers of a composite reverse osmosis membrane by impedance spectroscopy, streaming and membrane potentials, salt diffusion and X-ray photoelectron spectroscopy measurements, Journal of Membrane Science, 183 (2001) 135-146.

[15] J. Geens, B. Van der Bruggen, C. Vandecasteele, Characterisation of the solvent stability of polymeric nanofiltration membranes by measurement of contact angles and swelling, Chemical Engineering Science, 59 (2004) 1161-1164.

[16] W. Lee, C.H. Ahn, S. Hong, S. Kim, S. Lee, Y. Baek, J. Yoon, Evaluation of surface properties of reverse osmosis membranes on the initial biofouling stages under no filtration condition, Journal of Membrane Science, 351 (2010) 112-122.

[17] R. Sheikholeslami, J. Bright, Silica and metals removal by pretreatment to prevent fouling of reverse osmosis membranes, Desalination, 143 (2002) 255-267.

[18] D. Wu, X. Liu, S. Yu, M. Liu, C. Gao, Modification of aromatic polyamide thin-film composite reverse osmosis membranes by surface coating of thermo-responsive copolymers P(NIPAM-co-Am). I: Preparation and characterization, Journal of Membrane Science, 352 (2010) 76-85.

[19] A.I. Schafer, A.G. Fane, T.D. Waite, Nanofiltration: Principles and Aplications, in, Elsevier Advanced Technology, Oxford, 2005.

[20] A.K. Ghosh, E.M.V. Hoek, Impacts of support membrane structure and chemistry on polyamide-polysulfone interfacial composite membranes, Journal of Membrane Science, 336 (2009) 140-148.

[21] T. Shintani, A. Shimazu, S. Yahagi, H. Matsuyama, Characterization of methyl-substituted polyamides used for reverse osmosis membranes by positron annihilation lifetime spectroscopy and MD simulation, Journal of Applied Polymer Science, 113 (2009) 1757-1762.

[22] S.Y. Kwak, S.G. Jung, Y.S. Yoon, D.W. Ihm, Details of surface features in aromatic polyamide reverse osmosis membranes characterized by scanning electron and atomic force microscopy, Journal of Polymer Science Part B: Polymer Physics, 37 (1999) 1429-1440.

[23] S. Sourirajan, Polyamide membranes, in: Reverse Osmosis and Synthetic Membranes, National Research Council Canada, Ottawa, 1977.

4. Effect of supercritical CO_2 flux, temperature and processing time on physicochemical and morphological properties of commercial reverse osmosis membranes[1]

4.1. Introduction

Gas separation with polymer membranes is a well known technology and broadly used in chemical industries in various applications. Among many separation/purification processes with membranes, CO_2/CH_4 gas separation has been one of the most common applications. During this process, gaseous feed stream can reach pressures of up to 60 bar [1]. Such operating conditions have led to the fabrication of different modified polymer membranes to be able to maintain the membrane performance (selectivity, permeability) throughout processing. The main motivation behind the intense research on membrane properties has been the strong interaction of CO_2 with polymer materials as discussed in Chapter 2 (Section 2.3.2) at high pressures and better understanding of such interactions would improve membrane performance.

The operating conditions of the supercritical carbon dioxide (SC-CO_2) extraction-membrane separation coupled process could be much higher than 70 bar where CO_2 is in the supercritical state (>73.8 bar). Despite the existing research focused on high pressure CO_2 gas separations, the use of much higher CO_2 pressures at supercritical conditions would require more research to understand the changes at higher pressures due to plasticization of the polymer membranes in an effort to maintain the membrane efficiency and to develop optimal coupled processes.

[1] A version of this chapter has been accepted for publication. Akin and Temelli 2011. The Journal of Supercritical Fluids. in press, doi:10.1016/j.supflu.2011.03.011

Most of the polymer membranes used with the current investigations under SC-CO_2 conditions has been commercial thin film polyamide reverse osmosis (RO) membranes produced by interfacial polymerization. In order to assess the effect of CO_2 on polymer membranes, the physicochemical properties of the membrane and plasticization phenomena should be well understood [2-6].

Although previous studies have demonstrated that the coupled SC-CO_2 extraction and membrane separation process looks promising, studies on the effect of SC-CO_2 on the membranes have been scarce. Therefore, the purpose of this study was to investigate the effect of temperature and flux of pure SC-CO_2 at constant pressure over processing times of 0-8 h on the physicohemical and morphological properties of the most commonly used commercial polyamide membranes by using contact angle, attenuated total reflection - Fourier transform infrared spectroscopy (ATR-FTIR) and field emission - scanning electron microscopy (FE-SEM).

4.2. Material and methods

4.2.1. Membranes

Two RO membranes (AK, SG) were kindly provided by GE Osmonics (Minnetonka, MN, USA). The virgin membranes were cleaned according to the protocols described in Chapter 3 (Section 3.2.1). The detailed physicochemical characterization of the membranes was reported in Chapter 2 and the effect of SC-CO_2 processing is investigated in this study considering the suggested structures presented once again in Fig. 4-1 based on the initial characterization. Bone dry CO_2 (99.9% purity) with liquid withdrawal dip tube was from Praxair Canada Inc. (Mississauga, ON, Canada).

4.2.2. SC-CO_2 processing of membranes

The flow diagram of the supercritical system is presented in Fig. 4-2. This system was designed and built in-house, modifying another unit in our laboratory and using certified high pressure parts. Equipment considerations discussed

previously in Chapter 2 (Section 2.3.1) were taken into account with utmost care and testing was performed to ensure reproducible operation of the system. Flat plate membranes were carefully placed in the membrane module (Millipore Corp., Bedford, MA, USA). Membrane module was a dead-end filter module with 9.6 cm^2 active filtration area, which was designed to accommodate one flat plate membrane (47 mm diameter) for each experiment. Initially, valves V-3, V-4, V-6 and V-7 were kept open while the other valves were closed. Then, valve V-1 was opened and the feed pressure was set to 120 bar by using a syringe pump (Model D260, ISCO-Teledyne Inc., Lincoln, NE, USA). Valve V-2 was slowly opened and the system was filled with CO_2 and pressurized slowly (~0.2 bar/sec) to avoid possible compaction in the membrane structure. When the system pressure reached 120 bar, temperature was set using the heaters around the vessel (180 mL) and the membrane module.

Then, valve V-7 was closed to build up the transmembrane pressure by adjusting the back pressure regulator (V-8) (TESCOM 26-1721, Mississauga, ON, Canada). The pressure differential between the upstream and downstream was monitored by two pressure gauges (GE Druck, Leicester, UK). A flow meter (Alicat Scientific, Tucson, AZ, USA) was used to monitor the CO_2 flow under ambient conditions. At the end of the targeted processing time, depressurization of the system was achieved by closing valve V-2, and opening valves V-7 and V-8. Depressurization was performed slowly over 30 min to minimize any damage to the membrane structure.

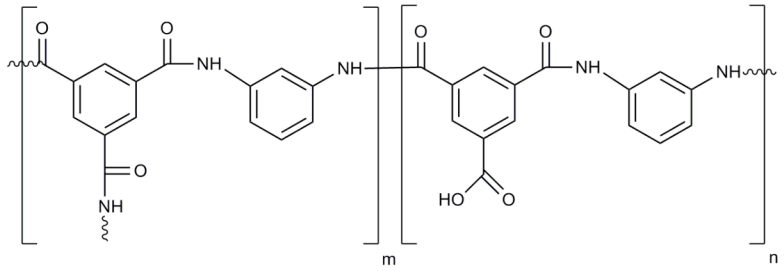

AK - Interfacially formed fully aromatic polyamide

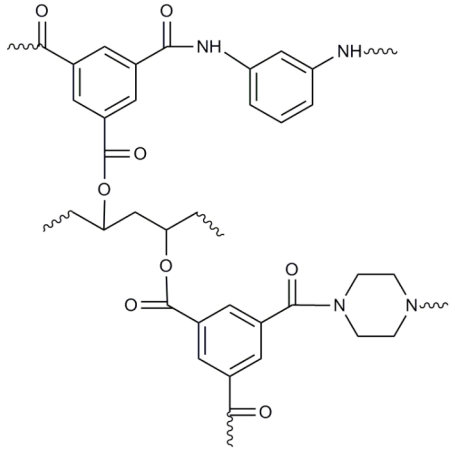

SG - Polyesteramide

Figure 4-1. The suggested chemical structures of AK and SG membranes based on analysis described in Chapter 2.

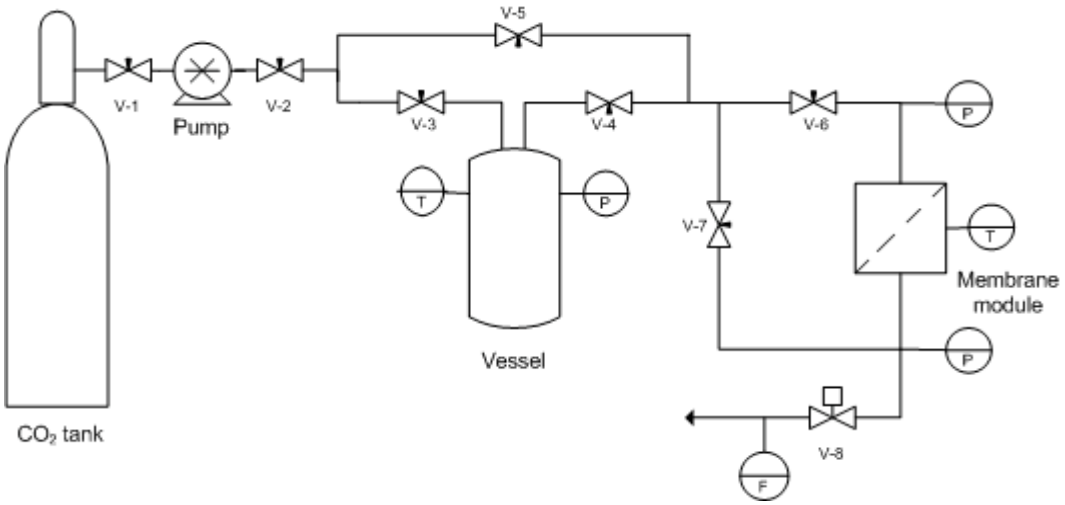

Figure 4-2. Flow diagram of the supercritical CO_2 extraction – membrane separation coupled system (T: thermometer, P: pressure gauge, V: valve, F: flowmeter).

Both AK and SG membranes were processed at different temperature (40 and 80 C°) and flow conditions (50 and 200 kg/m^{2}h) at 120 bar. These conditions were defined as mild (120 bar, 40 °C, 50 kg/m^{2}h), high flux (120 bar, 40 °C, 200 kg/m^{2}h) and high temperature (120 bar, 80 °C, 50 kg/m^{2}h) processing for presentation of results. Increasing the temperature from 40 to 80 ^{o}C had a negligible effect on flux at the constant transmembrane pressure of 6 and 10 bar for SG and AK, respectively. This was because flux is a function of the ratio density/viscosity and both density and viscosity show a substantial drop with such a temperature increase. The membranes were kept under the above processing conditions for 0, 0.5, 2, 4 and 8 h. Then, the system was depressurized (~1 bar/s) and the membranes were removed for analysis. At the pressurization/ depressurization rates employed, no deformation of membrane integrity was observed in the SEM images obtained at low magnification levels. Membrane processing at each condition was performed in duplicate.

4.2.3. Characterization of membranes

4.2.3.1. Contact angle by sessile drop method

Contact angles of the dry membranes were measured using FTA 200 contact angle analyzer (Ten Angstroms, Folio Instruments, Kitchener, ON, Canada) using the sessile drop method as described in Chapter 3 (Section 3.2.2).

4.2.3.2. ATR-FTIR

ATR-FTIR spectra were obtained using a Nicolet 8700 FTIR spectrometer coupled to a germanium crystal operated at 45°C using OMNIC 6.2 software (Thermo Electron Corp., Hampton, NH, USA) as described in Chapter 3 (Section 3.2.5).

4.2.3.3. FE-SEM

FE-SEM images of the cross-section and top layer of AK and SG membranes were taken using JEOL 6301F field emission scanning electron microscope (Tokyo, Japan) with Si diode detector as described in Chapter 3 (Section 3.2.6).

4.3. Results and discussion

4.3.1. Contact angle

The functional groups in the membrane structure, which could potentially be responsible for surface hydrophilicity should be well characterized to be able to explain any potential alteration of surface properties. Chemical structure of the virgin membranes used in this study was studied in detail and reported previously in Chapter 3. The suggested chemical structures of AK and SG membranes are presented again in Fig. 4-1 for ease of discussion here. In the case of uncoated and unmodified surfaces, carboxyl groups and amide N-H groups are the main contributors to the surface hydrophilicity of interfacially formed polyamide reverse osmosis membranes. The position and density of these groups may vary due to polymerization reaction conditions resulting in different contact angles of

the top selective layers. AK membrane was found to be produced by interfacial reaction between an amine monomer, m-phenyl diamine (m-PDA) and trimesoyl chloride (TMC) and exhibited relatively higher contact angle than many other commercial RO membranes produced via the same method [7-9]. Piperazine monomer was used during polymerization of SG membrane while PVA was also found to be involved in this step. As a result, ester bond formation during polymerization with TMC caused a decrease in the number of free carboxyl groups and the presence of piperazine monomer resulted in relatively less N-H bonds in the structure. Consequently, the surface hydrophobicity of the SG membrane was increased due to both of these modifications in the membrane structure.

The change in surface hydrophilicity upon CO_2 exposure with time was shown in Figs. 4-3a and 3b for AK and SG membranes, respectively. SG membrane did not show a substantial change whereas AK membrane exhibited increasing hydrophobicity with processing time. The increase in hydrophobicity was substantial at the end of 8 h for high flux and high temperature processing for AK membrane. The mild processing conditions did not affect surface hydrophilicity at the end of 8 h. Hydrophilicity of SG membrane did not show any change except for high flux processing, when the contact angle showed a drop but the change was not as prominent as that in AK.

a) **b)**

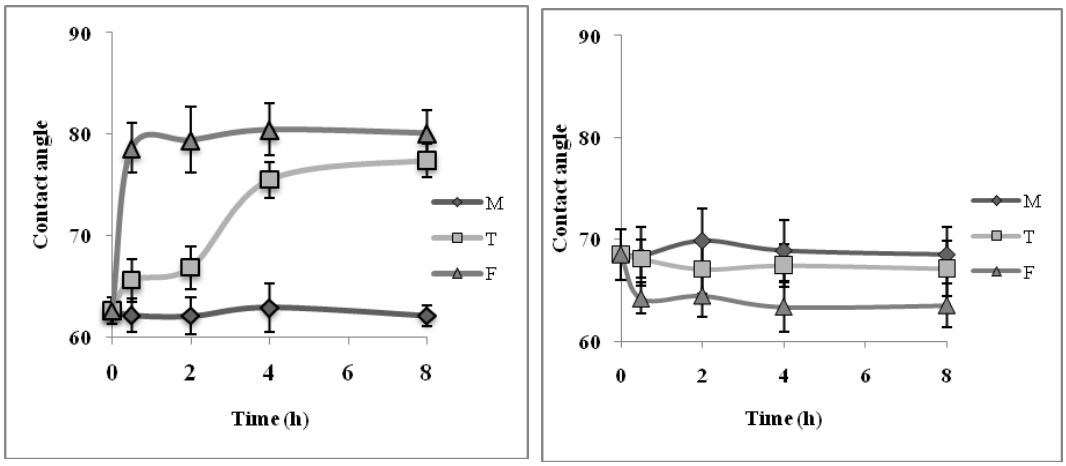

Figure 4-3. Contact angle of membranes processed under different conditions up to 8 h: (a) AK membrane, (b) SG membrane (M: mild, T: high temperature, F: high flux)

In the case of high flux processing, it was hypothesized that the amount of CO_2 passing in between the carboxyl groups of the neighbouring chains was increased. Higher penetration rate of CO_2 molecules would prevent the interaction between carboxyl groups and decrease the cohesive energy density by eliminating intense hydrogen bonding between polymer chains, which in turn would alter the structure of hydrogen-bonded groups. CO_2 interaction with hydrogen at high flux conditions increased the surface hydrophobicity to its maximum after 0.5 h for the AK membrane. It took 4 h for the AK membrane to reach maximum hydrophobicity when it was processed at 80 °C. These results showed that SC-CO_2 processing at higher temperature and higher flux affected the intermolecular hydrogen bonding in favour of CO_2 molecules to interact with the hydrogen of carboxyl and amide groups. The effect of high flux was more immediate compared to that of high temperature due to the alteration of surface hydrophilicity in the first 0.5 h of processing.

The substantial change in surface hydrophobicity of AK membrane with high temperature and high flux processing could be explained with the alteration of hydrogen-bonded groups. High temperature processing would most likely affect the polymer chain structure by increased thermal energy transferred to the network. Additional thermal energy could affect polymer-polymer interactions by loosening the chain restrictions. The mobility of the polymer chains could increase the distance between the intermolecular hydrogen bonding groups, resulting in a decrease in the degree of interaction between polymer chains. Thus, the reduced cohesive energy density would make it more likely for carboxyl and amide groups to be affected by CO_2 molecules.

The interaction of CO_2 with polar groups where the oxygen of CO_2 would interact with hydrogen has been reported previously [10]. Although these interactions were relatively smaller than intermolecular hydrogen bonding in the polymer network, extreme processing conditions were found to be effective in diminishing these forces by accommodating CO_2 to interact with hydrogen of carboxyl and amide groups.

Cross-linking in the SG membrane structure was suggested to be formed via esterification of carboxyl groups with hydroxyl groups of PVA (Fig. 4-1) (Chapter 3). The covalent bonds of such cross-links are much stronger than the hydrogen bonding associated with the AK membrane discussed above. Most of the available nitrogen would form tertiary amides due to the abundance of piperazine monomer over m-PDA during the polymerization reaction. This situation possibly caused a decrease in the extent of hydrogen bonding of N-H contrary to that in the AK membrane. Thus, the change in the surface hydrophilicity of the SG membrane over 8 h of processing was not as prominent as that observed in the AK membrane and was independent of processing conditions. This could be explained by the lack of hydrogen bonding groups in the SG membrane structure.

4.3.2. ATR-FTIR

ATR-FTIR spectra give detailed information about the functional groups present in the top 1-2 µm when equipped with an angled crystal tool. In this study, CO_2 effect related to the top polyamide layer of the membranes was investigated. Fig. 4-4 showed the change in the absorbance for AK and SG membranes processed under mild conditions for 0 and 8 h. This spectra covered the region between 1200 - 1800 cm^{-1}, including both polysulfone and polyamide layers. The decrease in the absorbance after 8 h was most probably due to a decrease in the concentration of the polymer, which may reflect the swelling of the structure [11]. Since it is not always feasible to use FTIR results quantitatively, no correlation could be established between processing time and absorbance. Detailed information on these membranes were given in Chapter 3.

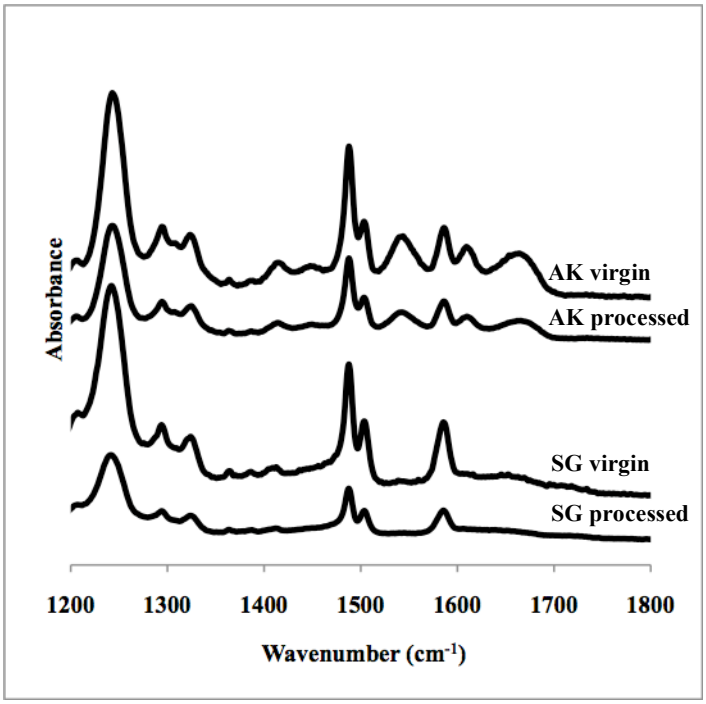

Figure 4-4. Absorbance between 1200 – 1800 cm^{-1} for AK and SG membranes processed under mild conditions for 0 and 8 h.

The interactions of CO_2 with hydrogen-bonded groups and carbonyl groups were investigated in detail by normalizing the spectra to compare the absorbance due to different processing conditions. The spectra were presented in two ranges (Figs. 4-5 and 4-6). The first range of 1500-1800 cm^{-1} (Fig. 4-5) covered the main characteristic functional groups of polyamide thin film membranes and exhibited amide and carbonyl groups between 1520-1625 cm^{-1} (Fig. 4-5a) and 1632-1683 cm^{-1} (Fig. 4-5b), respectively. Amide groups were assigned to amide 2 band whereas carbonyl groups belonged to amide 1 band. The effect of CO_2 processing on these groups was presented after the spectra in this region (1500-1800 cm^{-1}) were normalized relative to aromatic stretching vibration of the polsulphone layer at 1587 cm^{-1} (Fig. 4-5a and b). Because the intensity of the peaks was very low and no change was observed, the spectra of SG membrane were not presented in this region. The second region was between 2800-3600 cm^{-1} (Fig. 4-6), which focused on the chemical characteristics of the very top layer (<200 nm) [12]. The spectra in this region were normalized according to aromatic C-H stretching vibrations at 3000-3100 cm^{-1}.

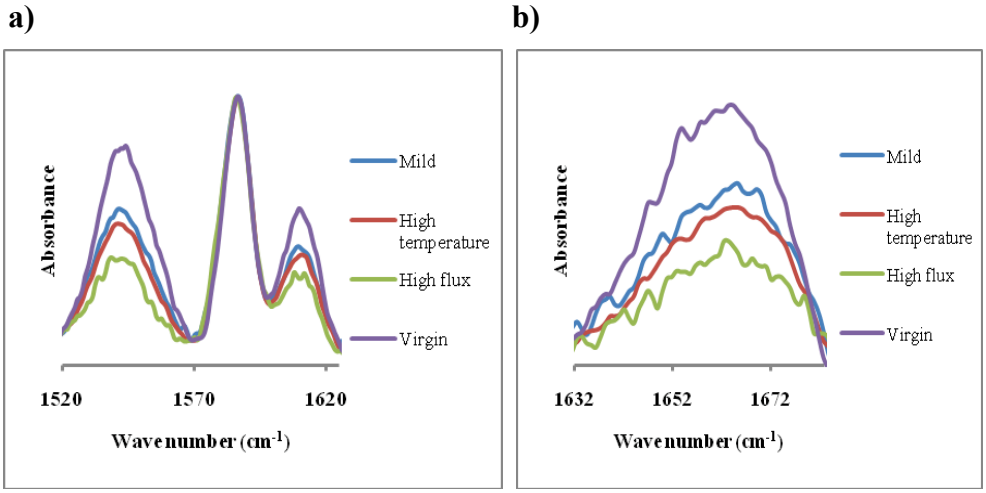

Figure 4-5. The spectra of AK membranes between 1500 – 1800 cm^{-1} normalized relative to aromatic stretching vibration of polsulphone layer at 1587 cm^{-1} for membranes processed at different conditions (a) absorbance between 1520 – 1620 cm^{-1} for the N-H groups (b) absorbance at 1663 cm^{-1} for the carbonyl groups.

Fig. 4-5a depicted the absorbance of the N-H groups for AK membranes processed at different conditions with SC-CO_2. The largest decrease in absorbance was observed with the membranes processed under high flux for 8 h. The membranes processed at high temperature were affected more than the membranes processed under relatively mild conditions but less than the membranes processed under high flux. These results were consistent with the contact angle results where high flux effect was the most prominent after 0.5 h of processing.

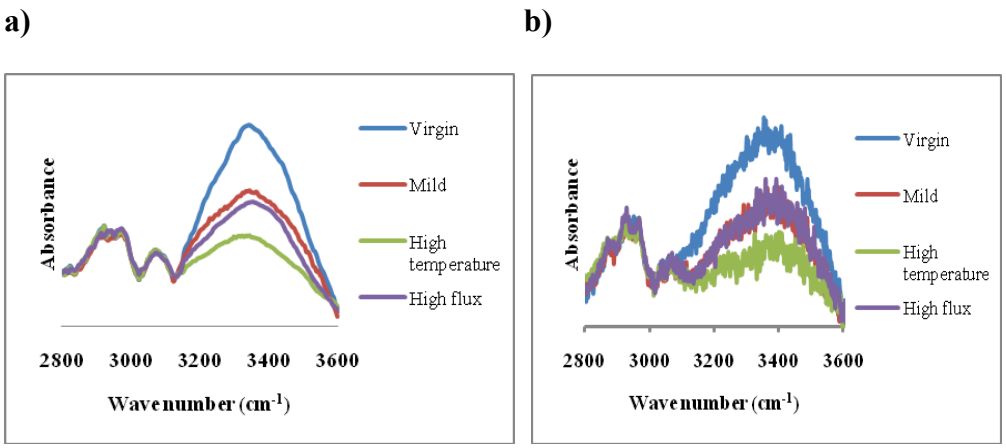

Figure 4-6. Absorbance between 2800 – 3600 cm^{-1} for O-H and N-H groups after processing at different conditions which were normalized according to aromatic C-H stretching vibrations at 3000-3100 cm^{-1} (a) AK and (b) SG membranes.

Carbonyl group interactions with CO_2 have been investigated extensively [3, 13-15]. Koros [14] indicated that the carbonyl groups had the strongest effect on plasticization of the polymer network. CO_2 also has the potential to have hydrogen bonding interactions. Oxygen atoms of CO_2 were reported to form conventional hydrogen bonds [10]. The change in the intensity of the peak associated with the carbonyl groups of AK membrane at 1663 cm^{-1} at different processing conditions was presented in Fig. 4-5b. The results were similar to

those obtained for the N-H groups (Fig. 4-5a) where the greatest effect was observed with the membranes processed under high flux.

The second region involved the peaks associated with O-H functional groups in addition to N-H groups. AK and SG exhibited large peaks centered at 3330 cm^{-1} (Fig. 4-6a) and 3405 cm^{-1} (Fig. 4-6b), respectively. The peaks were due to N-H and O-H stretching vibrations. These peaks were more prominent for the SG membrane compared to AK. Based on previous detailed analysis of the virgin membranes, it was suggested that the peak at 3405 cm^{-1} mostly belonged to the O-H groups of PVA used during polymerization reaction of SG membrane whereas the same peak centered at 3330 cm^{-1} for AK membrane belonged to the top polyamide layer (Chapter 3).

The spectra in Figs. 4-6a and 4-6b present the effect of processing conditions on O-H and N-H groups for AK and SG membranes, respectively. Unlike the high flux being the major effect on N-H groups (Fig. 4-5), high temperature was found to have the greatest effect on N-H and O-H groups in this region. The least affected membranes were the ones processed under mild conditions consistent with the results with N-H and carbonyl groups in the first region.

4.3.3. FE-SEM

Virgin AK and SG membrane surfaces exhibited structures consisting of a network of polymer strands and packed globules, as was shown in Figs. 3-9(c) and 3-9(f), respectively. FE-SEM images of AK membranes processed under different conditions were presented in Fig. 4-7. Many of the polymer strands in the AK membrane formed bead-like, globular structures, which resembled microcapsules after 8 h processing. The formation of these structures varied with time depending on the processing conditions. There were no visible beads in the membranes processed under mild conditions until 8 h of processing (Figs. 4-7 a-c). However, when the temperature was increased to 80 °C, beads were observed

at the end of 4 h (Figs. 4-7 d-f). The fastest bead formation occurred with high flux processing after 0.5 h (Figs. 4-7 g-i).

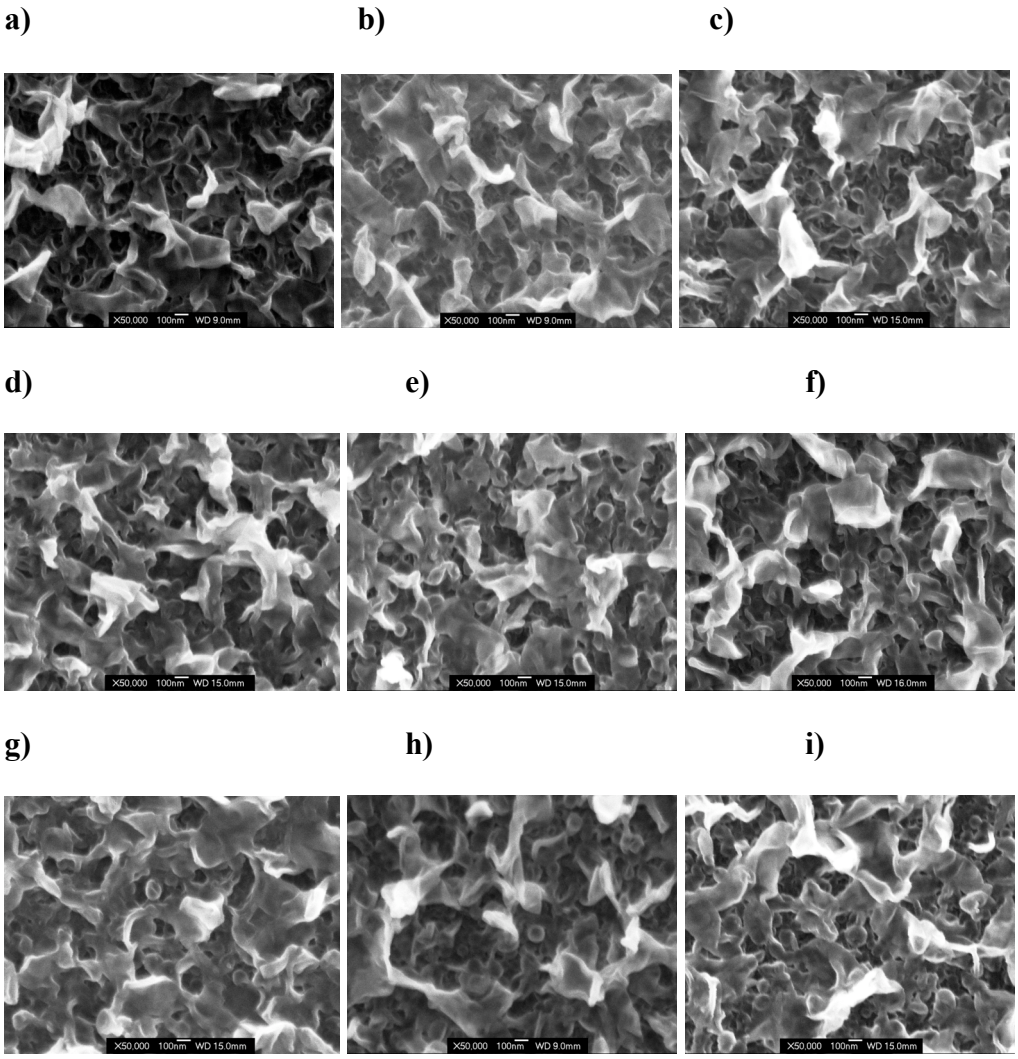

Figure 4-7. FE-SEM images of AK membrane processed under different conditions for different processing times at 120 bar (x50,000 magnification): (a) 40 °C, 50 kg/m^{2}h, 0.5 h, (b) 40 °C, 50 kg/m^{2}h, 2 h, (c) 40 °C, 50 kg/m^{2}h, 8 h, (d) 80 °C, 50 kg/m^{2}h, 0.5 h, (e) 80 °C, 50 kg/m^{2}h, 2 h, (f) 80 °C, 50 kg/m^{2}h, 8 h, (g) 40 °C, 200 kg/m^{2}h, 0.5 h, (h) 40 °C, 200 kg/m^{2}h, 2 h, (i) 40 °C, 200 kg/m^{2}h, 8 h.

FE-SEM images of SG membranes processed for 8 h were presented in Fig. 4-8. The surface structure of SG membrane was not as open as AK membrane so that the FE-SEM images could only exhibit the smooth top surface of SG after CO_2 processing. SG membranes did not show any morphological difference in their top surface under different processing conditions.

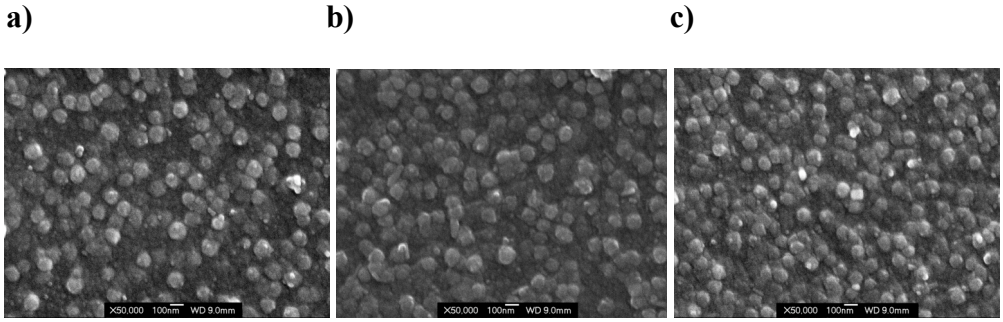

Figure 4-8. FE-SEM images of SG membrane processed under different conditions for 8 h at 120 bar (x50,000 magnification): (a) 40 °C, 50 kg/m^{2}h, (b) 80 °C, 50 kg/m^{2}h, (c) 40 °C, 200 kg/m^{2}h.

Although hydrogen bonds are classified as the strongest intermolecular bonds, their bond energy is very small compared to that of intramolecular covalent bonds [16]. As discussed above, alteration of surface hydrophobicity was probably due to the interaction of CO_2 with hydrogen bonds. However, the interaction of CO_2 with many other groups was reported to affect the solubility and diffusivity properties of membranes, which could potentially impact the morphology due to swelling [3, 17]. For example, Semenova *et al.* [18] demonstrated that the swelling of the polymer network was due to the interaction of CO_2 with polar groups resulting in the loosening of the binding between the polymer chains. Thus, the segmental mobility due to loosened chain restrictions would result in morphological changes in the polymer network.

CO_2 interaction in the polymer structure was mostly found to be stronger with functional groups having high electron donating nature [19]. Thus, it is

essential to know the existence and amount of such groups in the membrane network to assess their potential interaction with CO_2. Oxygen sources in the structures of both membranes were the carboxyl, ester and carbonyl groups connected to benzene rings. Nitrogen elements formed secondary and tertiary amides in the structures where AK membrane only accommodated secondary amides. Kilic *et al.* [13] reported that structures containing carbonyl groups and tertiary amines were expected to show morphological changes due to swelling with exposure to high pressure CO_2. They demonstrated that one of the polymers, poly N,N-dimethylacrylamide (PDMAA), which included both carbonyl groups and tertiary amines, possibly encapsulated CO_2 at 450 bar and 22 °C. The encapsulation process was assumed to be in part due to the carbonyl-CO_2 and tertiary amine-CO_2 interactions, which trapped CO_2 in the network. The final structure most probably accommodated CO_2-philic groups (carbonyl and tertiary amines) inside the capsules. Unlike the liquid state conditions tested by Kilic *et al.* [13], supercritical conditions were applied during the processing of the membranes in this study. In addition to the higher diffusivity provided by supercritical conditions, penetration of CO_2 molecules into the membrane network was increased together with the mobility of the molecules due to the pressure differential applied across the membranes. These effects could have further triggered the morphological changes observed in the AK membranes after CO_2 exposure. Morphological change in molecular scale was most probably responsible for the bead-like structure formation, which could be detected at ~0.1 micron scale in FE-SEM images.

A direct correlation between the extent of damage to the intermolecular hydrogen bonds and capsule formation could not be established. The AK membranes processed under high flux showed increased hydrophobicity within 30 min (Fig. 4-3a) but had a different time scale in terms of bead formation. Similarly, high temperature treated membranes reached maximum hydrophobicity after 4 h, while the bead-like structure started to appear after 2 h. These results were in agreement with Bos *et al.* [3] who stated that the observation of

plasticization phenomena with one characterization technique did not imply the occurrence in another one at the same time. In addition, the membranes processed under mild temperature and flux conditions did not show any change in terms of contact angle but exhibited bead formation at the end of 8 h. These findings indicate that intermolecular hydrogen bond interactions could not be the only reason responsible for the morphological changes observed in the AK membrane. On the other hand, loosened network due to diminished intermolecular hydrogen bonds could probably trigger the morphological change by accommodating CO_2 molecules and enhance the process.

4.4. Conclusions

The effects of SC-CO_2 processing at different temperature (40 and 80 °C), flux (50 and 200 kg/m^2h) and time (0-8 h) and at constant pressure (120 bar) were investigated on commercial reverse osmosis thin film polyamide membranes. m-PDA-based polyamide membrane, AK, showed prominent changes both chemically and morphologically. This was due to the presence of excess amount of hydrogen-bonded groups in its structure. Contact angle and ATR-FTIR results demonstrated that high flux had the most immediate effect on AK membrane hydrophobicity and amide and carbonyl groups, respectively. SG membrane did not show any substantial difference in its hydrophobicity, regardless of processing conditions. This was most likely due to reduced level of hydrogen bonding in its network, replaced by the covalent bonds formed during esterification with PVA. The ATR-FTIR spectra exhibited that hydroxyl groups of both membranes were mostly affected by high temperature processing unlike amide and carbonyl groups in their structure.

To the best of our knowledge, there were no previous studies focusing on the morphological changes due to SC-CO_2 processing of PA-based membranes using FE-SEM. The structure of AK membrane facilitated the observation of the changes in the membrane network. In the case of SG

membrane, probable PVA blending during polymerization reaction resulted in a closed network structure, which did not make it possible to probe morphological changes by FE-SEM. Formation of bead-like structures out of polymer strands of AK membrane was most likely due to strong self interactions of carbonyl and amide functional groups.

4.5. References

[1] C. Staudt-Bickel, W. J. Koros, Improvement of CO_2/CH_4 separation characteristics of polyimides by chemical crosslinking, Journal of Membrane Science, 155 (1999) 145-154.

[2] S. Kanehashi, T. Nakagawa, K. Nagai, X. Duthie, S. Kentish, G. Stevens, Effects of carbon dioxide-induced plasticization on the gas transport properties of glassy polyimide membranes, Journal of Membrane Science, 298 (2007) 147-155.

[3] A. Bos, I.G.M. Pünt, M. Wessling, H. Strathmann, CO_2-induced plasticization phenomena in glassy polymers, Journal of Membrane Science, 155 (1999) 67-78.

[4] A. Bos, I.G.M. Pünt, M. Wessling, H. Strathmann, Plasticization-resistant glassy polyimide membranes for CO_2/CO_4 separations, Separation and Purification Technology, 14 (1998) 27-39.

[5] J.H. Petropoulos, Plasticization effects on the gas permeability and permselectivity of polymer membranes, Journal of Membrane Science, 75 (1992) 47-59.

[6] S.R. Reijerkerk, K. Nijmeijer, C.P. Ribeiro Jr, B.D. Freeman, M. Wessling, On the effects of plasticization in CO_2/light gas separation using polymeric solubility selective membranes, Journal of Membrane Science, 367 (2011) 33-44.

[7] C.Y. Tang, Y.-N. Kwon, J.O. Leckie, Effect of membrane chemistry and coating layer on physiochemical properties of thin film composite polyamide RO and NF membranes: II. Membrane physiochemical properties and their dependence on polyamide and coating layers, Desalination, 242 (2009) 168-182.

[8] J. Geens, B. Van der Bruggen, C. Vandecasteele, Characterisation of the solvent stability of polymeric nanofiltration membranes by measurement of contact angles and swelling, Chemical Engineering Science, 59 (2004) 1161-1164.

[9] W. Lee, C.H. Ahn, S. Hong, S. Kim, S. Lee, Y. Baek, J. Yoon, Evaluation of surface properties of reverse osmosis membranes on the initial biofouling

stages under no filtration condition, Journal of Membrane Science, 351 (2010) 112-122.

[10] P. Raveendran, Y. Ikushima, S.L. Wallen, Polar Attributes of Supercritical Carbon Dioxide, Accounts of Chemical Research, 38 (2005) 478-485.

[11] N.M.B. Flichy, S.G. Kazarian, C.J. Lawrence, B.J. Briscoe, An ATR−IR Study of Poly (Dimethylsiloxane) under High-Pressure Carbon Dioxide: Simultaneous Measurement of Sorption and Swelling, The Journal of Physical Chemistry B, 106 (2001) 754-759.

[12] C.Y. Tang, Y.-N. Kwon, J.O. Leckie, Effect of membrane chemistry and coating layer on physiochemical properties of thin film composite polyamide RO and NF membranes: I. FTIR and XPS characterization of polyamide and coating layer chemistry, Desalination, 242 (2009) 149-167.

[13] S. Kilic, Y. Wang, J.K. Johnson, E.J. Beckman, R.M. Enick, Influence of tert-amine groups on the solubility of polymers in CO_2, Polymer, 50 (2009) 2436-2444.

[14] W.J. Koros, Simplified analysis of gas/polymer selective solubility behavior, Journal of Polymer Science, Polymer Physics Edition, 23 (1985) 1611-1628.

[15] S.P. Nalawade, F. Picchioni, L.P.B.M. Janssen, Supercritical carbon dioxide as a green solvent for processing polymer melts: Processing aspects and applications, Progress in Polymer Science, 31 (2006) 19-43.

[16] Y. He, B. Zhu, Y. Inoue, Hydrogen bonds in polymer blends, Progress in Polymer Science, 29 (2004) 1021-1051.

[17] A.F. Ismail, W. Lorna, Penetrant-induced plasticization phenomenon in glassy polymers for gas separation membrane, Separation and Purification Technology, 27 (2002) 173-194.

[18] S.I. Semenova, H. Ohya, S.I. Smirnov, Physical transitions in polymers plasticized by interacting penetrant, Journal of Membrane Science, 136 (1997) 1-11.

[19] Y. Akiyama, S. Fujita, H. Senboku, C.M. Rayner, S.A. Brough, M. Arai, An in situ high pressure FTIR study on molecular interactions of ketones, esters, and amides with dense phase carbon dioxide, The Journal of Supercritical Fluids, 46 (2008) 197-205.

5. Effect of supercritical CO_2 pressure on polymer membranes[1]

5.1. Introduction

In order to identify the effect of high pressure CO_2 on commercial membranes, clear understanding of the plasticization phenomena and potential changes in the physicochemical properties of these membranes is vital [1-3].

Permeability, selectivity and stability are the major factors while selecting the proper membrane for a certain application. Permeability and/or selectivity of various membranes in the supercritical carbon dioxide (SC-CO_2) coupled process applications have been reported by different researchers [4-11]. However, information related to the stability of polymer membranes used under SC-CO_2 environment is scarce. Therefore, the objectives of this study were to investigate the changes in physicochemical and morphological properties of two commercial reverse osmosis membranes (AK and SG) under different pressure, temperature, flux and processing time conditions by using contact angle, ATR-FTIR and FE-SEM analysis and to assess the effect of SC-CO_2 processing on membrane performance by determining CO_2 flux and oleic acid retention.

5.2. Materials and methods

5.2.1. Membranes and materials

Two RO membranes (AK, SG) were kindly provided by GE Osmonics (Minnetonka, MN, USA). The virgin membranes were cleaned as described in Chapter 3 (Section 3.2.1).

[1] A version of this chapter has been submitted for publication. Akin and Temelli 2011. Journal of Membrane Science.

5.2.2. SC-CO_2 processing of membranes

The original system that was described in Chapter 4 (Fig. 4-2) was modified as shown in Fig. 5-1 to introduce and collect lipid samples. The system was operated according to the protocol described in Chapter 4 (Section 4.2.2). The additional oil separator allowed collection of lipid samples from the permeate upon depressurization.

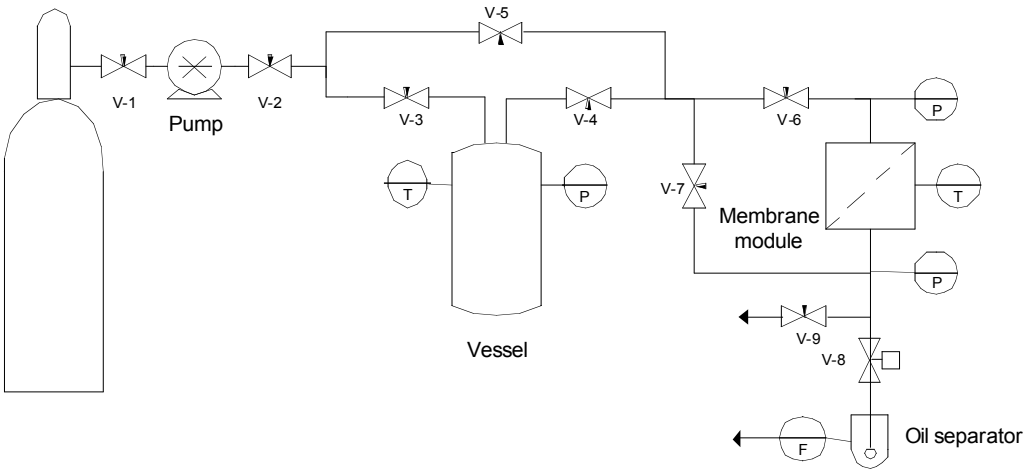

Figure 5-1. Flow diagram of the modified supercritical CO_2 – membrane separation coupled system (T: thermometer, P: pressure gauge, V: valve, F: flowmeter).

In order to determine the effect of supercritical conditions on membrane performance with no CO_2 transport, membranes were placed in the vessel (180 mL) at 280 bar and temperatures of 40 and 80 °C were applied for up to 5 days. Then, they were placed in the module for the determination of CO_2 flux and oleic acid retention as described later.

Potential hysteresis on membrane flux was tested after the system was pressurized to 120 bar at 40 °C and CO_2 flux was monitored with increasing and

decreasing transmembrane pressure (ΔP) values. ΔP was increased from 10 to 40 bar by 10 bar increments and 1 h processing at each step. Then, the same procedure was followed by decreasing (ΔP) back to 10 bar.

Membranes were first processed with pure CO_2 and then the system was depressurized for analysis of the membranes. In order to reveal the effect of SC-CO_2 processing and depressurization steps on CO_2 flux and oleic acid retention, the same membranes were used without removing them from the module. Retention and flux experiments were done at 120 bar and 40 °C upon repressurization of the system followed by filtration for up to 2 h.

Both AK and SG membranes were processed at three levels of pressures (120, 200 and 280 bar). The effect of pressure was compared at different temperature (40 and 80 °C) and flux conditions (50 and 200 kg/m^2h) for contact angle measurements. These conditions were defined as mild (40 °C, 50 kg/m^2h), high flux (40 °C, 200 kg/m^2h) and high temperature (80 °C, 50 kg/m^2h) processing for presentation of results. Processing with pure SC-CO_2 under different conditions was applied for up to 24 h. Membranes, which were depressurized right after their flux was measured were specified as processing time of 0 h. Membrane processing at each condition was performed in triplicate.

5.2.3. Characterization of membranes

5.2.3.1. Contact angle by sessile drop method

Contact angles of the dry membranes were measured using FTA 200 contact angle analyzer (Ten Angstroms, Folio Instruments, Kitchener, ON, Canada) using the sessile drop method as described in Chapter 3 (Section 3.2.2). Contact angles were measured to determine the effect of feed pressure (120, 200 and 280 bar) after processing the membranes at mild (40 °C, 50 kg/m^2h), high temperature (80 °C, 50 kg/m^2h) and high flux (40 °C, 200 kg/m^2h) conditions for up to 24 h.

5.2.3.2. ATR-FTIR

ATR-FTIR spectra were obtained using a Nicolet 8700 FTIR spectrometer coupled to a germanium crystal operated at 45°C using OMNIC 6.2 software (Thermo Electron Corp., Hampton, NH, USA) as described in Chapter 3 (Section 3.2.5). Membranes were analyzed after being processed for 24 h at two different pressures (120 and 280 bar) at mild (40 °C, 50 kg/m^{2}h) conditions.

5.2.3.3. FE-SEM

FE-SEM images of the cross-section and top layer of AK and SG membranes were taken using JEOL 6301F field emission scanning electron microscope (Tokyo, Japan) with Si diode detector as described in Chapter 3 (Section 3.2.6). Membranes were analyzed after up to 24 h processing under mild (40 °C, 50 kg/m^{2}h), high temperature (80 °C, 50 kg/m^{2}h) and high flux (40 °C, 200 kg/m^{2}h) conditions.

5.2.3.4. Determination of CO_2 flux and oleic acid retention

In order to calculate the CO_2 flux (kg/m^{2}h), the permeate flow rate was measured in volume (at ambient conditions), multiplied by CO_2 density at those conditions [12] and divided by the area of the exposed membrane (9.6 cm^2).

Variation of flux at constant pressures of 120 and 280 bar was tested at ΔP of 10 bar and presented as normalized flux values. Normalized flux values were calculated by dividing the actual flux at a given processing time (P) by the initial flux at time zero (P_0) for each membrane at the corresponding pressure.

For the oleic acid retention experiments, 30 g oleic acid was placed in the vessel of the system depicted in Fig. 5-1. The vessel was pressurized to the set pressure by opening valves V-1, V-2, V-3 and closing valves V-4 and V-5. Oleic acid+SC-CO_2 mixture was stirred for at least 3 h before it was fed to the membrane module at operating conditions. Then, valves V-2, V-3 and V-4 were closed and V-5, V-7 and V-9 were opened to depressurize the lines except the

vessel. After pure SC-CO_2 processing was applied as explained above, the system was depressurized and then repressurized to 120 bar. Oleic acid+SC-CO_2 was fed to the membrane module by closing valve V-5 and opening valves V-3 and V-4. At the end of 2 h filtration, depressurization of the system was achieved by closing valves V-2, V-3 and V-4 and opening V-5, V-7 and V-9.

Oleic acid retention was determined at 120 bar and 40 °C. Samples were weighed after being collected in the oil separator (Fig. 5-1) upon depressurization with and without the use of a membrane. When membranes were used, CO_2 flow rate corresponding to a flux of 50 kg/m^2h was recorded by the flow meter and the same flow rate was applied during the process without the use of membranes. Samples were collected until 50 L CO_2 (at ambient conditions) was collected as permeate (corresponding to ~2 h filtration). Retention factor was calculated according to Eq. (5-1).

$$\%R = \left(1 - \frac{Cp}{Cf}\right) x\ 100 \qquad (5\text{-}1)$$

where C_p and C_f represent the total amount of oleic acid collected in milligrams with and without the use of membrane, respectively.

5.3. Results and discussion

Alteration of surface properties could only be explained with sufficient information related to the surface physicochemical structure. A detailed characterization of the virgin membranes used in this study was reported previously in Chapter 3. Esterification of free carboxyl groups and the existence of piperazine monomer in the SG membrane resulted in a relatively different chemical structure than AK membrane as was shown in Fig. 4-1. As a result, AK membrane was found to have more hydrogen bonds in its structure compared to the SG membrane.

5.3.1. Contact angle

The change in contact angles of the membranes could be a good indicator of the potential interaction between the polar functional groups and CO_2. The effect of pressure on contact angles of AK membranes treated at mild processing conditions is presented in Fig. 5-2a. Contact angle of AK membrane remained almost constant over 24 h processing with CO_2 at 120 bar. When the system pressure was increased to 200 bar, there was a slight increase in the contact angle after 8 h. This behaviour was also observed at 280 bar but the contact angle reached a higher value after 24 h compared to that of membranes processed at 200 bar.

Under high temperature conditions (Fig. 5-2b), the effects of processing at pressures of 200 and 280 bar on the contact angle of AK membrane were similar, where there was a dramatic increase in contact angles within 2 h followed by a slight increase thereafter with the contact angles reaching 80° and 81° at the end of 24 h processing at 200 and 280 bar, respectively. On the other hand, contact angles of membranes processed at 120 bar showed an increase over the first 4 h and then remained almost constant after 8 h of processing, reaching 77°. High flux processing also had a prominent effect on surface hydrophobicity (Fig. 5-2c). Contact angles showed a dramatic increase in the first half hour and then increased slightly over 24 h processing at 280 bar, reaching 84°.

The AK membrane showed substantial differences in contact angles depending on processing conditions and time. The presence of excess amount of hydrogen bonds in the structure led to evident interactions with CO_2. The increase in contact angle due to different flux and temperature conditions at 120 bar was reported previously in Chapter 4 (Section 4.3.1) and now in this study it is demonstrated that an increase in pressure also causes additional alteration on surface hydrophobicity, especially with the membranes processed under high temperature and high flux conditions.

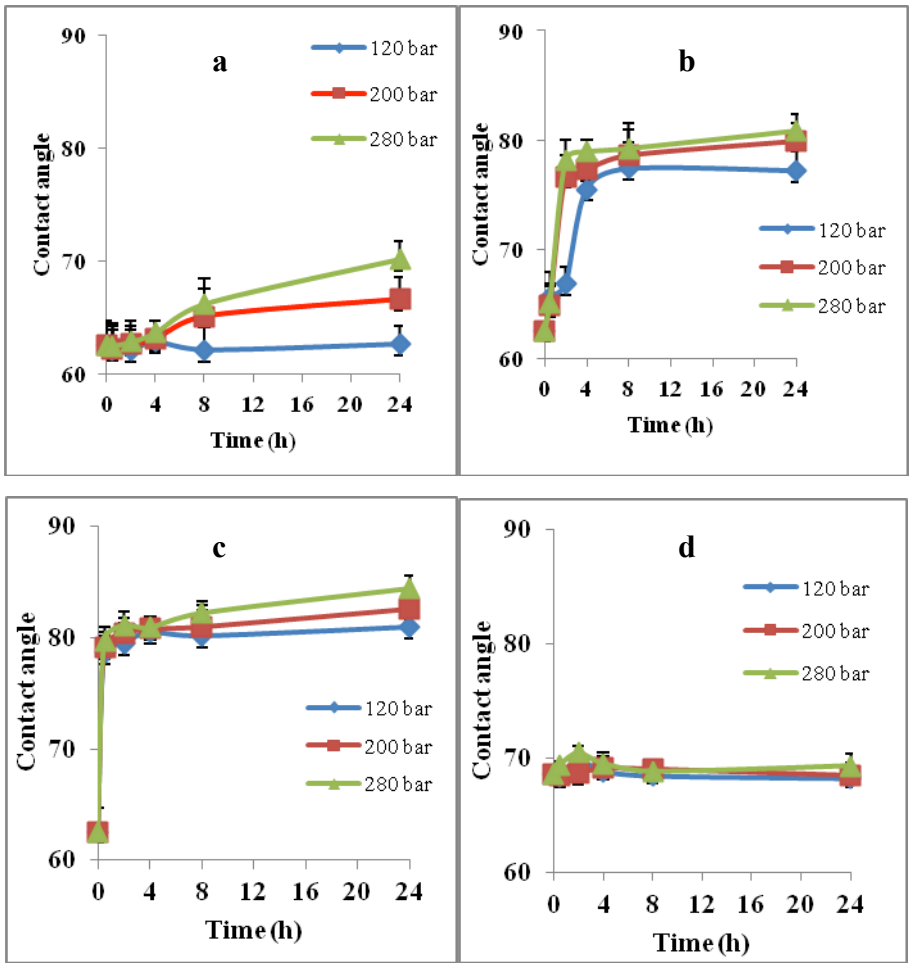

Figure 5-2. Contact angles of membranes processed under different pressure conditions up to 24 h: (a) AK membrane at mild conditions, (b) AK membrane at high temperature conditions, (c) AK membrane at high flux conditions and (d) SG membrane at mild conditions.

Since CO_2 is a strongly sorbing penetrant, higher penetrant concentrations due to higher feed pressure would cause more extensive interactions with the polar functional groups of the polymer material as well as plasticizing the polymer matrix via increasing polymer local segmental motion [13]. The interaction of CO_2 with polar groups where the oxygen of CO_2 would interact with hydrogen has been reported previously [14]. Although interactions between CO_2

and hydrogen were probably relatively smaller than intermolecular hydrogen bonding in the polymer network, extreme processing conditions were possibly more effective in diminishing these forces by accommodating CO_2 to interact with hydrogen of carboxyl and amide groups.

In the case of SG membrane, there was no substantial difference in contact angle (<3%) due to processing pressures as well as temperature, flux and processing time, thus the contact angle of SG membrane was only presented under mild conditions (Fig. 5-2d). These results were as expected based on the suggested chemical structure of the SG membrane (Fig. 4-1), where the SG membrane had relatively less hydrogen bonds due to esterification and the type of monomer used during polymerization (Chapter 3). The lack of hydrogen bonding in the structure resulted in less interaction with CO_2.

5.3.2. ATR-FTIR

ATR-FTIR spectra provided information for the top 1-2 μm of the thin film membranes. This region had the functional groups corresponding to the polyamide selective layer and the polysulphone sublayer. Previous investigations did not include transport of CO_2 through the polymer network at a certain transmembrane pressure as driving force. Besides, the effect of CO_2 depressurization after processing was not evaluated for polymer membranes using FTIR analysis [15].

Flichy *et al.* [15] postulated that the decrease in absorbance compared to the original polymer was due to the decrease in the concentration of the polymer exhibiting the swelling of the structure upon diffusion of small molecules. In order to determine the specific effect of CO_2 on carbonyl, amide and hydroxyl groups, the change in absorbance was presented by normalizing the spectra after processing under different pressure conditions. Based on previous FTIR analysis of the virgin membranes (Chapter 3, Section 3.3.3), the region between 1500-1800 cm^{-1} was found to be the fingerprint region for AK and SG membranes

exhibiting major differences, which consisted of amide and carbonyl groups (Fig. 5-2). Because of the very low intensity of the peaks associated with SG membrane, the spectra of SG were not presented in this region. The second region exhibited N-H and O-H groups between 2800-3600 cm^{-1} for both membranes (Fig. 5-4). The spectra in the first and second regions were normalized according to aromatic stretching vibration of polysulphone layer at 1587 cm^{-1} (Fig. 5-3) and aromatic C-H stretching vibrations at 3000-3100 cm^{-1} (Fig. 5-4a and 5-4b).

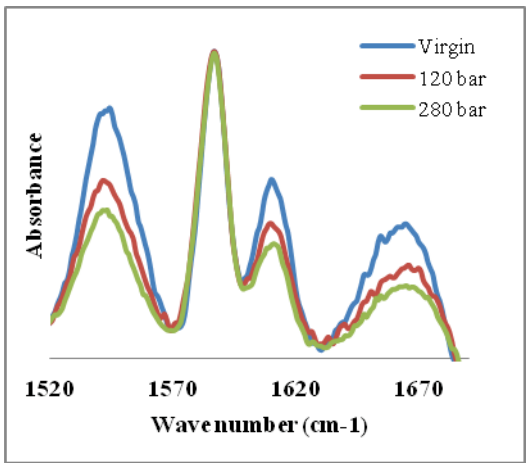

Figure 5-3. The spectra of AK membranes between 1500 – 1800 cm^{-1} normalized relative to aromatic stretching vibration of polsulphone layer at 1587 cm^{-1} for membranes processed at different conditions at mild conditions.

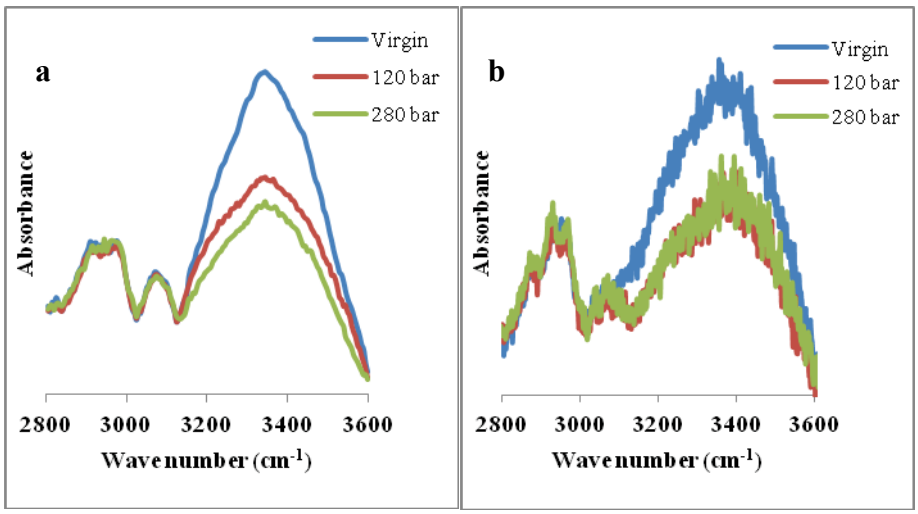

Figure 5-4. Absorbance between 2800 – 3600 cm^{-1} for O-H and N-H groups of (a) AK and (b) SG after processing at different pressures at mild conditions which were normalized according to aromatic C-H stretching vibrations at 3000-3100 cm^{-1}.

AK membrane showed peaks at 1541 cm^{-1} and 1609 cm^{-1}, which were assigned to amide 2 band and aromatic amide, and amide 1 band, respectively [16]. The peak at 1663 cm^{-1} was assigned to C=O stretching vibration of amide 1 band. SG membrane had much weaker peaks at 1541 cm^{-1} and 1609 cm^{-1} due to weaker N-H vibrations. In addition, SG membrane had a peak at 1653 cm^{-1} due to C=O stretching. SG membrane spectra also had a peak at 1730 cm^{-1}, which was assignable to C=O stretching observed in esters [16].

The effect of pressure was depicted at mild conditions at 120 and 280 bars after 24 h processing (Fig. 5-3) and AK membranes processed at 280 bars exhibited a larger decrease in the absorbance of N-H and carbonyl groups. Although polymer free-volume and chain flexibility contribute to increased plasticization of a polymer by CO_2, the dominant effect was reported to be the specific interactions between CO_2 and polymer structure [17]. Hydrogen bonding capability of the amide group in AK membrane could initiate simultaneous interaction with the oxygen of CO_2 [18, 19]. Besides, specific interactions

between carbonyl groups and CO_2 are well known where carbonyl groups can act as Lewis acid and CO_2 as a Lewis base [2, 20-22]. Pressure effect is evident for the degree of interaction of CO_2 with polymers, which increases with increasing level of sorption. These interactions can also lead to swelling of the polymer network as a function of pressure [17].

The region between 2800-3600 cm^{-1} involved the peaks of O-H and N-H functional groups for AK membrane. It was previously reported (Chapter 3, Section 3.3.3) that the peak at 3405 cm^{-1} mostly belonged to the O-H groups of polyvinyl alcohol (PVA) likely used during polymerization reaction of SG membrane whereas the same peak centered at 3330 cm^{-1} for AK membrane belonged to the top polyamide layer. As shown in Figs. 5-4a and 5-4b, the decrease in absorbance was slightly larger with AK membrane after 24 h processing compared to SG membrane. This may be due to the different sources of O-H groups arising from the different chemical structures of the two membranes. Since the peaks of SG were mostly found to be associated with PVA in this region, interaction of CO_2 with N-H groups could be another reason for the slightly different behaviour of the two membranes in this region.

5.3.3. FE-SEM

As reported previously in Chapter 3 (Section 3.3.4), FE-SEM images of AK membrane exhibited a network of polymer strands with relatively high surface roughness whereas SG membrane consisted of packed globules with a more smooth surface. PVA blending during SG membrane fabrication probably resulted in a completely different surface structure, which made it hard to observe any morphological changes due to the tight packing. On the other hand, AK membrane had a relatively open surface making it possible to see higher penetration depths through its surface. FE-SEM images of AK membranes were presented after processing at mild, high temperature and high flux conditions up to 24 h (Figs. 5-5 and 5-6).

Increasing the processing time up to 24 h, increased the extent of bead-like structure formation on the surface of AK membranes. Virgin membrane (Fig. 5-5a) and the membranes, which were exposed to CO_2 at 280 bar for 24 h was also presented at mild (Fig. 5-5b), high temperature (Fig. 5-5c) and high flux (Fig. 5-5d) conditions to depict morphological changes.

Morphological changes in the polymer strands of AK membrane were also observed at different processing times and conditions (Fig. 5-6). Processing the membrane at 280 bar had a prominent effect on membrane morphology. Bead-like, globular structure formation was observed in the polymer strands after 4 h of continues CO_2 flow through the membrane under mild conditions. A similar structural change did not occur until 8 h when the membranes were processed at 120 bar (Figs. 5-6a and b).

High temperature processing at 120 and 200 bar revealed the formation of bead-like structures at the end of 4 h unlike processing under mild conditions. Increasing the pressure to 280 bar accelerated this morphological change, which made the beads appear after 2 h processing (Figs. 5-6c and d). In the case of high flux processing bead-like structures appeared at the end of 0.5 h at all pressures (Figs. 5-6e and f).

On the other hand, SG membranes processed for 24 h under different conditions did not show any morphological change when compared with the virgin membrane as shown in Fig. 5-7 for membranes processed at 120 and 280 bar under mild conditions. Surface structure of SG was not as open as AK membrane so that FE-SEM images could only exhibit the smooth top surface of the membranes. Possible PVA blending during fabrication of SG membranes was suggested to form cross-linking resulting in a decrease in the hydrogen bonding sites. Although the interaction of CO_2 with many other groups was reported before [23, 24], alteration of surface hydrophobicity as demonstrated above for

the AK membrane was probably due to the interaction of CO_2 with hydrogen bonds.

As Semenova *et al.* [25] indicated, the interaction of CO_2 with polar groups would result in the loosening of the binding between the polymer chains. Thus, the segmental mobility due to loosened chain restrictions seemed more likely in the case of AK membrane with excess amount of hydrogen bonding in the structure, resulting in the morphological changes in the polymer network as observed in the SEM images.

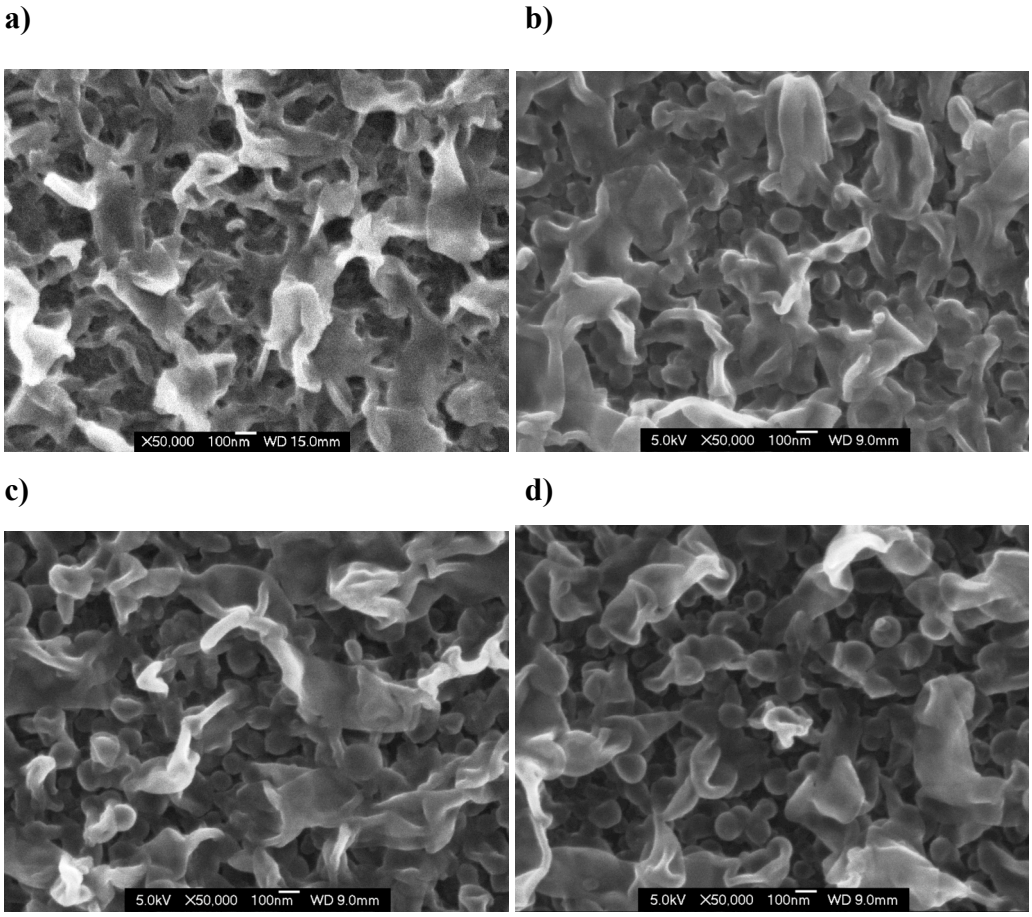

Figure 5-5. FE-SEM images of AK membranes processed at 280 bar for 24 h (x50,000 magnification): (a) virgin, (b) mild, (c) high temperature, (d) high flux conditions

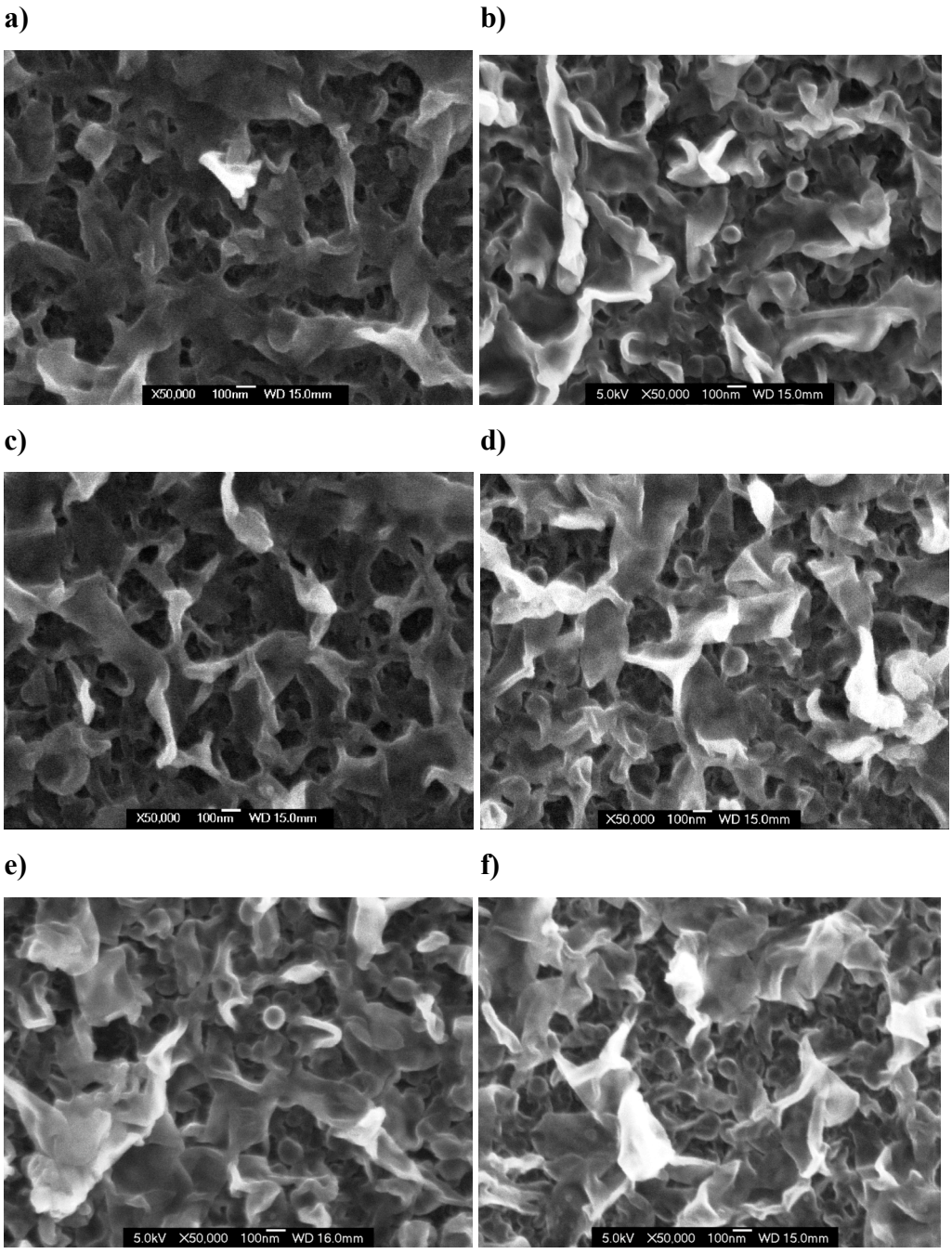

Figure 5-6. FE-SEM images of AK membrane processed under different pressures, different processing times at mild, high temperature and high flux conditions (x50,000 magnification): (a) 120 bar, 4 h, mild conditions ,(b) 280 bar, 4 h, mild conditions ,(c) 120 bar, 2 h, high temperature conditions, (d) 280 bar, 2 h, high temperature conditions, (e) 120 bar, 0.5 h, high flux conditions and (f) 280 bar, 0.5 h, high flux conditions

a) **b)** **c)**

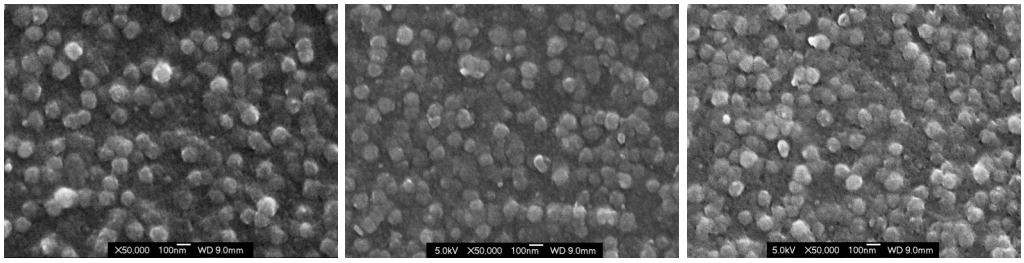

Figure 5-7. FE-SEM images of SG membranes processed at (a) 120 bar and (b) 280 bar for 24 h at mild conditions (x50,000 magnification)

Information on the morphological changes in polymer networks due to high pressure CO_2 processing has been scarce. Recently, Kilic *et al.* [20] reported that a polymer containing carbonyl and tertiary amine groups, poly N, N-dimethylacrylamide, formed capsul-like structures due to carbonyl-CO_2 and tertiary amine-CO_2 interactions. The bead-like structure formation observed in this study is in agreement with those findings even though the processing conditions are different. Supercritical state conditions were applied in this study unlike the liquid state conditions tested by Kilic *et al.* [20]. Penetration of CO_2 through the polymer network was achieved by applying transmembrane pressure across the membrane, which in turn proved to be detrimental for the polymer network as discussed above in terms of contact angle and FTIR results.

As presented in the FE-SEM images (Fig. 5-6), increasing the pressure initiated the structural changes earlier in AK membranes. In order to demonstrate the effect of CO_2 flow on morphological changes, membranes were kept under mild and high temperature conditions at 280 bar with CO_2 but without flow up to 5 days. FE-SEM images exhibited that the bead formation was not observed even after 5 days under these conditions. Based on these results, it could be hypothesized that CO_2 transport driven by transmembrane pressure is the main reason for the morphological changes observed in the AK membrane. Effects of

pressure and temperature under supercritical conditions were considerable contributors by accelerating the process of morphological change. Increasing the processing time up to 24 h enhanced the formation of bead-like structures and increased the extent of such structures on the top surface of AK membrane. On the other hand, although SG membrane did not exhibit such morphological changes that could be observed in the FE-SEM images, CO_2 flux and oleic acid retention experiments were performed to reveal any potential structural deformation associated with both membranes, which might in turn affect their performance.

5.3.4. CO_2 flux and oleic acid retention

Previous studies with lipid components involving coupled SC-CO_2 and membrane technologies focused on the efficiency of separation in terms of selectivity and permeability of solute components to determine the appropriate membrane for the targeted separation [4-6, 11]. Since polymer materials are known to have strong interactions with CO_2 under high pressure, it is evident that the stability of polymer-based membranes is an important issue regarding the durability of the membrane structure to withstand the supercritical operating conditions.

The effect of ΔP on flux was evaluated by applying compression/ decompression cycles for both membranes (Fig. 5-8). No hysteresis effect was observed for both membranes indicating that compaction was not an issue on permeate flux up to the transmembrane pressure of 40 bar.

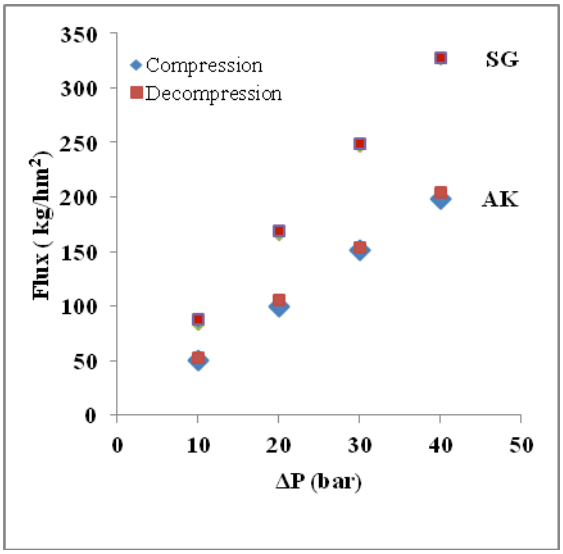

Figure 5-8. Flux of pure CO_2 during compression and decompression through AK and SG membranes at 40 °C and 120 bar.

Variation of flux was exhibited at constant pressures of 120 and 280 bar up to 180 min for both membranes at a ΔP of 10 bar (Fig. 5-9). Normalized flux values were determined to evaluate the change in flux with processing time. The initial increase was due to sudden relaxation of the polymer structure to form a new organizational state upon introduction of SC-CO_2. Flux exponentially increased until it reached 5% more than its initial value. AK membrane reached that level in a shorter period of time than SG membrane under both pressures of 120 and 280 bar (Figs. 5-9a and 5-9b). Since the AK membrane has excess of hydroxyl groups in its structure, hydrogen bonds reflected a relatively higher chain mobility especially in the first hour of processing, which required less relaxation time under SC-CO_2 environment. At 280 bar, the time required to reach 5% increase in flux was shorter than that at 120 bar, especially with AK membrane (60 vs 90 min). That was most probably due to less chain mobility at 120 bar needing longer time to complete the initial relaxation.

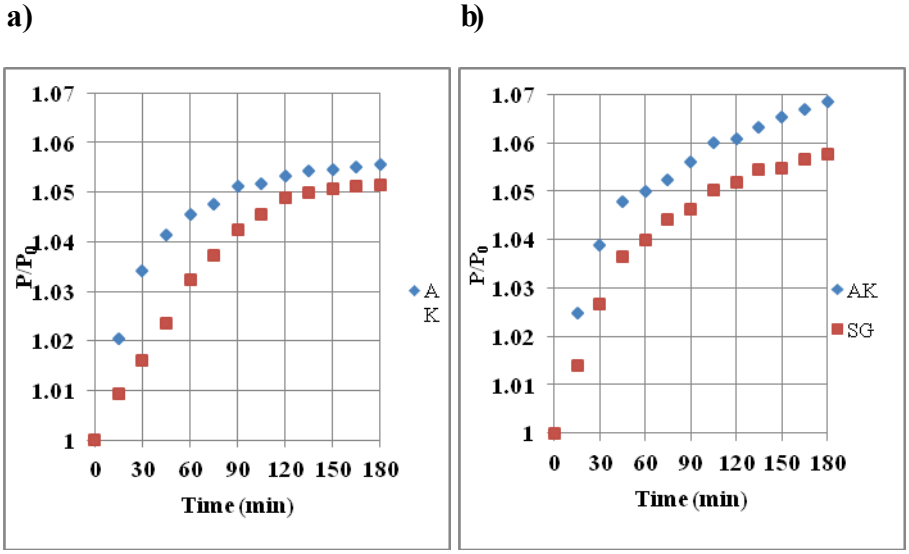

Figure 5-9. Variation of flux through AK and SG membranes at 40 °C at (a) 120 bar and (b) 280 bar up to 3 h processing at constant ΔP of 10 bar (P: flux at that particular time, P_0: initial flux at time 0)

Membranes showed a relatively higher increase in flux during the first 2 h of processing compared to the whole 24 h period. AK membrane had a greater increase in flux at 280 bar at the end of 24 h. AK and SG exhibited 16% and 10% increase in their flux at 280 bar while it was 12% and 8% at 120 bar at the end of 24 h compared to their initial value at time zero, respectively. The major reason behind the increase during the 24 h period was most probably due to rigid chains of glassy polymer structures, which are not in equilibrium state, requiring more time to reach a new organizational state compared to the polymers having much more mobile chains [26]. Increasing pressure up to 280 bar further affected swelling of the polymer network and resulted in a higher flux at the end of 24 h.

There was a decrease in the flux when the pressure was increased at constant ΔP of 10 bars for both membranes (Fig. 5-10). Flux (J, kg/m^2h) through polymeric membranes under supercritical conditions has been described as a

function of density (ρ, kg/m^3) /viscosity (μ, Pa.s) as shown in Eq. (5-2) where β is a constant and represents membrane structural parameter [27].

$$J = \beta \frac{\rho}{\mu} x \Delta P \qquad (5\text{-}2)$$

Both viscosity and density of CO_2 shows an increase when pressure is increased from 120 to 280 bar [12]. Since the increase in viscosity is greater than that for density with a pressure change from 120 to 280 bar, the flux was found to be lower at higher CO_2 pressures when ΔP was kept constant.

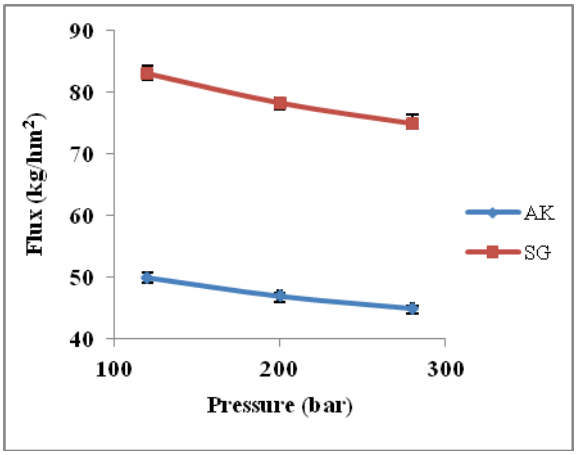

Figure 5-10. Effect of feed pressure on CO_2 flux at constant ΔP of 10 bar at 40 °C

In a membrane separation application with SC-CO_2, three major steps are involved: 1) Pressurization, 2) Processing with SC-CO_2 and 3) Depressurization. Table 5-1 exhibits the CO_2 flux and oleic acid retention of the membranes, which were previously processed with pure SC-CO_2 (0, 0.5, 8, 24 h) and left in the membrane module following depressurization to determine the change in their performance compared to their virgin conditions. Membranes, which were depressurized right after their flux was measured at 120 bar did not exhibit any change in their CO_2 flux and oleic acid retention upon depressurization compared to their virgin counterparts. That was due to insufficient time of interaction between the polymer network and SC-CO_2 and those conditions were defined as

'0 h', which exhibited the same results as unprocessed (virgin) membranes. AK membrane showed a higher level of increase in flux than SG membrane depending on the time of processing. Flux of AK increased to 61 kg/m^{2}h upon depressurization after 0.5 h processing. The flux reached its maximum level of 77 kg/m^{2}h after 24 h processing upon depressurization. In the case of SG membranes, there was no substantial increase in flux after 0.5 h processing whereas retention was down to 74% and 73% at the end of 8 and 24 h processing upon depressurization, respectively. These results showed that SC-CO_2 processing time had a strong effect on flux determined over 2 h following depressurization for both membranes. Besides, AK membrane was affected more than SG as the flux was prominently increased at the end of 0.5 h. Increasing processing time did not show any substantial difference after 8 h processing since the flux for both membranes almost levelled off.

Table 5-1. Performance of AK and SG membranes upon depressurization after SC-CO_2 processing

AK	**Processing time (h)**			
	0	**0.5**	**8**	**24**
Flux[a]	50 ± 2.4	61 ± 2.1	74 ± 3.1	77 ± 2.2
Retention (%)[b]	75 ± 0.8	72 ± 1.3	67 ± 1.9	66 ± 1.5
SG				
Flux[a]	83 ± 2.4	84 ± 1.8	108 ± 2.6	111 ± 2.9
Retention (%)[b]	79 ± 1.1	79 ± 1.5	74 ± 0.4	73 ± 1.2

[a] SC-CO_2 processing at 120 bar 40 °C, flux reported as kg/m^2.h with ΔP of 10 bar. Mean ± standard deviation based on 3 determinations

[b] Oleic acid retention at 120 bar 40 °C with ΔP of 10 bar. Mean ± standard deviation based on 3 determinations

The overall changes observed in the physicochemical and morphological properties of both membranes reflect most probably the sum of changes taking place in all of these steps. The changes as a result of the interactions during processing were most likely triggered upon depressurization of the system due to extremely high feed pressures achieved with the application of SC-CO_2. Depressurization reflected the effect of processing conditions on the membranes, which helped with probing any alterations in their structures.

Increase in flux could be explained as the increase in sorption and specific volume upon removal of CO_2 to reach atmospheric pressure. This effect was explained as the formation of new Langmuir sorption sites or enlargement of the existing ones by Wonders and Paul [28]. Transport of CO_2 under supercritical conditions have certain interactions with the polymer materials as presented. The weakening of the structures has further led to a structural reorganization upon depressurization leaving increased volume of microvoids in the network. Both membranes underwent a structural reorganization upon CO_2 removal. AK membrane was found to be affected more severely most likely due to excess of relatively weaker hydrogen bonds in its structure compared to the SG membrane, which was covalently cross-linked.

Oleic acid retentions of processed membranes were compared to evaluate any changes in the reorganized network due to SC-CO_2 processing and depressurization. As shown in Table 5-1, retention showed some decrease for both membranes with processing time upon depressurization. Oleic acid retention of AK and SG was about 9% and 6% less than those of the corresponding virgin membranes, respectively, when membranes processed with SC-CO_2 for 24 h was used after depressurization. These results showed that there was a change in the membrane structure due to processing and depressurization. The change in the structure was most probably associated with Langmuir sorption sites, which

resulted in an apparent increase in flux while retention rates were relatively less affected at the end of processing for both membranes.

5.4. Conclusions

The effect of SC-CO_2 processing pressure on physicochemical and morphological properties of two commercial polyamide membranes was presented in detail to investigate the stability of polyamide membranes under supercritical processing conditions. Contact angle measurements exhibited the effect of relatively hydrophobic CO_2 on hydrophilic groups accommodated on membrane surface. The prominent change associated with AK membrane was mainly the result of excess amount of hydrogen bonds in its structure rather than the cross-linked structure of SG membrane where the hydrogen bonding groups were replaced by cross-linking. Amide, carbonyl and hydroxyl groups showed the highest drop in absorbance upon CO_2 processing due to Lewis acid-base interactions. These interactions increased with pressure. Besides, increasing density of CO_2 at higher pressures accelerated the morphological changes in the structure of AK membrane while SG membrane structure did not exhibit any difference.

Lewis acid-base interactions were believed to play an important role during reorganization of the polymer structures upon depressurization. CO_2 flux increased for both membranes with processing time after depressurization. This increase was found to be higher with AK membrane mostly due to increased chain mobility and higher interactions with CO_2 provided by excess of hydrogen bonds in its network. Another reason for the relatively higher flux of AK could be the higher surface hydrophobicity arising from SC-CO_2 – polar group interactions. Higher hydrophobicity on the top surface could lead to higher dissolution rates of SC-CO_2 resulting in higher flux compared to its virgin form. Retention of oleic acid was decreased by up to 9% when AK membranes were used. SG membranes

proved to be more resistant under supercritical conditions as a result of their covalently cross-linked structures.

5.5. References

[1] S. Kanehashi, T. Nakagawa, K. Nagai, X. Duthie, S. Kentish, G. Stevens, Effects of carbon dioxide-induced plasticization on the gas transport properties of glassy polyimide membranes, Journal of Membrane Science, 298 (2007) 147-155.

[2] A. Bos, I.G.M. Pünt, M. Wessling, H. Strathmann, CO_2-induced plasticization phenomena in glassy polymers, Journal of Membrane Science, 155 (1999) 67-78.

[3] J.H. Petropoulos, Plasticization effects on the gas permeability and permselectivity of polymer membranes, Journal of Membrane Science, 75 (1992) 47-59.

[4] C.B. Spricigo, A. Bolzan, R.A.F. Machado, L.H.C. Carlson, J.C.C. Petrus, Separation of nutmeg essential oil and dense CO_2 with a cellulose acetate reverse osmosis membrane, Journal of Membrane Science, 188 (2001) 173-179.

[5] L.H.C. Carlson, A. Bolzan, R.A.F. Machado, Separation of d-limonene from supercritical CO_2 by means of membranes, The Journal of Supercritical Fluids, 34 (2005) 143-147.

[6] J.M.L.N. de Moura, L.A.G. Gonçalves, L.A.V. Sarmento, J.C.C. Petrus, Purification of structured lipids using $SCCO_2$ and membrane process, Journal of Membrane Science, 299 (2007) 138-145.

[7] L.A.V. Sarmento, C.B. Spricigo, J.C.C. Petrus, L.H.C. Carlson, R.A.F. Machado, Performance of reverse osmosis membranes in the separation of supercritical CO_2 and essential oils, Journal of Membrane Science, 237 (2004) 71-76.

[8] A. Pietsch, W. Hilgendorff, O. Thom, R. Eggers, Basic investigation of integrating a membrane unit into high-pressure decaffeination processing, Separation and Purification Technology, 14 (1998) 107-115.

[9] L.A.V. Sarmento, R.A.F. Machado, J.C.C. Petrus, T.R. Tamanini, A. Bolzan, Extraction of polyphenols from cocoa seeds and concentration through polymeric membranes, The Journal of Supercritical Fluids, 45 (2008) 64-69.

[10] S.J. Sarrade, G.M. Rios, M. Carlès, Supercritical CO_2 extraction coupled with nanofiltration separation: Applications to natural products, Separation and Purification Technology, 14 (1998) 19-25.

[11] W. Artz, T. Kinyanjui, M. Cheryan, Deacidification of soybean oil using supercritical fluid and membrane technology, Journal of the American Oil Chemists' Society, 82 (2005) 803-808.

[12] E.W. Lemmon, M.O. McLinden, D.G. Friend, Thermophysical Properties of Fluid Systems, in: NIST Chemistry WebBook, NIST Standard Reference Database Number 69, P.J. Linstrom, W.G. Mallard (Eds.) National Institute of Standards and Technology, Gaithersburg, MD, http://webbook.nist.gov (retrieved Nov. 30, 2010)

[13] W.J. Koros, M.W. Hellums, Gas separation membrane material selection criteria: Differences for weakly and strongly interacting feed components, Fluid Phase Equilibria, 53 (1989) 339-354.

[14] P. Raveendran, Y. Ikushima, S.L. Wallen, Polar Attributes of Supercritical Carbon Dioxide, Accounts of Chemical Research, 38 (2005) 478-485.

[15] N.M.B. Flichy, S.G. Kazarian, C.J. Lawrence, B.J. Briscoe, An ATR−IR Study of Poly (Dimethylsiloxane) under High-Pressure Carbon Dioxide: Simultaneous Measurement of Sorption and Swelling, The Journal of Physical Chemistry B, 106 (2001) 754-759.

[16] C.Y. Tang, Y.-N. Kwon, J.O. Leckie, Effect of membrane chemistry and coating layer on physiochemical properties of thin film composite polyamide RO and NF membranes: I. FTIR and XPS characterization of polyamide and coating layer chemistry, Desalination, 242 (2009) 149-167.

[17] P. Vitoux, T. Tassaing, F. Cansell, S. Marre, C. Aymonier, In Situ IR Spectroscopy and Ab Initio Calculations To Study Polymer Swelling by Supercritical CO_2, The Journal of Physical Chemistry B, 113 (2009) 897-905.

[18] A.F. Ismail, W. Lorna, Penetrant-induced plasticization phenomenon in glassy polymers for gas separation membrane, Separation and Purification Technology, 27 (2002) 173-194.

[19] P. Raveendran, S.L. Wallen, Cooperative C−H···O Hydrogen Bonding in CO2−Lewis Base Complexes: Implications for Solvation in Supercritical CO_2, Journal of the American Chemical Society, 124 (2002) 12590-12599.

[20] S. Kilic, Y. Wang, J.K. Johnson, E.J. Beckman, R.M. Enick, Influence of tert-amine groups on the solubility of polymers in CO_2, Polymer, 50 (2009) 2436-2444.

[21] W.J. Koros, Simplified analysis of gas/polymer selective solubility behavior, Journal of Polymer Science, Polymer Physics Edition, 23 (1985) 1611-1628.

[22] S.P. Nalawade, F. Picchioni, L.P.B.M. Janssen, Supercritical carbon dioxide as a green solvent for processing polymer melts: Processing aspects and applications, Progress in Polymer Science, 31 (2006) 19-43.

[23] A. Bos, I.G.M. Pünt, M. Wessling, H. Strathmann, Plasticization-resistant glassy polyimide membranes for CO_2/CH_4 separations, Separation and Purification Technology, 14 (1998) 27-39.

[24] S.P. Nalawade, F. Picchioni, J.H. Marsman, L.P.B.M. Janssen, The FT-IR studies of the interactions of CO_2 and polymers having different chain groups, The Journal of Supercritical Fluids, 36 (2006) 236-244.

[25] S.I. Semenova, H. Ohya, S.I. Smirnov, Physical transitions in polymers plasticized by interacting penetrant, Journal of Membrane Science, 136 (1997) 1-11.

[26] J.S. Chiou, D.R. Paul, Effects of CO_2 exposure on gas transport properties of glassy polymers, Journal of Membrane Science, 32 (1987) 195-205.

[27] V.E. Patil, L.J.P. van den Broeke, F.F. Vercauteren, J.T.F. Keurentjes, Permeation of supercritical carbon dioxide through polymeric hollow fiber membranes, Journal of Membrane Science, 271 (2006) 77-85.

[28] A.G. Wonders, D.R. Paul, Effect of CO_2 exposure history on sorption and transport in polycarbonate, Journal of Membrane Science, 5 (1979) 63-75.

6. Performance characterization of polyamide reverse osmosis membranes upon supercritical CO_2 processing[1]

6.1. Introduction

Many applications of solute component separations, including essential oils, fatty acids and caffeine have been investigated along with separation of ethanol and processing of petroleum products using integrated SC-CO_2 extraction – membrane separation processes over the last decade employing organic and inorganic membranes [1-10]. Some of the studies focused on the viscosity effect and transport of SC-CO_2 through the membrane network [11-13]. Most of these studies focused on the permeability and selectivity of membranes under extreme processing conditions associated with the use of SC-CO_2. Although stability is one of the most important factors affecting membrane performance, reports on the stability of membranes processed under supercritical conditions is scarce. Since the use of organic membranes is very popular due to their availability and low cost, stability is even more important if polymer membranes are to be selected for use in coupled SC-CO_2 extraction – membrane systems.

Interactions between CO_2 and polymer structure can adversely affect the membrane performance depending on the polymer material and processing conditions. These interactions were previously reported, targeting different functional groups associated with different polymer materials [14-24]. The effect of SC-CO_2 on polymer membrane structure can be considered in two different parts: swelling behaviour during processing and reorganization of the polymer network upon depressurization. Changes in the physicochemical and morphological properties of two polyamide membranes upon SC-CO_2 processing

[1] A version of this chapter has been submitted for publication. Akin and Temelli 2011. The Journal of Supercritical Fluids.

under different temperature and pressure conditions were previously characterized (Chapters 4 and 5). The objective of this study was to investigate the effect of those morphological and physicochemical changes on the performance of the same two commercial polyamide membranes (AK and SG). The effects of different temperature, transmembrane pressure (ΔP), processing time and depressurization rate conditions during processing were assessed by measuring CO_2 flux and oleic acid retention as indicators of performance and stability.

6.2. Materials and methods

6.2.1. Membranes and materials

Two reverse osmosis (RO) membranes (AK and SG) were kindly provided by GE Osmonics (Minnetonka, MN, USA). The virgin membranes were cleaned as described in Chapter 3 (Section 3.2.1). Detailed characterization of the membranes used in this study was reported previously in Chapter 3, which demonstrated the fully aromatic polyamide structure of AK and the polyesteramide nature of the SG membrane. Oleic acid was obtained from Fischer Scientific (Ottawa, ON, Canada). Bone dry, liquid withdrawal CO_2 was from Praxair Canada Inc. (Mississauga, ON, Canada).

6.2.2. Supercritical system and processing protocols

The flow diagram of the supercritical system was presented in Fig. 5-1. The system was operated according to the protocol described in Chapter 4 (Section 4.2.2). The additional oil separator allowed collection of lipid samples from the permeate upon depressurization.

A two-step protocol was followed for the evaluation of membrane performance under supercritical conditions. In the first step, membranes were processed by passing pure SC-CO_2 through them at different temperatures (40, 60 and 80 °C) and transmembrane pressures (10, 20, 30 and 40 bar) for different periods of time (0, 2, 8 and 24 h). In the second step, the change in performance due to the initial CO_2 processing time and conditions was investigated. Oleic acid

retention and CO_2 flux were determined in the second step as indicators of performance at 120 bar and 40 °C with a ΔP of 10 bar right after pure CO_2 processing with no depressurization in between the two steps.

In order to reveal the effect of depressurization, the system pressure was released to ambient pressure after the first step of SC-CO_2 processing and then followed by repressurization of the system to 120 bar and setting the temperature to 40 °C for the second step of performance evaluation by flux and retention analysis at ΔP of 10 bar.

6.2.2.1. Protocol for SC-CO_2 processing

For SC-CO_2 processing of the membranes, flat plate membranes were carefully placed in the module (Fig. 5-1). Valve V-2 was slowly opened and the system was filled with CO_2 and pressurized slowly (~0.2 bar/sec) to avoid possible compaction in the membrane structure. When the target pressure was reached (120 bar), temperature was set using the heater around the membrane module and the controller it is attached to. Then, valve V-7 was closed to build up the transmembrane pressure (ΔP) by adjusting the back pressure regulator (BPR) (V-8).

Both AK and SG membranes were processed at different temperature (40 and 80 °C) and ΔP conditions (10, 20, 30 and 40 bar) at 120 bar. Membranes were kept under these conditions up to 24 h. Membrane processing at each condition was performed in triplicate.

Potential hysteresis on membrane flux was tested after the system was pressurized to 120 bar at 40 °C and CO_2 flux was monitored with increasing and decreasing ΔP values. ΔP was increased from 10 to 40 bar by 10 bar increments and 1 h processing at each step.

In order to determine the effect of supercritical conditions on membrane performance with no CO_2 transport, membranes were kept in the module at 120 bar and 40 °C for up to 24 h. Then, ΔP was set to 10 bar for CO_2 flux analysis.

6.2.2.2. Protocol for performance determination with CO_2 flux upon depressurization

Processing which involved a depressurization step was only performed at 120 bar 40 °C. Depressurization of the system in between the two processing steps was achieved by closing the valves V-2, V-3 and V-4 and opening V-5, V-7 and V-9 (Fig. 5-1) at two different rates (0.1 and 5 bar/s) after corresponding processing times. This step of the process was performed at the rate of 0.1 bar/s unless specified. Desired depressurization rate was achieved by manually adjusting the BPR. Then, in order to analyze the change in CO_2 flux, the system was repressurized by following the protocol for SC-CO_2 processing without removing the membranes in the module.

Depressurization/repressurization process was repeated up to 4 times to investigate its effect on membrane performance. Depressurization and repressurization were performed as described above. At each step, the system was pressurized 15 min after depressurization. Flux was measured 15 min after the system was repressurized to 120 bar and ΔP was set to 10 bar. At each cycle, membranes were processed with pure CO_2 for 2 h.

CO_2 flux was determined as described in Chapter 5 (Section 5.2.3.4).

6.2.2.3. Protocol for performance determination with oleic acid retention upon depressurization

In order to determine the change in retention performance of the membranes oleic acid was used as the solute component. Initially, oleic acid (30 g) was placed in the extractor and the vessel was pressurized to the set pressure by opening valves V-1, V-2, V-3 while keeping valves V-4 and V-5 closed (Fig. 5-1). Temperature was set to the desired level using the heater around the extractor and the controller it is attached to at the same time when the extractor was being pressurized to the set pressure. Then, valves V-2, V-3 and V-4 were closed and V-5, V-7 and V-9 were opened to depressurize the lines except the extractor. Thus, oleic acid+SC-CO_2 mixture was kept at 120 bar and 40 °C in the vessel, which

was ready to be fed to the membrane module after the system was repressurized as described in the protocol for SC-CO_2 processing. Oleic acid+SC-CO_2 mixture was stirred at least for 3 h before it was fed to the membrane module at operating conditions by closing valve V-5 and opening valves V-3 and V-4.

Oleic acid retention was calculated as described in Chapter 5 (Section 5.2.3.4).

6.2.2.4. Statistical analysis

Data are presented as mean ± standard deviation based on triplicate experiments. Statistical analysis of the data was performed for only depressurization rate results using SPSS software (version 10.0) applying 95% confidence interval.

6.3. Results and discussion

6.3.1. Effect of ΔP

Pure SC-CO_2 transport through two RO membranes was measured at 120 bar and 40 °C to demonstrate the dependence of flux on pressure differential across the membrane. There was a linear increase in flux with ΔP for both membranes with SG membrane showing higher flux levels at each ΔP (Fig. 6-1). No hysteresis was observed with increasing and decreasing ΔP for both membranes.

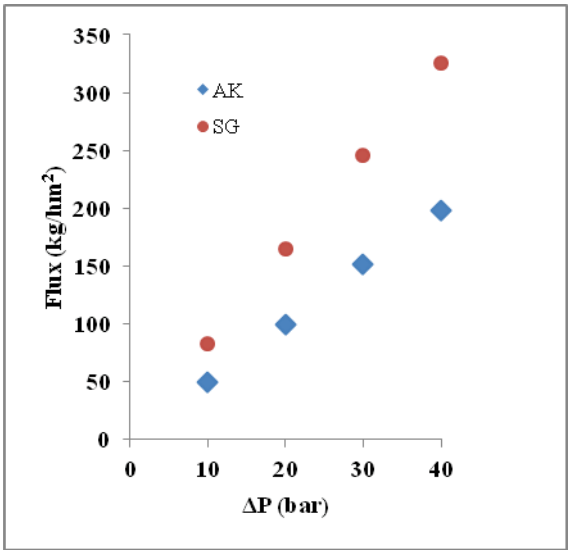

Figure 6-1. CO_2 flux as a function of ΔP at 120 bar and 40 °C for AK and SG membranes

In order to verify the effect of ΔP on flux, membranes were exposed to SC-CO_2 up to 24 h. The effect of processing time on permeate flux at constant ΔP was exhibited in Figs. 6-2a and b for AK and SG membranes, respectively. It was found that flux was reduced compared to the virgin membranes at ΔP values higher than 20 bar after 24 h processing. Although there was no substantial difference in flux after the first hour (%5) upon application of high ΔP values (30 and 40 bar), flux started to decrease after 2 h and remained almost constant after 12 h of processing. The decrease in flux was reduced with decreasing ΔP. That was most likely due to the prominent effect of compaction on membrane structure at high ΔP applications. The reduction in flux was ~20% for both membranes at ΔP of 40 bar whereas it was ~8% for processing at ΔP of 30 bar and there was no substantial difference between the two membranes. Relatively low pressure differential across the membrane, 10 and 20 bar, resulted in an increase in flux (~10%) unlike high ΔP values at the end of 24 h for both membranes.

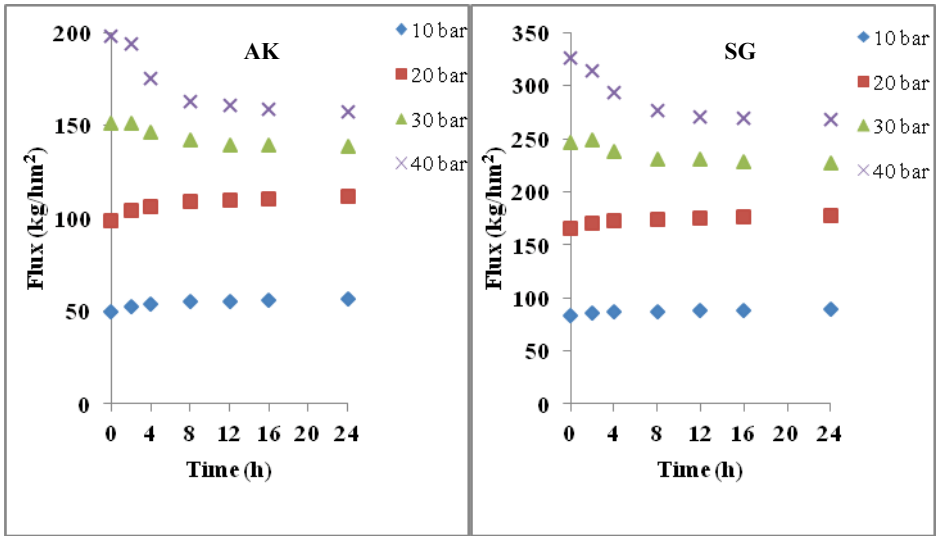

Figure 6-2. CO_2 flux as a function of processing time at different ΔP values for AK and SG membranes at 120 bar and 40 °C.

The reason for the increase in flux for ΔPs of 10 and 20 bar over the 24 h period was probably the interaction of SC-CO_2 with the polymer network, affecting the rigid chains of glassy polymer structures by increasing their mobility. An increase in ΔP increased the permeate flux whereby the amount of CO_2 passing in between the neighbouring chains was increased. Higher CO_2 flux would especially prevent the interaction between carboxyl groups by decreasing the cohesive energy density due to alteration of the polymer structure (Chapter 4). The decrease in flux at high ΔP processing (30 and 40 bar) could be explained by the suppression of swelling behaviour by compaction of the polymer network.

In order to evaluate the change in membrane performance due to compaction, oleic acid retention of both membranes was measured right after processing of the membranes at different ΔP values for up to 24 h (Table 6-1). ΔP was fixed at 10 bar after each membrane was processed for up to 24 h without any depressurization/repressurization to exclude any other effect on membrane structure and the oleic acid was immediately fed to the membrane module for determination of the effect of compaction and/or swelling. All oleic acid retention

results were compared with those for virgin membranes, which were not processed with SC-CO_2 previously.

AK and SG membranes, which were processed for up to 24 h at a ΔP of 10 and 20 bar exhibited retention factors similar to that of the virgin membrane (Table 6-1). Although there was a slight increase in CO_2 flux after 24 h processing, oleic acid retention factors remained almost constant. Membranes processed at ΔP of 30 bar showed relatively higher retention factors than those at 10 and 20 bar due to compaction. The highest retention factor was observed with the membranes processed at ΔP of 40 bar. There was almost no oleic acid collected in the permeate during the first hour of processing. Higher retention factors at greater ΔP values could be due to the prominent compaction of the membrane structure as a result of the high pressure differential applied across the membrane for 24 h.

Processing time was also an important factor on CO_2 flux and oleic acid retention. High ΔP processing (30 and 40 bar) did not show a continuous trend of decrease in flux after 8 h (Fig. 6-2); however, increasing processing time substantially increased oleic acid retention due to intense compaction at high ΔPs of 30 and 40 bar (Table 6-1).

Table 6-1. Oleic acid retention of AK and SG membranes right after processing (without depressurization) at different ΔP conditions up to 24 h at 120 bar and 40 °C.

Membrane		Retention (%)[a]			
	ΔP (bar)	Processing time (h)			
		0	2	8	24
AK					
	10	75 ± 0.8	75 ± 1.2	74 ± 1	73 ± 1.4
	20	75 ± 0.8	75 ± 1.1	73 ± 0.6	73 ± 1.8
	30	75 ± 0.8	76 ± 0.9	78 ± 0.4	80 ± 0.8
	40	75 ± 0.8	77 ± 1.3	81 ± 1.6	88 ± 1.8
SG					
	10	79 ± 1.1	79 ± 1	79 ± 2.1	79 ± 1.8
	20	79 ± 1.1	79 ± 2.2	79 ± 1.5	78 ± 1.5
	30	79 ± 1.1	79 ± 1	82 ± 1.2	85 ± 0.8
	40	79 ± 1.1	80 ± 0.6	86 ± 2.4	90 ± 1.6

[a]: Retention was measured at 120 bar 40 °C immediately after the membranes were processed and the retention factors were calculated upon collecting samples for 2 h. Mean ± standard deviation based on three determinations.

6.3.2. Effect of temperature

Both membranes were exposed to temperatures of 40, 60 and 80 °C at 120 bar and a ΔP of 10 bar for up to 24 h. The change in CO_2 flux was presented for both membranes in Fig. 6-3. CO_2 flux at each temperature was normalized based on the flux obtained at 40 °C for a clear demonstration of the differences due to processing and to avoid the variance of flux due to the slight changes in density/viscosity (ρ/μ) of CO_2 at different temperatures. Thus, results were presented as percentage increase during processing. AK membranes processed at 60 °C showed slightly more increase than membranes processed at 40 °C at the end of 24 h processing unlike SG membranes. The main difference was observed

with membranes processed at 80 °C. There was a substantial increase in flux at the end of 24 h at high temperature for both membranes. Increase in flux at 80 ^{o}C with AK was 45% while it was 25% for SG over that at 40 ^{o}C. That was due to the excess amount of hydrogen bonding in the structure of AK membrane compared to the covalently cross-linked SG membrane. Previously, it was postulated that high temperature processing effect was due to increased thermal energy transferred to the network, which loosened the polymer chain restrictions (Chapter 4). Polymer chain mobility resulted in a higher increase in the flux of AK due to increased distance between the intermolecular hydrogen bonding groups, resulting in a decrease in the degree of interaction between polymer chains.

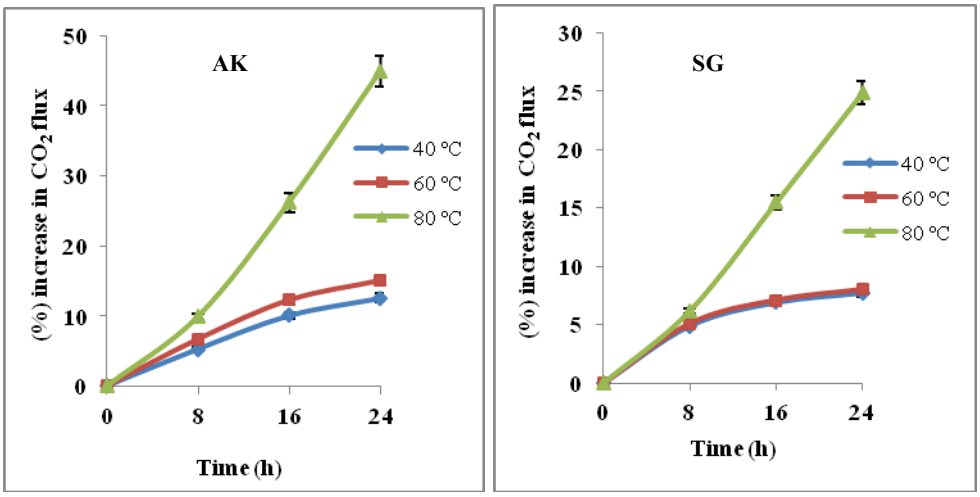

Figure 6-3. CO_2 flux as a function of processing time at different temperatures and 120 bar for AK and SG membranes

In order to analyze the effect of temperature on membrane performance, membrane module temperature was cooled down to 40 °C for subsequent CO_2 flux and oleic acid retention analysis for both membranes after higher temperatures were applied in order to be consistent with performance testing of all the membranes in this study. During the cooling step, flux exhibited a sharp decrease approaching zero because of the sudden contraction in the structures of

both membranes processed at 80 °C. This behaviour was mainly due to sudden cooling over 5 min to set the module temperature to 40 °C. That was an important indication of intense polymer segmental mobility due to temperature changes in the polyamide network. Flux was constant 10 min after the module temperature was set to 40 °C and it was 7.7-13.1% higher than that for virgin AK and SG membranes due to swelling after 24 h processing for both AK and SG membranes processed at 40 and 60 °C (Table 6-2). Membranes processed at 80 °C for 24 h resulted in a relatively higher flux at 40 °C. That was due to high temperature CO_2 processing, which loosened the polymer network, increasing the distance between polymer segments. This structural change was more effective on AK membrane. However, the effect of processing at 80 °C for 24 h on membrane structure was not completely reversible. Expanded polymer structure of both membranes was found to partially move back in their space and contracted when tested at 40 °C. However, flux values were still substantially higher than that for the virgin membranes, 24.2 and 13.9% higher for AK and SG, respectively (Table 6-2).

Oleic acid retention showed similar trends to that of CO_2 flux upon processing the membranes at different temperatures (Table 3). AK membrane exhibited slightly more decrease than SG membrane in terms of the oleic acid retention factor after being processed at 40 and 60 °C. On the other hand, SG membrane was found to be more resistant to higher temperature processing by almost maintaining the same retention factor as that of the virgin SG membranes. Membranes processed at 80 °C exhibited a substantial decrease in oleic acid retention for both membranes upon 8 h processing. After 24 h at 80 ^{o}C, there was a drop of 14% and 8% in oleic acid retention for AK and SG, respectively.

Table 6-2. Increase in CO_2 flux (%) compared to virgin AK and SG membranes right after processing (without depressurization) at different temperature conditions up to 24 h at 120 bar with ΔP of 10 bar.

Membrane		**Flux(%)[a]**		
	T (°C)	**Processing time (h)**		
		2	**8**	**24**
AK				
	40	5.3 ±0.2	10.1 ± 0.2	12.6 ± 0.4
	60	5.5 ± 0.5	10.5 ± 0.1	13.1 ± 0.1
	80	7.3 ± 0.6	16.8 ± 0.9	24.2 ± 0.8
SG				
	40	4.9 ± 0.1	6.3 ± 0.6	7.7 ± 0.4
	60	5 ± 0.1	6.5 ± 0.3	8 ± 0.3
	80	5.5 ± 0.3	7.4 ± 0.2	13.9 ± 0.7

[a] Flux was measured 15 min after the system temperature reached 40 °C at 120 bar, immediately after corresponding processing time and temperature. Mean ± standard deviation based on three determinations.

6.3.3. Effect of depressurization

Although operating temperature and ΔP are in the range of common membrane separations, high feed pressures are unique to membrane applications with SC-CO_2. The effect of CO_2 on polymer structures was investigated previously [17, 24]. Adverse effects of high pressure CO_2 resulting in swelling and plasticization in membrane structure has been one of the challenging factors limiting the use of supercritical fluids with polymer membrane applications. Another important issue, which must be taken into consideration with high pressure applications is depressurization of the system upon completion of the separation process. Especially high pressure drops might result in severe damage to the polymer structure, which in turn would affect membrane efficiency. Many blisters or microstructures might be formed by irreversible deterioration of the membrane structure upon sudden drop in pressure, which is referred to as

'explosive deterioration failure' (XDF) [25]. The resistance of a polymer network to XDF is related to physicochemical properties of polymer structure and operating conditions.

Table 6-3. Oleic acid retention factor of AK and SG membranes right after processing at different temperature conditions up to 24 h at 120 bar with ΔP of 10 bar.

Membrane		**Retention (%)**[a]		
	T (°C)	**Processing time (h)**		
		2	**8**	**24**
AK				
	40	75 ± 0.8	74 ± 0.6	73 ± 1.2
	60	75 ± 1.1	73 ± 0.2	71 ± 0.5
	80	72 ± 1.8	66 ± 1.3	58 ± 2.4
SG				
	40	79 ± 1.1	79 ± 1.3	79 ± 0.6
	60	79 ± 2.1	79 ± 2.4	79 ± 1.9
	80	77 ± 0.2	73 ± 2	69 ± 1.1

[a] Oleic acid retention factor was measured 15 min after the system temperature reached 40 °C at 120 bar, immediately after corresponding processing time and temperature. Mean ± standard deviation based on three determinations.

In order to evaluate the behaviour of polyamide membranes upon depressurization, AK and SG membranes were processed at 120 bar and 40 °C for various processing times prior to depressurization. Different depressurization rates were also applied to determine the resistance of the polyamide network. The effect of depressurization was analyzed in terms of the effect on CO_2 flux and oleic acid retention upon reuse of the membranes under supercritical conditions.

Depressurization of membranes was applied after 2, 8 and 24 h processing at 120 bar and 40 °C. Then, flux was measured at 120 bar and 40 °C at a ΔP of 10

bar following repressurization and the results are presented in Fig. 6-4. The lowest increase in flux was observed with SG membranes processed for 2 h. The increase in flux was greater with increasing processing time for both membranes and it levelled off after 8 h (Fig. 6-4).

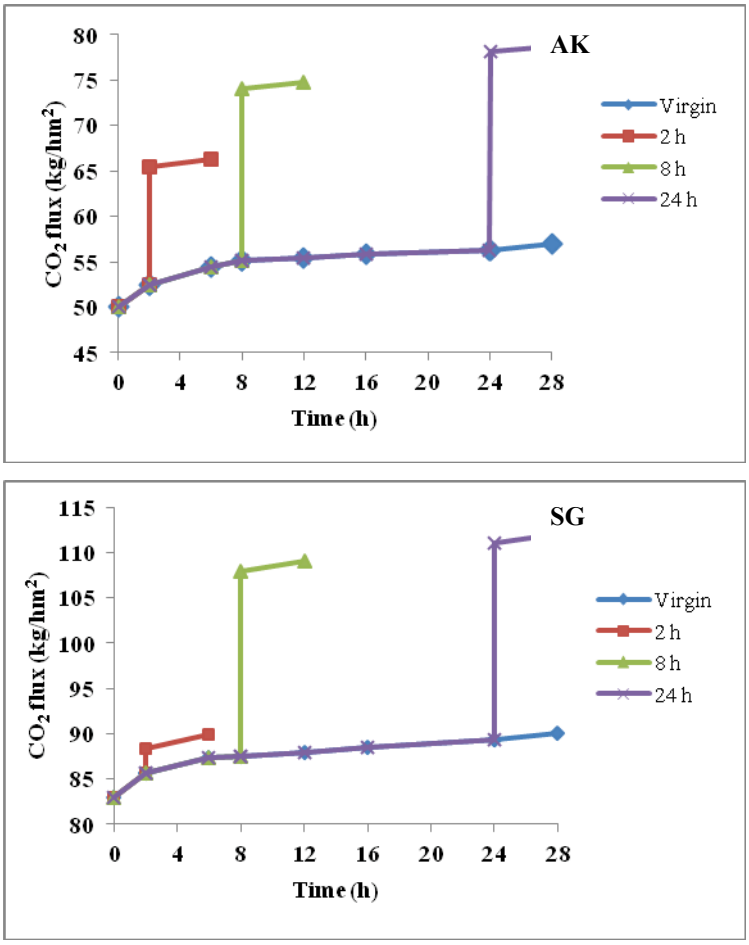

Figure 6-4. Effect of processing time on CO_2 flux upon depressurization at 120 bar and 40 °C for AK and SG membranes

The highest increase was observed with AK membranes processed for 24 h. At each processing time, SG membrane exhibited a lower increase in flux compared to AK membrane upon depressurization. At the end of 24 h processing, flux was increased by 54% and 33% for AK and SG, respectively, upon depressurization/repressurization. Although hydrogen bonds are known to provide robust structures, depressurization was found to have a severe effect on the

reorganization of the polyamide network resulting in a much higher CO_2 flux. Covalently cross-linked structure of SG membrane proved to be more resistant to the depressurization effect.

In order to determine the effect of depressurization rate on membrane performance, two different rates were tested. The system was depressurized from 120 bar at the rates of 0.1 and 5 bar/s for both membranes. CO_2 flux (Table 6-4) and oleic acid retentions (Table 6-5) of AK and SG were compared after depressurization. The different depressurization rates applied did not result in any substantial difference in flux or oleic acid retention for both membranes. These results showed that faster expansion of CO_2 would not cause greater deterioration of the polymer networks investigated in this study.

Table 6-4. Increase in CO_2 flux (%) compared to virgin membranes upon depressurization at different rates for both membranes after different processing times at 120 bar and 40 °C at ΔP of 10 bar

Membrane		**Flux***		
	Rate (bar/s)	**Processing time (h)**		
		2	**8**	**24**
AK				
	0.1	31% ± 1.6[a]	50% ± 4.2[b]	55% ± 2.8[b]
	5	33% ± 2.1[a]	54% ± 2.3[b]	59% ± 3.3[b]
SG				
	0.1	6% ± 2.5[c]	30% ± 2.4[d]	33% ± 2.7[d]
	5	6% ± 1.6[c]	32% ± 3.3[d]	32% ± 4.6[d]

* Flux was measured 15 min after the system was repressurized to 120 bar at 40 °C, after corresponding processing time and depressurization. Mean ± standard deviation based on three determinations.

[a-d] Means with different superscript letters are significantly different ($p<0.05$) for each membrane.

Table 6-5. Oleic acid retention factors upon depressurization at different rates for both membranes after different processing times at 120 bar and 40 °C at ΔP of 10 bar.

Membrane		**Retention (%)**[a]		
	Rate (bar/s)	**Processing time (h)**		
		2	**8**	**24**
AK				
	0.1	70 ± 1.6	67 ± 1.9	66 ± 1.5
	5	70 ± 2.1	65 ± 1.1	64 ± 1.6
SG				
	0.1	78 ± 1.8	74 ± 0.4	73 ± 1.2
	5	78 ± 2.2	74 ± 0.3	72 ± 1.9

[a] Oleic acid retention factor was measured 15 min after the system was repressurized to 120 bar at 40 °C by collecting oleic acid samples for 2 h, after corresponding processing time and depressurization. Mean ± standard deviation based on three determinations.

Oleic acid retention factors showed that there was no explicit damage in the structures of membranes causing blisters or microvoid formation. Depressurization most likely caused formation of new Langmuir sorption sites or enlargement of the existing ones as stated by Wonders and Paul [26]. Since the decrease in oleic acid retention factor after high temperature processing was much more prominent than other conditions, enlargement or expansion of existing Langmuir sorption sites rather than the formation of new ones could be the reason in that case.

The most important parameter affecting membrane performance was found to be CO_2 transport across the membrane. When the membranes were left in the module up to 24 h with no flux, there was no difference in flux upon depressurization. Thus, SC-CO_2 processing time was very important for the reorganization of polymer structure when there was CO_2 transport across the membrane. Although SG membrane was proven to be more resistant to

supercritical conditions compared to the AK membrane, processing times of up to 8 h was long enough to observe a change in membrane performance via CO_2 flux and oleic acid retention upon depressurization.

Membranes were processed at 120 bar 40 °C for 2 h to determine the effect of repeated depressurization/repressurization cycles on membrane flux at a ΔP of 10 bar. As depicted in Fig. 6-5, flux exhibited an increase after each step for both membranes but the degree of increase was higher with the AK membrane. The overall increase in CO_2 flux after the fourth cycle was more than 2 fold for AK membrane whereas it was only 20% more for the SG membrane (Fig. 6-5). This result indicated that reuse of the same polyamide membrane by repressurization of the feed streams would be affecting the performance by reorganization of the polymer network on each cycle upon CO_2 transport and depressurization.

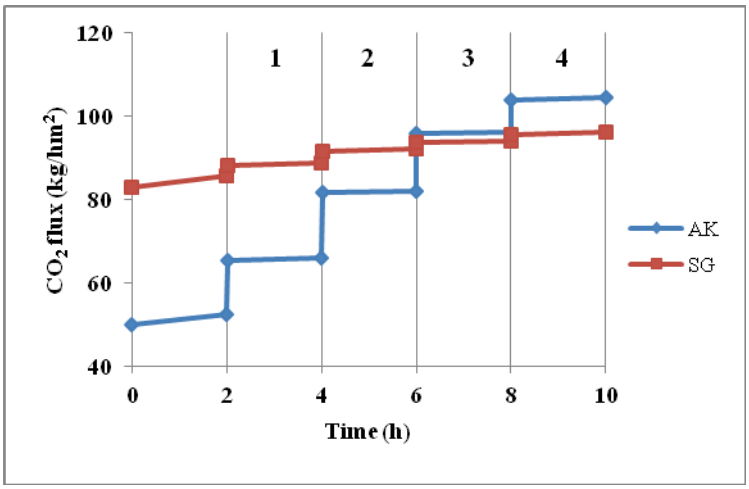

Figure 6-5. Effect of repeated depressurization/repressurization cycles on membrane flux at 120 bar and 40 °C and ΔP of 10 bar

6.4. Conclusions

The effects of different temperature, transmembrane pressure, time and depressurization on the performance and stability of polyamide membranes during

SC-CO_2 processing were investigated. Although CO_2 flux showed a linear increase with increasing ΔP, processing time was found to be an important factor affecting membrane performance at ΔPs of 30 and 40 bar. Membrane structures were adversely affected due to compaction at high ΔP resulting in lower flux and higher oleic acid retention rates measured immediately after processing. Temperature was another important parameter, which loosened the polymer chains and expanded the polymer network. AK membrane was affected to a greater extent than the covalently cross-linked SG membrane due to the excess hydrogen bonding in its structure upon exposure to high temperature. Processing at 80 °C caused partially irreversible changes in membrane structure resulting in lower oleic acid retentions when tested at mild conditions right after processing.

Depressurization of the system caused reorganization of the polymer network most likely via expansion of existing Langmuir sorption sites or formation of new ones. Processing time had a prominent effect on reorganization by causing an increase in CO_2 flux upon depressurization. Oleic acid retention was not affected as much as CO_2 flux most likely due to slight changes in Langmuir sorption sites, which were more effective on transport of much smaller CO_2 molecules than oleic acid. Application of depresurization/repressurization cycles was tested to simulate the potential effects on reuse of the same membrane material. It was demonstrated that polyamide structure continued to expand with each cycle applied, resulting in higher CO_2 flux than the previous one. This was an important indication of the fact that polyamide-based membranes tested in this study were not stable under supercritical conditions, especially upon application of depressurization. Although the two depressurization rates tested did not show a significant difference for both membranes, changes in the flux and retention were found to be substantial enough to question the stability of the membranes to be used during SC-CO_2 applications. However, relatively more resistant structure of the covalently cross-linked SG membrane could possibly be used as a model to develop more stable membranes targeting SC-CO_2 applications.

6.5. References

[1] C.B. Spricigo, A. Bolzan, R.A.F. Machado, L.H.C. Carlson, J.C.C. Petrus, Separation of nutmeg essential oil and dense CO_2 with a cellulose acetate reverse osmosis membrane, Journal of Membrane Science, 188 (2001) 173-179.

[2] L.H.C. Carlson, A. Bolzan, R.A.F. Machado, Separation of d-limonene from supercritical CO_2 by means of membranes, The Journal of Supercritical Fluids, 34 (2005) 143-147.

[3] J.M.L.N. de Moura, L.A.G. Gonçalves, L.A.V. Sarmento, J.C.C. Petrus, Purification of structured lipids using $SCCO_2$ and membrane process, Journal of Membrane Science, 299 (2007) 138-145.

[4] L.A.V. Sarmento, C.B. Spricigo, J.C.C. Petrus, L.H.C. Carlson, R.A.F. Machado, Performance of reverse osmosis membranes in the separation of supercritical CO_2 and essential oils, Journal of Membrane Science, 237 (2004) 71-76.

[5] A. Pietsch, W. Hilgendorff, O. Thom, R. Eggers, Basic investigation of integrating a membrane unit into high-pressure decaffeination processing, Separation and Purification Technology, 14 (1998) 107-115.

[6] L.A.V. Sarmento, R.A.F. Machado, J.C.C. Petrus, T.R. Tamanini, A. Bolzan, Extraction of polyphenols from cocoa seeds and concentration through polymeric membranes, The Journal of Supercritical Fluids, 45 (2008) 64-69.

[7] S. Sarrade, C. Guizard, G.M. Rios, New applications of supercritical fluids and supercritical fluids processes in separation, Separation and Purification Technology, 32 (2003) 57-63.

[8] S.J. Sarrade, G.M. Rios, M. Carlès, Supercritical CO_2 extraction coupled with nanofiltration separation: Applications to natural products, Separation and Purification Technology, 14 (1998) 19-25.

[9] W. Artz, T. Kinyanjui, M. Cheryan, Deacidification of soybean oil using supercritical fluid and membrane technology, Journal of the American Oil Chemists' Society, 82 (2005) 803-808.

[10] S.I. Semenova, H. Ohya, T. Higashijima, Y. Negishi, Separation of supercritical CO_2 and ethanol mixtures with an asymmetric polyimide membrane, Journal of Membrane Science, 74 (1992) 131-139.

[11] V.E. Patil, J. Meeuwissen, L.J.P. van den Broeke, J.T.F. Keurentjes, Permeation of supercritical fluids across polymeric and inorganic membranes, The Journal of Supercritical Fluids, 37 (2006) 367-374.

[12] V.E. Patil, L.J.P. van den Broeke, F.F. Vercauteren, J.T.F. Keurentjes, Permeation of supercritical carbon dioxide through polymeric hollow fiber membranes, Journal of Membrane Science, 271 (2006) 77-85.

[13] A.W. Verkerk, P. van Male, M.A.G. Vorstman, J.T.F. Keurentjes, Properties of high flux ceramic pervaporation membranes for dehydration of alcohol/water mixtures, Separation and Purification Technology, 22-23 (2001) 689-695.

[14] S. Kanehashi, T. Nakagawa, K. Nagai, X. Duthie, S. Kentish, G. Stevens, Effects of carbon dioxide-induced plasticization on the gas transport properties of glassy polyimide membranes, Journal of Membrane Science, 298 (2007) 147-155.

[15] A. Bos, I.G.M. Pünt, M. Wessling, H. Strathmann, CO_2-induced plasticization phenomena in glassy polymers, Journal of Membrane Science, 155 (1999) 67-78.

[16] J.H. Petropoulos, Plasticization effects on the gas permeability and permselectivity of polymer membranes, Journal of Membrane Science, 75 (1992) 47-59.

[17] A.F. Ismail, W. Lorna, Penetrant-induced plasticization phenomenon in glassy polymers for gas separation membrane, Separation and Purification Technology, 27 (2002) 173-194.

[18] S.P. Nalawade, F. Picchioni, J.H. Marsman, L.P.B.M. Janssen, The FT-IR studies of the interactions of CO_2 and polymers having different chain groups, The Journal of Supercritical Fluids, 36 (2006) 236-244.

[19] S.I. Semenova, H. Ohya, S.I. Smirnov, Physical transitions in polymers plasticized by interacting penetrant, Journal of Membrane Science, 136 (1997) 1-11.

[20] N.M.B. Flichy, S.G. Kazarian, C.J. Lawrence, B.J. Briscoe, An ATR−IR study of poly (dimethylsiloxane) under high-pressure carbon dioxide: Simultaneous measurement of sorption and swelling, The Journal of Physical Chemistry B, 106 (2001) 754-759.

[21] J.D. Wind, S.M. Sirard, D.R. Paul, P.F. Green, K.P. Johnston, W.J. Koros, Relaxation dynamics of CO_2 diffusion, sorption, and polymer swelling for plasticized polyimide membranes, Macromolecules, 36 (2003) 6442-6448.

[22] W.J. Koros, M.W. Hellums, Gas separation membrane material selection criteria: Differences for weakly and strongly interacting feed components, Fluid Phase Equilibria, 53 (1989) 339-354.

[23] P. Vitoux, T. Tassaing, F. Cansell, S. Marre, C. Aymonier, In situ IR spectroscopy and ab initio calculations to study polymer swelling by supercritical CO_2, The Journal of Physical Chemistry B, 113 (2009) 897-905.

[24] J.S. Chiou, D.R. Paul, Effects of CO_2 exposure on gas transport properties of glassy polymers, Journal of Membrane Science, 32 (1987) 195-205.

[25] S.A.E. Boyer, M.-H. Klopffer, J. Martin, J.-P.E. Grolier, Supercritical gas–polymer interactions with applications in the petroleum industry. Determination of thermophysical properties, Journal of Applied Polymer Science, 103 (2007) 1706-1722.

[26] A.G. Wonders, D.R. Paul, Effect of CO_2 exposure history on sorption and transport in polycarbonate, Journal of Membrane Science, 5 (1979) 63-75.

7. Membrane separation of lipids using supercritical CO_2 as a solvent[1]

7.1. Introduction

Supercritical carbon dioxide (SC-CO_2) is a great alternative to replace organic solvents used for the extraction and recovery of high-value components due to its tunable dissolving power. SC-CO_2 has advantages over organic solvents regarding its low viscosity and high diffusivity properties. Easy removal from extracted components makes its use very promising due to more strict environmental regulations. On the other hand, recompression of gaseous CO_2 to SC-CO_2, and the need for powerful compression equipment are major drawbacks for the implementation of this technology [1].

Integration of a membrane separation unit with SC-CO_2 extraction process will lead to a reduction of the operating costs related to recompression of CO_2 gas to the supercritical conditions upon recycling and enhance overall process efficiency. SC-CO_2 extraction of lipids is a well-known technology and is already commercialized for some specialty oil applications [2, 3]. Many applications of lipid component separations, including fatty acids and triacylglycerols have been reported using this coupled process over the last decade employing organic and inorganic membranes [1, 4-12]. Besides, the use of SC-CO_2 as a solvent was proven to increase the flux via reducing the viscosity during transport through the membrane [9].

Polymer membranes are more commonly used over inorganic membranes due to their availability and lower cost. Most of the polymer membranes used with the current investigations under SC-CO_2 conditions has been commercial

[1] A version of this chapter will be submitted for publication. Akin and Temelli 2011. Journal of American Oil Chemists' Society.

thin film polyamide reverse osmosis (RO) membranes produced by interfacial polymerization.

Although there are several examples of this coupled technology employing food- related processes, membrane fouling is still one of the major problems faced during separations. In order to prove the advantages of the coupled process and demonstrate its potential not only for separation of lipids from CO_2 but also for the separation of different lipid components, more information is needed regarding the use of SC-CO_2, lipids and polymer membranes to reveal the effect of processing on the efficiency of separation. Therefore, the main goal of this study was to investigate the performance of five different commercial polymer membranes for the separation of oleic acid (OA) and triacylglycerol (TAG). The specific objectives were to determine CO_2 flux, oleic acid retention, total lipid yield and TAG separation factor over time for each membrane for better understanding of membrane performance under supercritical conditions. The effect of pure SC-CO_2 addition on membrane fouling was also evaluated during processing of lipid components.

7.2. Materials and methods

7.2.1. Membranes and materials

Five commercially available membranes, AK, SG, HL, DL, CE were kindly provided by GE Osmonics Inc. (Minnetonka, MN, USA). Physicochemical and morphological structures of these membranes were characterized in detail in previous studies [13-15]. The virgin membranes were cleaned according to protocols described in Chapter 3 (Section 3.2.1). Oleic acid was obtained from Fischer Scientific (Ottawa, ON, Canada). Bone dry CO_2 (99.9% purity) with liquid withdrawal dip tube was from Praxair Canada Inc. (Mississauga, ON, Canada). Canola oil purchased from a local store was used as the TAG source (>99% TAG content, containing oleic, linoleic and linolenic acids as the major fatty acids).

7.2.2. Processing procedures

The flow diagram of the modified supercritical system was presented in Fig. 5-1 and operation protocols were described in section 5.2.2.

7.2.3. SC-CO_2 + OA experiments

7.2.3.1. Processing

Oleic acid retention experiments were done as explained in section 5.2.3.4.

Potential hysteresis on membrane flux was tested after the system was pressurized to 120 bar at 40 °C and CO_2 flux was monitored with increasing and decreasing ΔP values. ΔP was increased from 10 to 40 bar by 10 bar increments and 1 h processing at each step.

In order to investigate the effect of fouling, oleic acid transport through the vessel was stopped after 2 h and 8 h of filtration by closing V-3 and V-4 and pure CO_2 was fed to the membrane module by opening valve V-5. Then, CO_2 flux was measured before and after feeding oleic acid to the system for all membranes upon 2 and 8 h processing. Then, ΔP was increased from 10 to 40 bar by 10 bar increments and 5 min processing at each step to determine the CO_2 flux at each ΔP. No cleaning was performed prior to the measurement of flux.

In order to determine the effect of pure SC-CO_2 addition on membrane fouling, SC-CO_2 was periodically added during oleic acid retention experiments performed using the SG membrane. Two hours after oleic acid was fed to the membrane module, valves V-3 and V-4 were closed and V-5 was opened. SC-CO_2 was fed for 30 min at the same pressure and temperature (120 bar, 40 °C) as oleic acid retention experiments while applying a ΔP of 10 bar. At the end of 30 min, V-5 was closed, and V-3 and V-4 were opened to feed oleic acid again to the membrane module. This process was repeated 3 times for up to 8 h of oleic acid processing and 1.5 h of pure SC-CO_2 addition. Flux was measured and recorded at the end of each hour during processing up to the total of 9.5 h processing.

7.2.3.2. Determination of CO_2 flux and oleic acid retention

Oleic acid retention and CO_2 flux were determined as described in Chapter 5 (Section 5.2.3.4).

7.2.4. SC-CO_2 + TAG + OA experiments

7.2.4.1. Processing

In an effort to determine the composition of the lipid mixture fed to the membrane module a relatively simpler system was used as shown in Fig. 7-1. The membrane module was disconnected and the samples were collected after they were dissolved in SC-CO_2 at different conditions. A total of 30 g lipid mixture (50:50, wt%) of OA+TAG was placed in the extraction vessel. Then, the vessel was pressurized by opening valves V-1, V-2 and V-3 while V-4 and V-5 were closed. When the pressure reached the desired level, V-3 was closed. Temperature was maintained constant at 40 °C at 120 bar. The OA+TAG+SC-CO_2 mixture was stirred at constant temperature and pressure for at least 3 h. Then, V-4 was slowly opened and the tubing between V-4 and V-5 was filled with the dissolved mixture. Next, V-4 was closed and V-5 was slowly opened to depressurize and collect the sample in the oil separator.

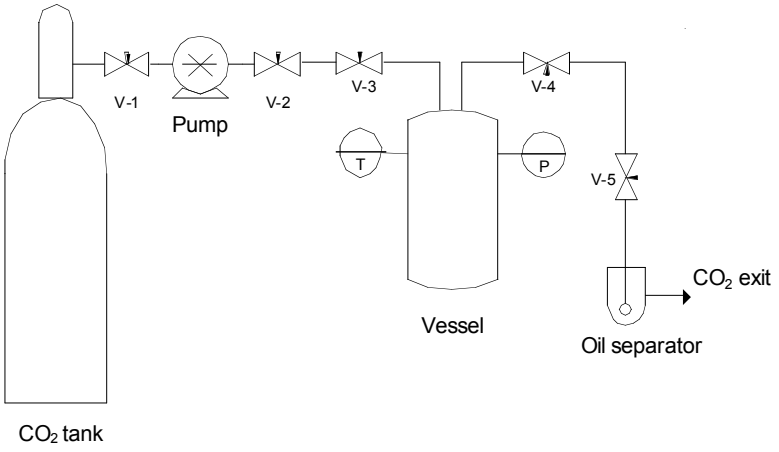

Figure 7-1. Flow diagram of the supercritical CO_2 extraction system

TAG and oleic acid mixture was then used to determine the separation efficiency of the membranes. In this case, the original coupled SC-CO_2 extraction – membrane separation system (Fig. 5-1) was employed. Oleic acid - TAG mixture was placed in the vessel. The same procedure of oleic acid retention experiments was applied during separation of the lipid mixture. The mixture was first dissolved in SC-CO_2 at 120 bar and 40 °C in the vessel before it was fed to the membrane module at a ΔP of 10 bar. Thus, inlet feed concentration to the membrane module was adjusted to be 50/50 (w/w) on a CO_2-free basis by initially placing 30 g mixture with a weight percentage of 78% TAG and 22% oleic acid in the vessel. Permeate lipid mixture from the module was collected until 100 L CO_2 permeated at ambient conditions. Total lipid yield was determined by weighing the samples collected upon depressurization at the end of this process after each membrane was tested.

2.4.2. Determination of TAG separation factor and total lipid yield

An automatic 'cool on column' injection gas chromatograph (GC, Varian 3400, Varian Inc., Walnut Creek, CA, USA) equipped with a flame ionization detector was used for the determination of oleic acid and TAG content of the samples.

Samples were silylated prior to injection to GC in order to increase the volatility of the components. Silylation was done using the method of Verleyen *et al.* [16] with some modification. Briefly, 10 mg of sample was weighed in a screw-capped test tube, and 50 µL of dilaurin (20 mg/mL chloroform) was added as an internal standard for the quantification of oleic acid and TAGs. The sample and internal standard mixture was dissolved in 0.5 mL of pyridine and 100 µL of *N*,*O*-bis-(trimethylsilyl)trifluoracetamide (BSTFA) containing 1% trimethyl-chlorosilane (TMCS) solution was added as silylation agent. Then, test tubes were placed in an oven at 70 °C for 20 min for completion of the silylation reaction. Samples were diluted with 1 mL of chloroform. Finally, 1 mL of silylated sample was transferred into a GC vial for injection onto the column.

An aliquot (1µL) was injected via automated cool on column injection onto a Restek MTX-Biodiesel TG column (15 m × 0.32 mm ID × 0.10 µm film thickness; Restek Corp., Bellefonte, PA, USA) with a retention gap (2 m × 0.53 mm ID). Hydrogen was used as the carrier gas at a head pressure of 103.4 kPa. Injector temperature was programmed from 70 °C to 340 °C at 150 °C/min, and held for 25 min. Column temperature was programmed with an initial hold at 50 °C for 1 min, followed by an initial increase to 180 °C at 15 °C/min, then another increase from 180 °C to 230 °C at 7 °C/min, and a final increase from 230 °C to 380 °C at 30 °C/min, and held for 8.2 min. Detector temperature was set at 380 °C.

In order to determine the efficiency of separation towards TAGs, a separation factor was used as defined by Semenova [12] in Eq. (7-2)

$$\alpha = \frac{Cpt}{Cft} \quad (7\text{-}2)$$

where C_{pt} and C_{ft}, represent the concentration (%, w/w) of TAG in the permeate and feed on CO_2-free basis, respectively. Higher retention of TAG compared to oleic acid by a particular membrane would lead to $\alpha<1$.

Total lipid amount in the permeate was collected up to 100 L CO_2 (measured at ambient conditions) transported through each membrane and samples were weighed and lipid amounts were recorded in triplicate experiments.

7.3. Results and Discussion

7.3.1. CO_2 flux and OA retention determination

Five different polymer membranes were tested under SC-CO_2 processing conditions. CO_2 flux was measured at 120 bar and 40°C with increasing ΔP values from 10 to 40 bar to assess the possibility of hysteresis. None of these commercial membranes were designed to work under supercritical conditions. Cellulose acetate membrane (CE) did not exhibit any flux at these conditions. Most probably the excess amount of OH groups present in the CE membrane structure

prevented CO_2 transport under the processing conditions investigated. CO_2 flux of the remaining four polyamide-based membranes was presented in Fig. 7-2, which showed a linear increase with ΔP. No hysteresis was observed for the membranes upon 1 h processing at each ΔP condition. HL membrane exhibited the highest flux while DL had the lowest.

Retention experiments were performed at the same conditions by using pure oleic acid. ΔP was fixed at 10 bar for all membranes during processing. The retention factors were presented for all four membranes in Fig. 7-3 as a function of processing time up to 8 h. Retention factor for the SG membrane was found to be more stable over time than that for the other membranes. Oleic acid retention was initially 79% for the SG membrane and did not show a substantial difference (<10%) up to 8 h processing. The retention factors obtained with AK and HL membranes showed a prominent decrease with processing time. Oleic acid retention gradually decreased from 75% to 45% for AK after 8 h whereas that for the HL membrane dropped from 76% to 30% within 4 h and then remained almost constant up to 8 h. DL membrane exhibited relatively different retention behaviour. Oleic acid retention gradually increased and reached 100% at the end of 6 h processing. Decrease in oleic acid retention with processing time for AK and HL membranes was probably due to the interactions between oleic acid and membrane structure. Hydrophilic end of oleic acid molecules could be interacting with the hydrophilic groups of the membrane leaving the hydrophobic ends of oleic acid molecules free throughout the structure. Since structure of AK and HL membranes are relatively more hydrophilic compared to SG membrane, this would most probably be the reason for unstable oleic acid retention factors during processing.

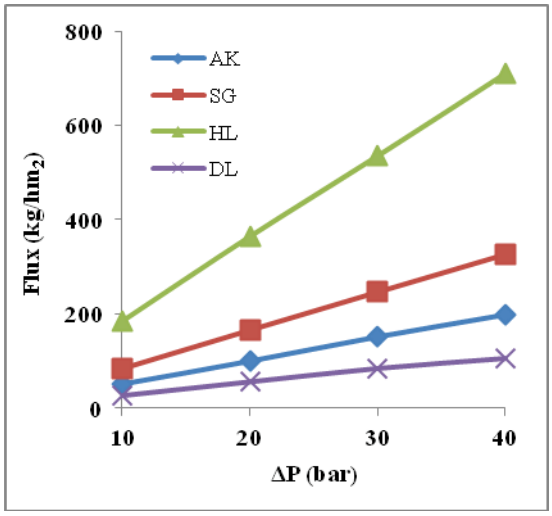

Figure 7-2. CO_2 flux as a function of ΔP at 120 bar and 40 °C for AK, SG, HL and DL membranes

The permeate CO_2 flux showed a decrease with processing time for all four membranes (Fig. 7-4). The lowest CO_2 flux was observed with DL membrane, which approached almost zero after 6 h processing. That was most probably the result of increasing oleic acid retention (Fig. 7-3), causing fouling on the membrane surface. Relatively lower initial CO_2 flux for DL membrane probably prevented the oleic acid transport resulting in its accumulation on the top surface, leading to concentration polarization. Although SG membrane exhibited the most stable retention factor, CO_2 flux showed a prominent drop to 30% of the initial value after 8 h. AK membrane exhibited relatively less decrease in flux (30%) up to 8 h processing compared to SG. The flux for HL membrane showed a substantial drop during the first 2 h of processing and then remained almost constant. Decrease in CO_2 flux for SG membrane was much smaller compared to the data reported by Carlson *et al.* [1]. This was most probably due to the use of essential oils in their experiments, resulting in much higher feed concentrations under similar processing conditions.

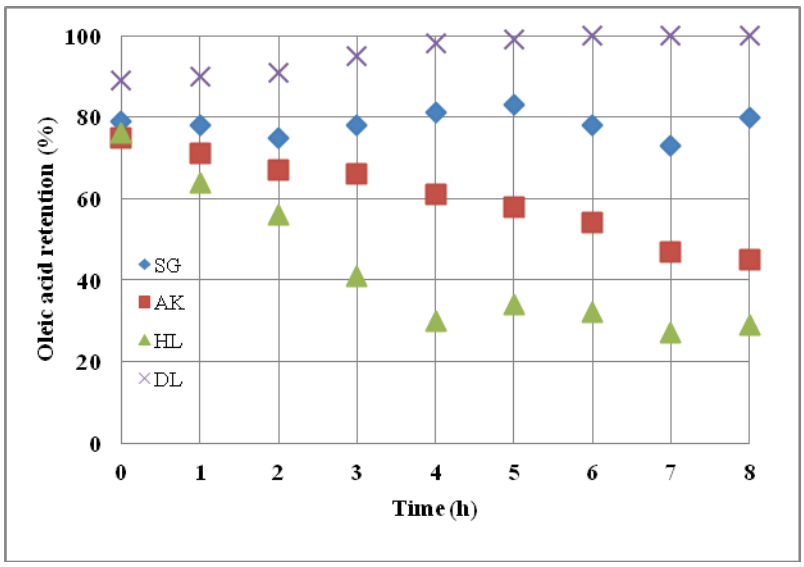

Figure 7-3. Oleic acid retention factor as a function of processing time for AK, SG, HL and DL membranes at 120 bar, 40 °C with ΔP of 10 bar

In this study, lower feed concentrations were reached due to the lower solubility of oleic acid compared to essential oils at 120 bar and 40 °C, which caused clogging of the membranes over longer processing times. Besides, formation of an additional lipid layer on top could be another important factor changing the nature of CO_2 – membrane interactions, leading to more complicated membrane – OA – CO_2 interactions.

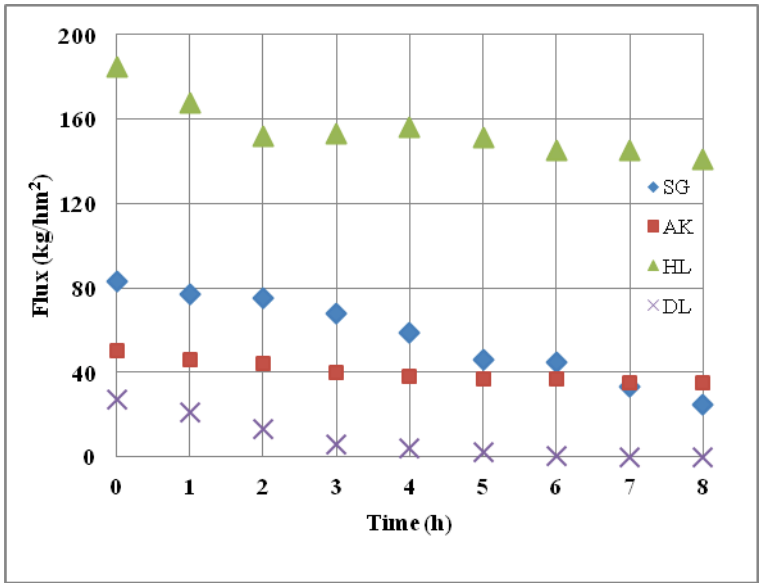

Figure 7-4. CO_2 flux as a function of processing time during oleic acid transport at 120 bar, 40 °C with ΔP of 10 bar

Accumulation of oleic acid on the membrane with time was expected, considering the dead-end filtration module employed. The degree of fouling on the membranes was assessed by the effect of ΔP on CO_2 flux. It was found that CO_2 flux was smaller than that for the virgin membranes and decreased with increasing processing time for all membranes (Fig. 7-5). The flux did not increase linearly with ΔP, which was in contrast with the virgin membranes where the flux increase with ΔP was linear. That was a clear indication of fouling of the membranes..

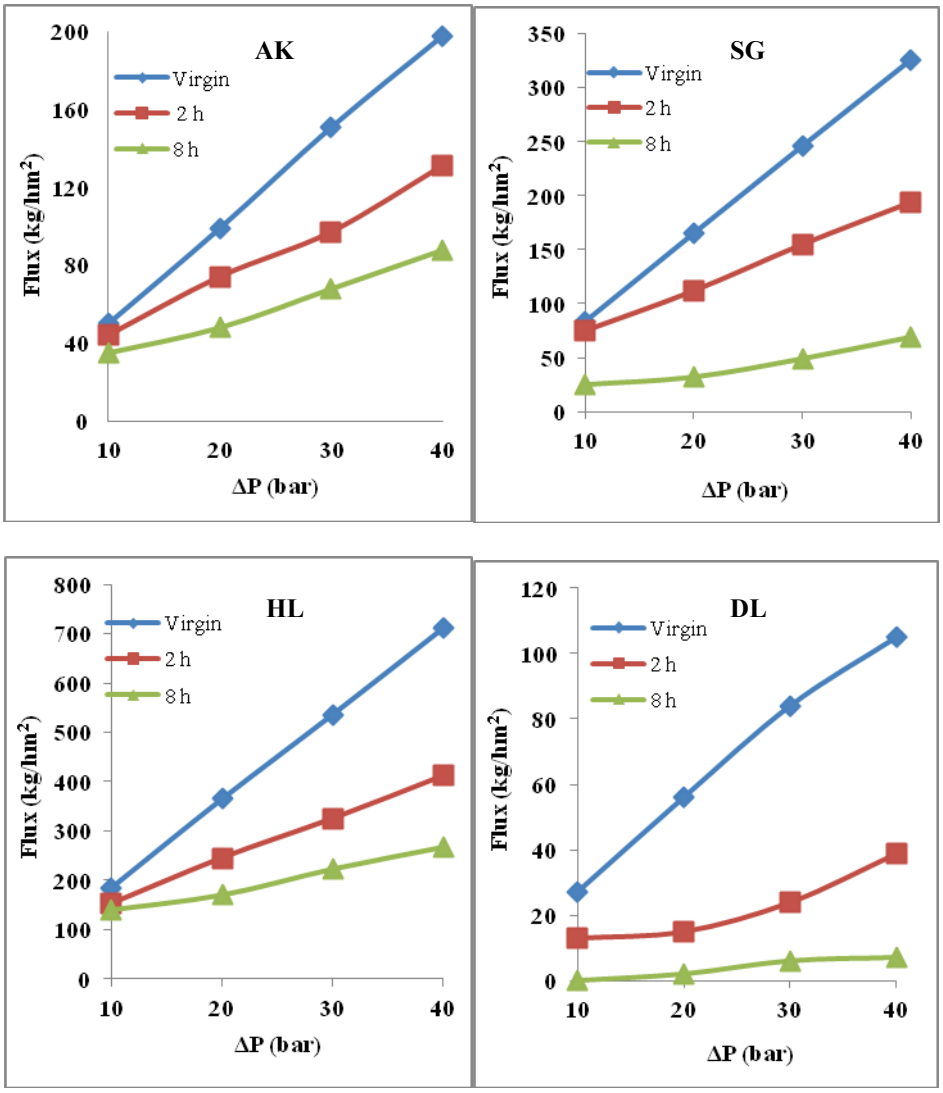

Figure 7-5. Dependence of SC-CO_2 flux on ΔP upon processing with oleic acid up to 8 h at 120 bar, 40 °C with ΔP of 10 bar.

Decreasing CO_2 flux during processing was the major drawback with SG membrane. In order to avoid the decrease in flux, pure SC-CO_2 was fed to the system for 30 min periods after every 2 h of processing. ΔP value of 10 bar was tested with pure SC-CO_2. Fig. 7-6 showed that periodic feeding of pure SC-CO_2 prevented the substantial drop in CO_2 flux. When pure CO_2 was added periodically, CO_2 flux was more than 3 times higher than that with no CO_2 addition at the end of 9.5 h processing. That was most probably due to cleaning of

the membrane structure causing a delay in oleic acid accumulation on the surface of the membrane.

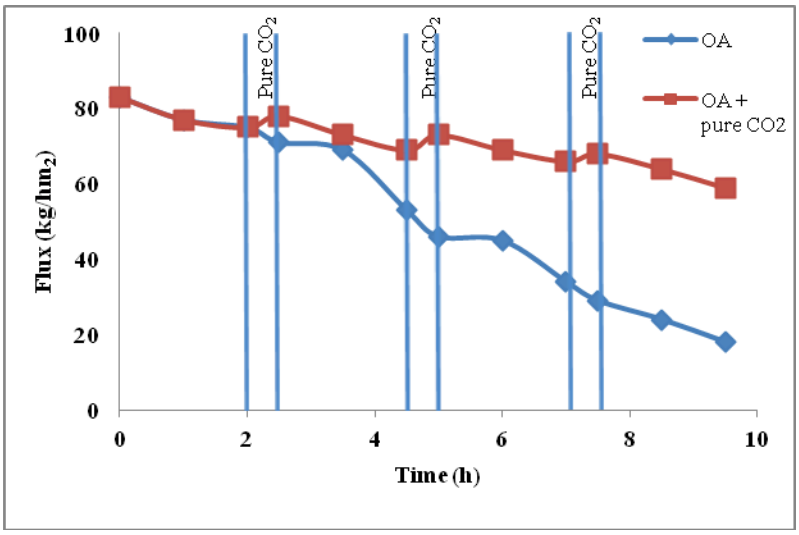

Figure 7-6. Effect of periodic (0.5 h) pure SC-CO_2 addition on CO_2 flux during oleic acid processing up to 8 h.

7.3.2. TAG separation factor and lipid yield determination

In order to evaluate the separation performance of the membranes a mixture of TAG and oleic acid (50/50 w/w) was fed to the membrane module at 120 bar and 40 °C with a ΔP of 10 bar for each membrane. Separation factor of $\alpha<1$ represented the higher retention of TAG compared to oleic acid by the corresponding membrane. Separation factors for AK, SG and HL were found to be similar and much smaller than that for the DL membrane (Fig. 7-7). Lipid yield was calculated as the total amount of lipid collected upon depressurization of the permeate stream per 100 L CO_2 (measured at ambient conditions) used during processing. Yields were exhibited for each membrane in Fig. 7-8. DL membrane had the lowest yield among all the membranes tested. HL and SG showed similar yields whereas yield of AK membrane was relatively smaller. SG membrane exhibited a lower separation factor for TAG compared to the other membranes. HL membrane had a slightly lower separation factor than that of AK. It also had a

reasonably high yield, which made it as promising as SG membrane for the separation of this lipid mixture. On the other hand, decreasing oleic acid retention factor of HL membrane during processing did not make it desirable for this separation.

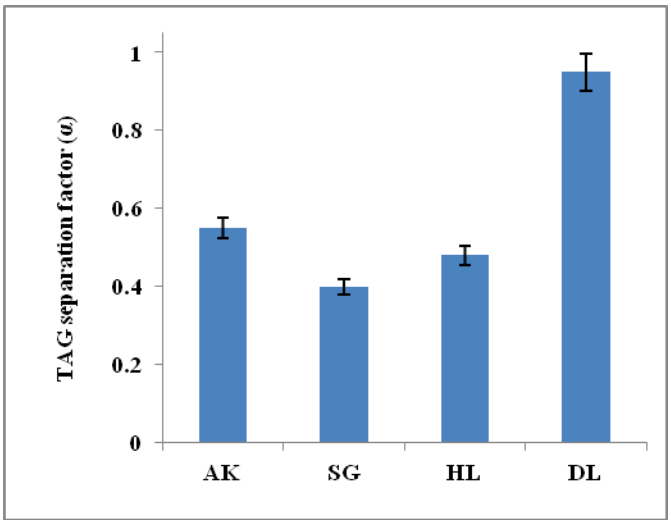

Figure 7-7. TAG separation factor for AK, SG, HL and DL membranes during separation of OA/TAG mixture (50/50 w/w). Error bars are based on 3 determinations.

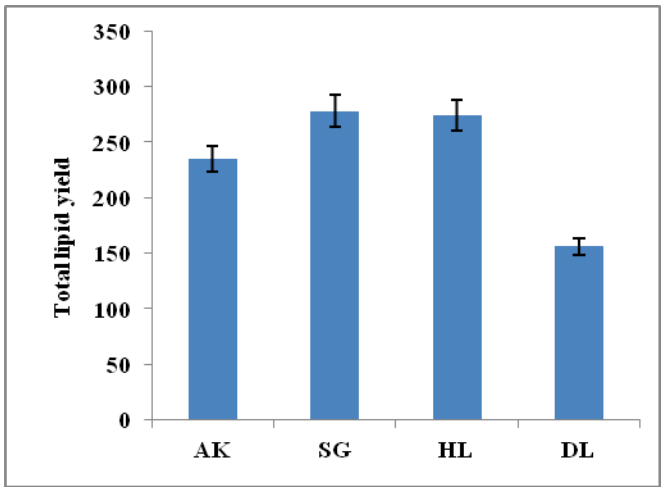

Figure 7-8. Total lipid yield (mg) at the end of 100 L CO_2 collected at the permeate for AK, SG, HL and DL membranes at 120 bar, 40 °C and ΔP of 10 bar. Error bars are based on 3 determinations.

7.4. Conclusions

All membranes except CE demonstrated CO_2 flux under supercritical conditions. DL membrane was not preferred due to the low TAG retention and low CO_2 flux. Among all the membranes tested, SG was found to be the only membrane, which exhibited consistent oleic acid retention throughout 8 h of processing. That was most probably due to presence of lipid molecules, like oleic acid, interacting with the membrane and thus altering the CO_2 – membrane interactions. Although permeate CO_2 flux showed a gradual decrease due to fouling of the membrane in the dead-end module, pure CO_2 introduction over short periods was shown to be effective in elimination of this drawback. Low TAG separation factor and reasonable yield of SG membrane made it the best choice for TAG/oleic acid separation among all the membranes tested at 120 bar and 40 °C. Integrating a high pressure membrane module equipped with the SG membrane into SC-CO_2 processing would add to the selective solubilisation of SC-CO_2 while maintaining the stability and separation efficiency throughout the process.

7.5. References

[1] L.H.C. Carlson, A. Bolzan, R.A.F. Machado, Separation of d-limonene from supercritical CO_2 by means of membranes, The Journal of Supercritical Fluids, 34 (2005) 143-147.

[2] F. Temelli, Perspectives on supercritical fluid processing of fats and oils, The Journal of Supercritical Fluids, 47 (2009) 583-590.

[3] F. Sahena, I.S.M. Zaidul, S. Jinap, A.A. Karim, K.A. Abbas, N.A.N. Norulaini, A.K.M. Omar, Application of supercritical CO_2 in lipid extraction - A review, Journal of Food Engineering, 95 (2009) 240-253.

[4] C.B. Spricigo, A. Bolzan, R.A.F. Machado, L.H.C. Carlson, J.C.C. Petrus, Separation of nutmeg essential oil and dense CO_2 with a cellulose acetate reverse osmosis membrane, Journal of Membrane Science, 188 (2001) 173-179.

[5] J.M.L.N. de Moura, L.A.G. Gonçalves, L.A.V. Sarmento, J.C.C. Petrus, Purification of structured lipids using $SCCO_2$ and membrane process, Journal of Membrane Science, 299 (2007) 138-145.

[6] L.A.V. Sarmento, C.B. Spricigo, J.C.C. Petrus, L.H.C. Carlson, R.A.F. Machado, Performance of reverse osmosis membranes in the separation of supercritical CO_2 and essential oils, Journal of Membrane Science, 237 (2004) 71-76.

[7] A. Pietsch, W. Hilgendorff, O. Thom, R. Eggers, Basic investigation of integrating a membrane unit into high-pressure decaffeination processing, Separation and Purification Technology, 14 (1998) 107-115.

[8] L.A.V. Sarmento, R.A.F. Machado, J.C.C. Petrus, T.R. Tamanini, A. Bolzan, Extraction of polyphenols from cocoa seeds and concentration through polymeric membranes, The Journal of Supercritical Fluids, 45 (2008) 64-69.

[9] S. Sarrade, C. Guizard, G.M. Rios, New applications of supercritical fluids and supercritical fluids processes in separation, Separation and Purification Technology, 32 (2003) 57-63.

[10] S.J. Sarrade, G.M. Rios, M. Carlès, Supercritical CO_2 extraction coupled with nanofiltration separation: Applications to natural products, Separation and Purification Technology, 14 (1998) 19-25.

[11] W. Artz, T. Kinyanjui, M. Cheryan, Deacidification of soybean oil using supercritical fluid and membrane technology, Journal of the American Oil Chemists' Society, 82 (2005) 803-808.

[12] S.I. Semenova, H. Ohya, T. Higashijima, Y. Negishi, Separation of supercritical CO_2 and ethanol mixtures with an asymmetric polyimide membrane, Journal of Membrane Science, 74 (1992) 131-139.

[13] C.Y. Tang, Y.-N. Kwon, J.O. Leckie, Probing the nano- and micro-scales of reverse osmosis membranes--A comprehensive characterization of physiochemical properties of uncoated and coated membranes by XPS, TEM, ATR-FTIR, and streaming potential measurements, Journal of Membrane Science, 287 (2007) 146-156.

[14] C.Y. Tang, Y.-N. Kwon, J.O. Leckie, Effect of membrane chemistry and coating layer on physiochemical properties of thin film composite polyamide RO and NF membranes: II. Membrane physiochemical properties and their dependence on polyamide and coating layers, Desalination, 242 (2009) 168-182.

[15] C.Y. Tang, Y.-N. Kwon, J.O. Leckie, Effect of membrane chemistry and coating layer on physiochemical properties of thin film composite polyamide RO and NF membranes: I. FTIR and XPS characterization of polyamide and coating layer chemistry, Desalination, 242 (2009) 149-167.

[16] T. Verleyen, R. Verhe, L. Garcia, K. Dewettinck, A. Huyghebaert, W. De Greyt, Gas chromatographic characterization of vegetable oil deodorization distillate, Journal of Chromatography A, 921 (2001) 277-285.

8. Effect of feed pressure on separation of lipid mixtures using supercritical CO_2 – membrane separation coupled system[1]

8.1. Introduction

Polymer membranes are economically more feasible than inorganic membranes. However, there is no polymer membrane commercially produced for SC-CO_2 applications. In order to maintain the highest efficiency throughout the separation for a particular process; the interactions among the polymer membrane, solute and solvent should be well understood. Especially, tunable properties of SC-CO_2 will most likely result in potential changes in such interactions depending on its density. Although several studies have reported on the characterization of commercial polymer membranes [1-3] studies focusing on the separation performance of membranes under SC-CO_2 conditions have been scarce. Therefore, the aim of this study was to investigate the effect of different pressure conditions of SC-CO_2 during the separation of oleic acid from a model mixture of oleic acid (OA) – triacylglycerol (TAG) using four commercially available polymer membranes on membrane performance, which was assessed in terms of CO_2 flux, OA retention, TAG/OA separation factor and total lipid yield in the permeate stream.

8.2. Materials and methods

8.2.1. Membranes and materials

Four polyamide based membranes, AK, SG, HL and DL were kindly provided by GE Osmonics Inc. (Minnetonka, MN, USA). Those membranes were previously characterized in detail in terms of their physicochemical properties (Chapter 3, [2, 3]). The virgin membranes were cleaned according to protocols described in Chapter 3 (Section 3.2.1). Oleic acid was obtained from Fischer

[1] A version of this chapter will be submitted. Akin and Temelli 2011. Separation and Purification Technology.

Scientific (Ottawa, ON, Canada). Bone dry CO_2 (99.9% purity) with liquid withdrawal dip tube was from Praxair Canada Inc. (Mississauga, ON, Canada). Canola oil purchased from a local store was used as a source of TAG (>99% TAG content containing oleic, linoleic and linolenic acids as the major fatty acids).

8.2.2. Determination of feed concentration to the membrane module

The concentration of the feed stream to the membrane module was determined using a simple system equipped with the extraction vessel but not the membrane module as described previously in Chapter 7 (Fig. 7-1). A 30 g lipid mixture (50% OA and 50% TAG (w/w)) was placed in the high pressure vessel and the vessel was pressurized by opening valves V-1, V-2 and V-3 while V-4 and V-5 were closed. When the pressure was set V-3 was closed. Temperature was maintained constant at 40 °C at all pressures tested (120, 200 and 280 bar). The mixture was stirred at set pressure at least for 2 h. Then, V-4 was slowly opened and the tubing between V-4 and V-5 was filled with the dissolved mixture. Next, V-4 was closed and V-5 was slowly opened to collect the sample in the oil separator upon depressurization. The concentrations of OA and TAG in the collected sample were determined as described later.

8.2.3. Procedure to run the coupled system

The flow diagram of the coupled system was presented in Fig. 5-1. The operating protocols of the system were similar to those described in Chapter 5 (Section 5.2.2). Oleic acid retention experiments were carried out as described in Chapter 7.

8.2.4. Determination of CO_2 flux and oleic acid retention

CO_2 flux and oleic acid retention was determined as previously described in Chapter 5 (Section 5.2.3.4).

In order to investigate the effect of fouling on ΔP, flux was held constant initially by setting ΔP at 10 bar. Then, ΔP was increased to keep the flux constant throughout processing. Two different pressures were tested (120 and 280 bar).

Experiments were continued until ΔP reached 30 bar and processing time for each condition was noted with increasing ΔP.

SC-CO_2 was periodically added during oleic acid retention experiments by using SG membrane at 120 and 280 bar to determine the effect of pure SC-CO_2 processing on membrane fouling. Two hours after oleic acid was fed to the membrane module, valves V-3 and V-4 were closed and V-5 was opened. SC-CO_2 was fed for 30 min at the same pressure and 40 °C with a ΔP of 10 bar. At the end of 30 min, V-5 was closed, and V-3 and V-4 were opened. This process was repeated 3 times up to 8 h of oleic acid processing and 1.5 h pure SC-CO_2 addition. Flux was measured and recorded at the end of each hour during processing up to the total of 9.5 h.

8.2.5. Determination of separation factor and total lipid yield

8.2.5.1. Processing

A total of 30 g mixture consisting of 50% OA and 50% TAG (w/w) was placed in the vessel for separation of TAG and yield experiments. The procedure performed with oleic acid was repeated for the separation of the mixture by feeding the SC-CO_2 + OA + TAG mixture to the membrane module. Pressure levels of 120 and 280 bar were tested.

8.2.5.2. Analysis of permeate

An automatic 'cool on column' injection gas chromatograph (GC, Varian 3400, Varian Inc., Walnut Creek, CA, USA) equipped with a flame ionization detector was used for the determination of oleic acid and TAGs in the permeate stream. The protocols used were similar to those described in Chapter 7 (Section 7.2.4.2).

In order to determine the efficiency of operation towards TAGs, a separation factor was used as defined by Semenova [4] in Eq. (8-1).

$$\alpha = \frac{\%Cpt}{\%Cft} \quad (8\text{-}1)$$

where C_{pt} and C_{ft}, represent the concentration (%, w/w) of TAG in the permeate and feed streams, respectively, on a CO_2-free basis. Higher retention of TAG compared to oleic acid by a particular membrane would lead to $\alpha<1$. Total lipid amount in the permeate was collected up to 100 L CO_2 (measured at ambient conditions) transported through each membrane and samples were weighed and lipid amounts were recorded.

8.3. Results and Discussion

8.3.1. Feed composition to the membrane module

A mixture of 50% oleic acid and 50% TAG (% w/w) was placed in the extraction vessel to determine the concentration of each component in the extract at the different operating conditions investigated. Three different pressures were tested (120, 200 and 280 bar) at 40 °C to determine its effect on the composition of the SC-CO_2 extract obtained (Table 8-1). Oleic acid concentration was the highest at the lowest pressure tested. That was due to the relatively smaller size of OA compared to TAG (MW_{OA}=282 g/mol and $MW_{Triolein}$=885 g/mol). Triolein can be taken to represent the TAGs present in the canola oil used in this study, considering that oleic acid the major fatty acid in canola oil. Solubilities of triolein and oleic acid increase with increasing CO_2 density in a binary mixture [5] as reported earlier by Guclu-Ustundag and Temelli. As expected, increasing pressure increased the concentration of TAG in the extract (Table 8-1).

Table 8-1. OA/TAG concentration of lipid extract at three different pressures (120, 200 and 280 bar) at 40 °C

Pressure (bar)	OA (%, w/w)	TAG (%, w/w)
120	87	13
200	67	33
280	58	42

Results showed that SC-CO_2 can be used to selectively extract the components by changing the CO_2 density. In addition, size difference between the OA and TAG molecules provides a potential opportunity to separate them using a membrane system. When the extract was then fed into the membrane module, OA permeated due to its relatively smaller size as discussed later. Integration of SC-CO_2 extraction and membrane separation for separation of lipid mixtures requires optimization of the processing conditions for each individual unit operation.

8.3.2. CO_2 flux and oleic acid retention

Four NF/RO membranes, AK, SG, HL and DL were tested for potential use in TAG/OA separations. Feed pressure and temperature were set at 120 bar and 40°C, respectively, during OA retention and CO_2 flux measurements. ΔP was adjusted to 10 bar during processing for all membranes. HL exhibited the highest CO_2 flux while DL had the lowest during 50 L CO_2 passing through the membrane and measured at ambient conditions (Fig. 8-1).

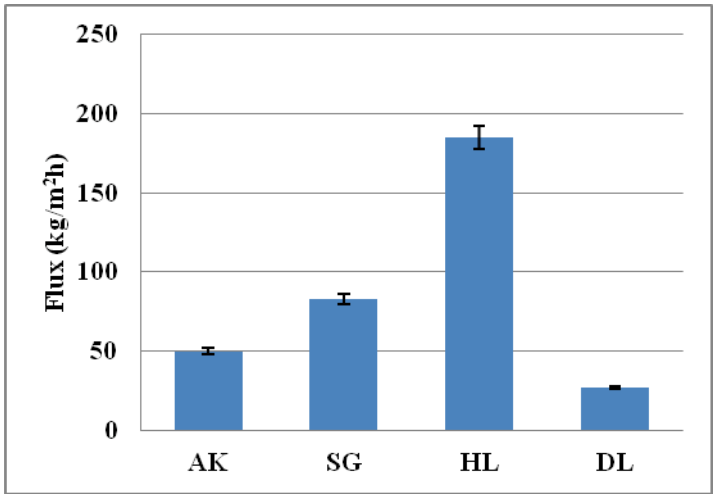

Figure 8-1. CO_2 flux of polymer membranes at 120 bar and 40 °C with ΔP of 10 bar. Error bars based on 3 determinations.

OA was used to assess the retention performance of the membranes. The oleic acid retention factor for AK, SG and HL were similar whereas the DL

membrane had a relatively much higher retention factor than the other membranes at 120 bar (Fig. 8-2).

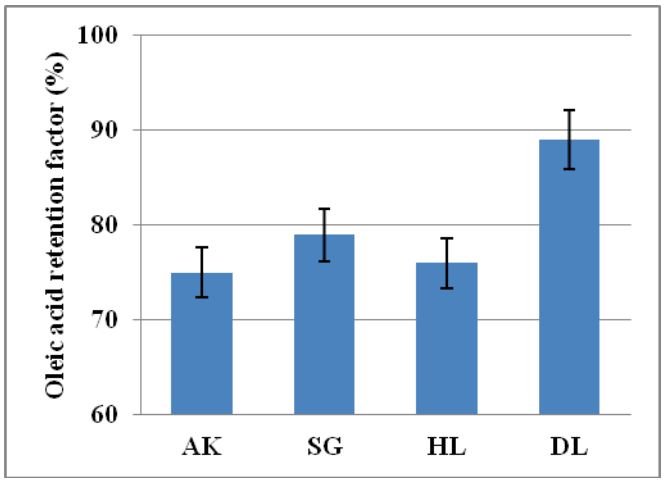

Figure 8-2. Oleic acid retention of polymer membranes at 120 bar and 40 °C with ΔP of 10 bar. Error bars based on 3 determinations.

Two different feed pressures (120 and 280 bar) were applied during retention experiments. Increasing the feed pressure resulted in a higher oleic acid concentration in the feed stream passing to the module. It is known that increasing CO_2 pressure increases the density, which in turn increases the solubility of oleic acid in CO_2 [5]. Greater accumulation of the solutes on membrane surface takes place especially when dead-end modules are used. Relatively lower CO_2 flux and higher oleic acid retention prevented the use of DL membrane at 280 bar most probably due to fouling of the membrane. Therefore, remaining experiments were performed using AK, SG and HL membranes.

8.3.3. OA/TAG mixture processing

One of the most important problems associated with membrane separation systems is fouling caused by accumulation of solute material on membrane surface and/or clogging of membrane pores. Fouling much more prominently occurs when dead-end filtration systems are used. An increase in feed pressure from 120 bar to 280 bar increases the solubility of the OA/TAG mixture in SC-

CO_2. In order to maintain the constant flux of 10 bar during processing, the change in ΔP with time was shown at 120 and 280 bar (Fig. 8-3). ΔP had to be increased at a much higher pace reaching 30 bar after 4 h of processing at 280 bar while it took more than 12 h to reach the same pressure difference at 120 bar. Higher pressure processing required higher ΔP values to keep the CO_2 flux at a constant level due to a substantial increase in the concentration of OA in the feed stream.

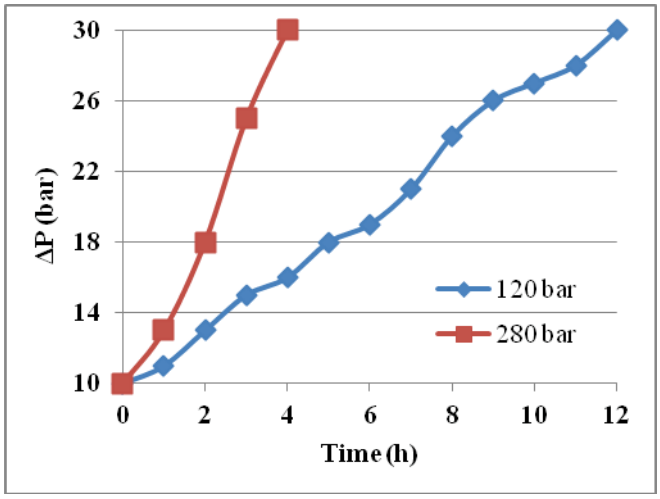

Figure 8-3. Change of ΔP during constant flux processing of SG membranes at 40 °C at two different pressures (120 and 280 bar) during OA/TAG mixture processing

Pure SC-CO_2 added periodically during OA/TAG separation at 120 and 280 bar to exhibit the effect of pure CO_2 addition on CO_2 flux at constant ΔP of 10 bar and the results are presented in Figure 8-4. Decrease in CO_2 flux was delayed substantially with pure CO_2 addition at 120 bar. On the other hand, there was a dramatic decrease in CO_2 flux at 280 bar (Fig. 8-4). In addition to the increase in the amount of solute components at 280 bar, higher TAG concentration in the feed stream caused a substantial increase in the accumulation of solute materials on the membrane surface. Periodic addition of pure CO_2 throughout separation at 280 bar did not show any promising effect to prevent

fouling. CO_2 flux remained almost the same compared with the process with no CO_2 addition.

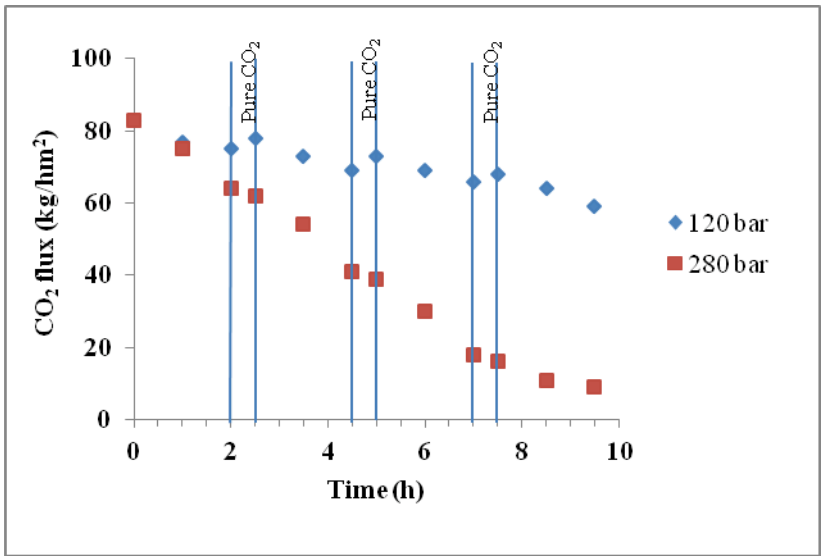

Figure 8-4. Effect of periodic (half hour) pure SC-CO_2 addition on CO_2 flux for SG membrane at different feed pressures during OA/TAG processing up to 8 h at 40 °C and ΔP of 10 bar

8.3.4. Determination of separation factors and total yield

As expected, increasing CO_2 density by increasing pressure at constant temperature (40 °C) decreased the selective solubilisation of oleic acid by increasing the concentration of TAG in the extracted mixture. In order to determine the effect of extraction pressure on the membrane separation process, AK, SG and HL membranes were used during the experiments. The effect of pressure and thus CO_2 density and composition of feed mixture on separation factor and total lipid yield was investigated.

Oleic acid separation factor (α_{OA}) was expected to be higher than 1 indicating higher concentration of oleic acid in the permeate stream whereas TAG separation factor (α_{TAG}) was expected to be less than 1 to exhibit greater retention of the relatively larger TAG molecules for an efficient separation. Separation factors of the membranes at two different feed pressures were depicted in Figs. 8-5a and b for TAG and OA separation factors, respectively. Both OA and TAG

separation factors showed a substantial drop with an increase in pressure from 120 to 280 bar. SG membrane showed almost no selectivity at 120 bar and proved to be not useful for OA/TAG separation at this pressure. HL membrane showed the highest α_{OA} and the lowest α_{TAG} and was the most efficient membrane for separation at 120 bar. Unlike at 120 bar, SG membrane's separation performance was similar to that of HL, which was substantially better than that of AK at 280 bar.

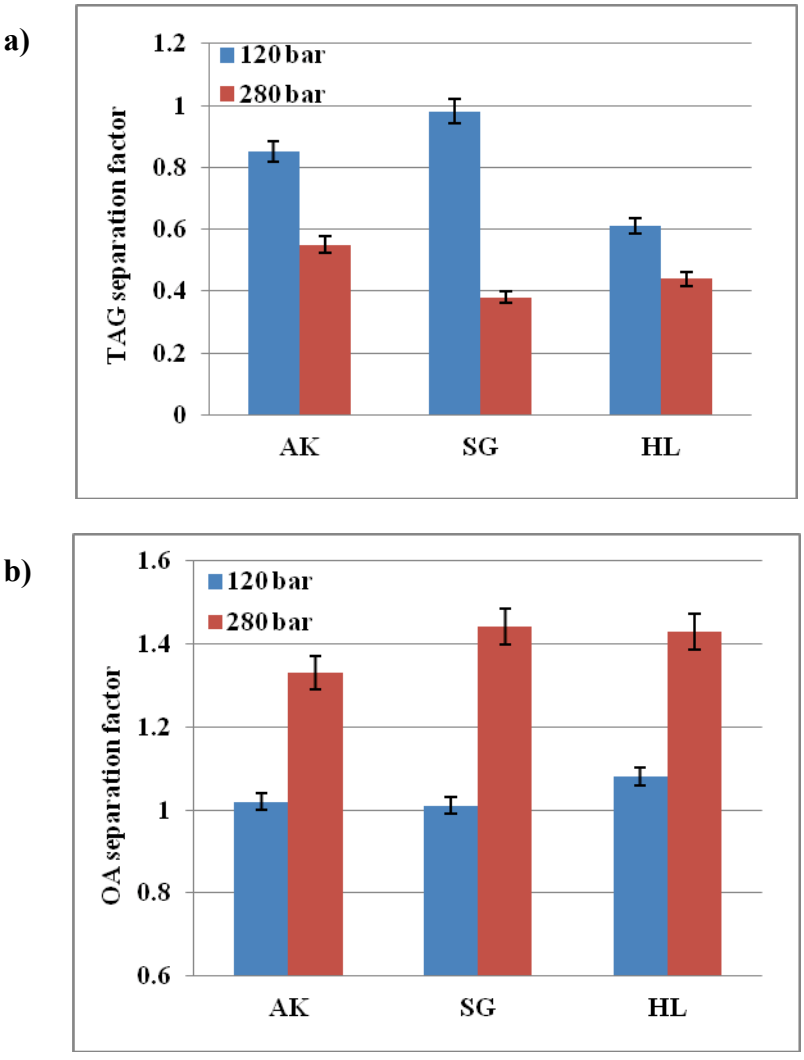

Figure 8-5. TAG (a) and OA (b) separation factors for AK, SG and HL membranes at two different pressures (120 and 280 bar) at 40 °C and ΔP of 10 bar. Error bars are based on 3 determinations.

The amounts of OA and TAG placed in the extraction vessel were kept constant and the mixture concentration reaching the membrane was changed due to the application of two different pressures. Thus, different concentrations fed to the membrane module were another important factor, which might have affected membrane performance throughout processing. Lower pressure extraction resulted in much higher OA concentration in the feed to the membrane module, which was most likely one of the reasons decreasing the efficiency of the membranes, possibly due to the interactions between the oleic acid and the membranes.

The overall effect of coupled SC-CO_2 extraction and membrane separation on oleic acid and TAG concentration in the permeate stream was exhibited in Fig. 8-6. HL and SG membranes were found to be the most efficient membranes during separation, which provided the lowest TAG and the highest OA concentrations in the permeate at 120 and 280 bar, respectively. The concentrations of the permeate streams were shown for HL and SG membranes, indicating the effect of each individual unit operation on the final concentration of the permeate after processing at 120 bar and 280 bar, respectively. The effect of membrane separation was much more prominent at higher pressures whereas SC-CO_2 effect was more dominant at lower pressures. Overall, processing at 120 bar provided the most efficient separation based on OA/TAG concentration of 92/8 (%, w/w) compared to 84/16 (%, w/w) at 280 bar processing. Although OA concentration in the permeate stream was substantially increased, multi-stage system usage might be necessary to increase the degree of separation.

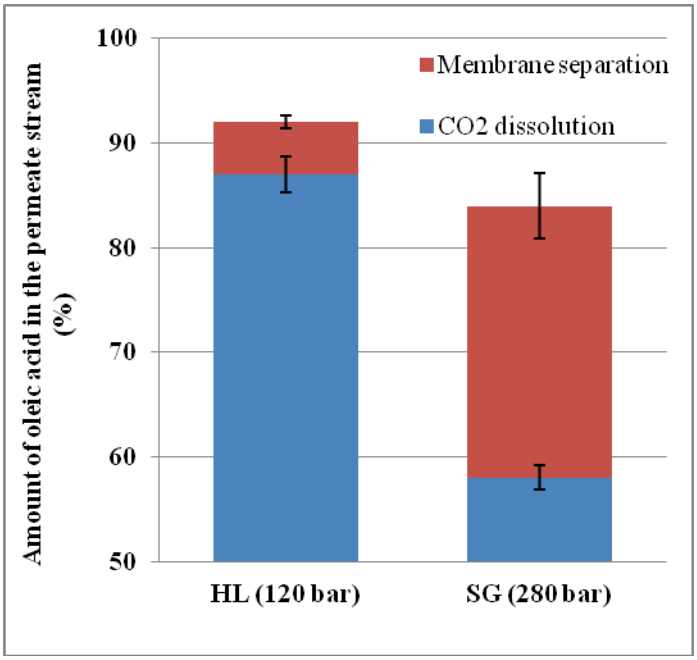

Figure 8-6. Effect of SC-CO_2 dissolution and membrane separation on oleic acid concentration in the permeate stream at 40 °C and ΔP of 10 bar for HL and SG membranes at 120 and 280 bar, respectively. Error bars based on 3 determinations.

An increase in pressure also resulted in prominent differences in total lipid yield (Fig. 8-7). Solubility of the mixture in SC-CO_2 increased substantially with pressure, which in turn increased the amount of lipids passing through the membrane. The highest yield at 280 bar was obtained with SG membrane, which was more than 7 fold higher compared to that at 120 bar. Total lipid yield increased by about 5 fold for AK and HL membranes when the pressure was increased to 280 bar. SG membrane was found to be the most efficient membrane due to its high separation factors and reasonable yield at 280 bar. On the other hand, HL membrane showed the best performance in terms of separation factors and had similar yield with SG at 120 bar.

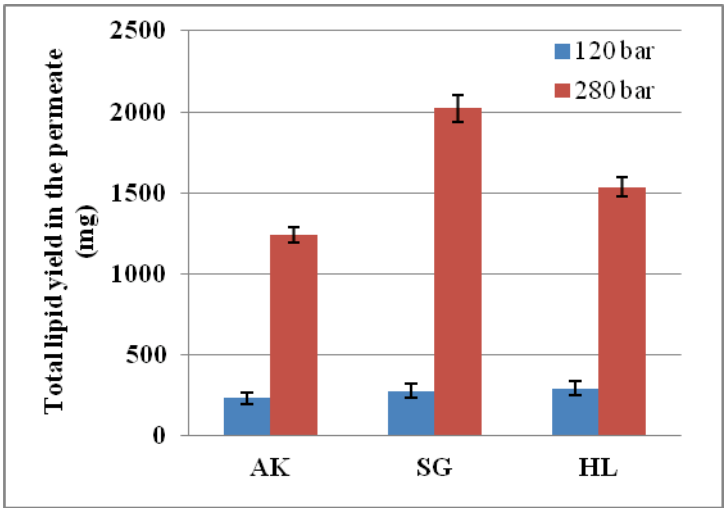

Figure 8-7. Effect of pressure on total lipid yield in the permeate stream at 40 °C and ΔP of 10 bar for AK, SG and HL membranes. Error bars based on 3 determinations.

8.4. Conclusions

Four commercial polyamide membranes were used during separation of OA/TAG mixture at two different pressures with SC-CO_2. HL showed the highest CO_2 flux while DL had the highest OA retention among all membranes tested. AK, SG and HL were proven to effectively operate under all pressure conditions tested. In this study, 50/50 (%, w/w) TAG/OA mixture was used as a model mixture. Two different pressures (120 and 280 bar) were tested at constant temperature (40 °C) during SC-CO_2 extraction and membrane separation with a constant ΔP of 10 bar.

Change in the solubility of lipids in CO_2 due to a change in pressure resulted in different TAG and OA concentrations in the feed stream reaching the membrane module after the solubilisation or extraction step. TAG concentration in the feed stream increased with increasing pressure. TAG and OA separation factors were calculated at two different pressures for AK, SG and HL membranes. HL was found to perform the best for both separation factors at 120 bar whereas SG showed a better TAG separation factor compared to AK and HL at 280 bar.

Increasing the processing pressure increased the dissolved lipid content resulting in higher yields in the permeate with all membranes. HL membrane exhibited the highest yield at 120 bar while SG had the best yield at 280 bar. Increase in the lipid yield due to higher solubility in CO_2 caused clogging of the membrane in a shorter period of time. Periodic addition of pure SC-CO_2 was not effective to prevent the delay of fouling at 280 bar unlike at 120 bar.

The coupled process exhibited higher OA concentration in the permeate stream at lower pressures whereas yield was substantially higher at higher pressures. Efficiency of the membranes varied depending on the processing parameters. These results proved that the interactions among solute, solvent and membrane network should be well understood to be able to increase the performance of the coupled systems. The optimum conditions should be adjusted by considering each individual unit operation involved in the overall separation process. Dead-end membrane modules did not show promising results when higher pressures were applied during the use of SC-CO_2 as solvent due to fouling.

8.5. References

[1] C.Y. Tang, Y.-N. Kwon, J.O. Leckie, Probing the nano- and micro-scales of reverse osmosis membranes--A comprehensive characterization of physiochemical properties of uncoated and coated membranes by XPS, TEM, ATR-FTIR, and streaming potential measurements, Journal of Membrane Science, 287 (2007) 146-156.

[2] C.Y. Tang, Y.-N. Kwon, J.O. Leckie, Effect of membrane chemistry and coating layer on physiochemical properties of thin film composite polyamide RO and NF membranes: II. Membrane physiochemical properties and their dependence on polyamide and coating layers, Desalination, 242 (2009) 168-182.

[3] C.Y. Tang, Y.-N. Kwon, J.O. Leckie, Effect of membrane chemistry and coating layer on physiochemical properties of thin film composite polyamide RO and NF membranes: I. FTIR and XPS characterization of polyamide and coating layer chemistry, Desalination, 242 (2009) 149-167.

[4] S.I. Semenova, H. Ohya, T. Higashijima, Y. Negishi, Separation of supercritical CO2 and ethanol mixtures with an asymmetric polyimide membrane, Journal of Membrane Science, 74 (1992) 131-139.

[5] Ö. Güçlü-Üstündag, F. Temelli, Correlating the solubility behavior of minor lipid components in supercritical carbon dioxide, The Journal of Supercritical Fluids, 31 (2004) 235-253.

9. Conclusions and Recommendations

Coupled supercritical CO_2 (SC-CO_2) extraction – membrane separation systems have potential to save energy while increasing the efficiency of the overall process. Although applications with lipid components give promising results for the coupled process, stability of the membranes during long term processing is still under investigation. Polyamide-based membranes are economically feasible and exhibit high retentions with their tight and robust structures. However, interactions between CO_2 and polyamide material under high pressures result in swelling, which might lead to plasticization in the membrane structure. In order to better establish the efficiency of the coupled processes, properties of the membrane material and the effect of processing conditions on the material must be well known. Subsequently, results regarding the performance of the membranes during lipid separations would provide better understanding of membrane behaviour under supercritical conditions.

Therefore, characterization of the four polyamide (PA) membranes was performed to identify the structure of the membranes by using advanced analysis techniques including X-ray photoelectron spectroscopy (XPS), attenuated total reflection - Fourier transform infrared spectroscopy (ATR-FTIR), contact angle, atomic force microscopy (AFM), field emission – scanning electron microscopy (FE-SEM) (Chapter 3). Results of the analysis suggested that AK and AG membranes were PA membranes formed via interfacial polymerization of m-phenylene diamine (m-PDA) and trimesoyl chloride (TMC) monomers. AG membrane had tighter structure due to higher cross-linking in its network. SG and SE membranes were suggested to be made of piperazine and m-PDA blend, which possibly also underwent esterification with PVA during thin film formation. SE membrane had higher salt rejection rates most likely due to higher m-PDA

concentrations used during polymerization compared to SG membrane. AK and AG membranes accommodated intermolecular hydrogen bonds as a result of close chain distances. SE and SG membranes were covalently cross-linked membranes lacking most of the amide hydrogen and carboxyl groups in their structure.

FE-SEM and AFM results exhibited that AK membrane had a rougher surface, which made it visible through couple hundred nanometers whereas SG membrane had relatively smoother and packed surface. Contact angle of both membranes were somewhat higher than many of the other commercially available polyamide-based membranes.

After the structures of the membranes were elucidated, the effects of SC-CO_2 processing at different temperature (40 and 80 °C), flux (50 and 200 kg/m^2h) and time (0-8 h) were investigated at constant pressure (120 bar) on AK and SG membranes (Chapter 4). AK exhibited prominent changes both chemically and morphologically due to the presence of excess amount of hydrogen-bonded groups. High flux had the most immediate effect on hydrophobicity of AK with a substantial increase in contact angle. SG membrane did not show any substantial difference in hydrophobicity at any processing condition due to its covalently cross-linked structure. Hydroxyl groups of both membranes were mostly affected by high temperature processing unlike amide and carbonyl groups. Surface structure of AK exhibited morphological changes forming bead-like structures out of polymer blends upon processing due to strong self interactions of carbonyl and amide functional groups. Molecular scale morphological change was most probably responsible for triggering the effect on formation of submicron scale bead-like structures on the surface of AK membrane. On the other hand, there was almost no change with SG membrane.

In addition to the temperature and flux parameters, the effect of SC-CO_2 processing pressure on physicochemical and morphological properties was also investigated (Chapter 5). Parallel to the previous results, there was a prominent

increase in the contact angle of AK membrane upon processing. In addition, carbonyl and hydroxyl groups showed the highest drop in absorbance upon CO_2 processing. Morphological changes in AK membrane accelerated with increasing CO_2 pressure whereas SG membrane structure did not exhibit any difference. SC-CO_2 processing caused swelling in membrane structure due to non-equilibrium state of glassy polymers. Increasing pressure resulted in an increase in interactions between the membrane and CO_2 and thus increased the CO_2 flux during processing due to higher degree of swelling. CO_2 flux increased for both membranes with processing time after depressurization/repressurization. This increase was found to be higher with AK membrane. Oleic acid retention of AK membrane was decreased up to 9%. SG membranes were more resistant due to their covalently cross-linked structures.

In order to reveal the effect of different temperature, transmembrane pressure, time and depressurization during pure SC-CO_2 processing, oleic acid was used during retention tests for AK and SG membranes (Chapter 6). Compaction due to high transmembrane pressure resulted in lower flux and higher oleic acid retention rates after processing. High temperature loosened the polymer chains and expanded the polymer network. High temperature effect was more prominent with AK membrane compared to the SG membrane. At 80 °C, processing caused irreversible effects on membranes resulting in lower oleic acid retentions upon testing at mild conditions right after processing.

New Langmuir sorption sites were created or the existing ones were most probably enlarged upon depressurization of the system. Processing time had a prominent effect on reorganization by causing an increase in CO_2 flux upon depressurization. Oleic acid retention was not affected as much as CO_2 flux most likely due to slight changes in Langmuir sorption sites, which were more effective on transport of much smaller CO_2 molecules than oleic acid.

After investigating the effect of pure SC-CO_2 processing on membranes, lipid separations were performed using model mixtures of oleic acid (OA) and triacylglycerol (TAG) (Chapter 7). Out of all the membranes tested (AK, SG, HL, DL and CE), only CE did not exhibit flux under supercritical conditions. DL membrane was not preferred due to low TAG retention and low CO_2 flux. SG was the only membrane, which exhibited consistent oleic acid retention throughout processing. Interactions between the lipid components and membrane should also be taken into account. Presence of lipid molecules most probably altered the CO_2 – membrane interactions and caused unstable oleic acid retentions on membranes having relatively more hydrophilic structures. Periodic pure CO_2 introduction over short periods was effective in the elimination of a gradual decrease in flux. High TAG separation factor and reasonable yield of SG membrane made it the best choice for TAG/oleic acid separations among all tested membranes at 120 bar and 40 °C.

Pressure was found to be strongly affecting the performance of each individual unit operation, SC-CO_2 extraction and membrane separation during the coupled process (Chapter 8). Separation of OA/TAG mixture was tested at two different pressures (120 and 280 bar) using SC-CO_2 with a constant ΔP of 10 bar and temperature of 40 °C. HL showed the highest CO_2 flux while DL had the highest OA retention among all membranes. TAG concentration in the feed stream increased with pressure. HL showed the best separation factor at 120 bar whereas SG was the best at 280 bar. Increasing the processing pressure increased the yield as a result of the increase in dissolved lipid content. HL membrane exhibited the highest yield at 120 bar while SG had the highest at 280 bar processing.

The findings summarized above proved that the interactions among solute, solvent and membrane network should be well understood to be able to increase the performance of the coupled systems. The conditions should be optimized by

considering each individual unit operation involved in the separation process. The dead-end membrane module did not show promising results when higher pressures were applied during the use of SC-CO_2 as solvent due to fouling.

With all the new data being generated, the research focusing on this process continues to grow at a much faster pace compared to its first decade. Besides, significant advances in research on supercritical fluids and membrane separations give rise to the possible alternatives for coupling these two techniques.

Even though the research is developing relatively quickly, commercial applications of such a coupled process have been lagging. One of the reasons for the delay in the progress in commercialization has been the lack of research on the development of membranes to work under the extreme processing conditions arising from the supercritical state of the fluids. Although inorganic membranes can withstand extreme high pressure and temperature conditions, their use in large scale is not economically feasible. On the other hand, polymer membranes have been used in many different industrial applications where they have also proven to be affordable and efficient. However, to the best of our knowledge, no polymer membrane has been produced to specifically work under supercritical conditions. Evidently, the use of commercial polyamide membranes during lipid and essential oil separations provided promising results in the last decade. The main disadvantage associated with commercial polyamide membranes is their relatively hydrophilic nature, resulting in high cohesive energy density of their network. However, it looks promising that this effect could be mitigated by modifications of the membrane structure, including esterification of hydrophilic groups by chemical cross-linking without sacrificing its separation performance. Once the plasticization effect is minimized through such cross-linking or other means, the coupled process has the potential to provide efficient separations by tuning the solvent conditions.

Although the industrial applications of supercritical processes have shown considerable growth, it is still relatively immature compared to membrane processes employed by many different industries. However, commercialization of supercritical fluid applications has increased over the past decade with the reduction in equipment cost and increasing restrictions on environmental regulations regarding the use of organic solvents. In addition, major developments in know-how over the last two decades make it more likely that we may see many more commercial applications in the near future. As the large-scale applications of supercritical processes grow, the research to make them more efficient and affordable will grow in parallel. In addition to the reduction of capital costs, the reduction of operating costs is also of much interest. At that point, integration of membranes into supercritical processes, targeting reduction of recompression costs will most likely provoke the investigations on membranes, which can efficiently function in supercritical processing. In this thesis research, a systematic approach was taken to first characterize the structure and morphology of selected commercial membranes, then assess the effect of SC-CO_2 processing on those membranes and finally evaluate their performance for oleic acid retention and OA/TAG separation. Throughout this thesis research, the effect of structure on performance and stability of the membranes was emphasized. As a result, structure – performance and structure – stability relationships were clearly identified. Characterization of complicated membrane structures was presented as one of the most important tools for proper membrane selection for targeted separations. Information on membrane–solute–solvent interactions, which is essential for efficient membrane separations was studied using polyamide – lipid – CO_2 interactions.

Application potential of a coupled SC-CO_2 extraction – membrane separation system was evaluated thoroughly from micro to macro level. Considering that the literature lacked information on the performance and stability of these processes, a coupled system was custom-designed to determine the

efficiency of polymer membranes when they were subjected to SC-CO_2 processing. Highly complicated and modified commercial polyamide membranes were characterized in detail to be able to clearly exhibit the effect of processing conditions on the structures of those polymer membranes. Nano-scale investigation of structures indicated the need for the fabrication of robust membranes based on covalently cross-linked and tight networks in order not to sacrifice efficiency due to swelling or plasticization during processing. Needless to say, energy savings associated with the coupled process can only be achieved by employing robust membranes under high pressure conditions. The type of polymer material used during processing must be evaluated along with the optimization of each unit operation individually. The findings emphasize the importance of each parameter, such as pressure, temperature, transmembrane pressure, depressurization rate, processing time, membrane materials and lipid components and the need to optimize them for efficient use of the coupled systems while maximizing both performance and stability.

FTIR and XPS are complementary techniques providing detailed information on the chemical structure of polymer membranes if data are analyzed properly. However, it could also be recommended to use time of flight – secondary ionization mass spectroscopy (TOF-SIMS) in addition to these two techniques for further characterization. TOF-SIMS can provide precise information especially on modification of a membrane with a known structure.

On the other hand, transmission electron microscopy can be used as an important tool to replace FE-SEM with higher resolutions. TEM images could be very helpful to determine the thickness of selective layer before and after processing with CO_2. Polyamide membranes have extremely thin layer on top, which makes it very difficult to isolate for TEM. Use of cryogenic conditions for isolation of the top layer could further help in characterization of the selective polyamide layer in more detail.

Since covalently cross-linked structures were found to have higher resistance to supercritical conditions, next step in membrane research could be modifications on membrane structure targeting formation of covalently bonded structures. This could lead to production of more stable membranes. Performance – stability relationship can be investigated to produce membranes which would work efficiently under supercritical conditions.

Using membrane modules working according to tangential flow mechanism will most likely have great impact on energy savings via recycling CO_2 in supercritical state. Since dead-end modules are prone to fouling during processing especially at high pressures, tubular modules could be recommended for processing at higher pressures while CO_2 is recycled.

The performance of the polyamide membranes used during TAG/OA separations was not highly efficient. A multi-stage system could be recommended to increase the efficiency of separation. Modifications on polyamide membranes can also be targeted to obtain higher degree of separation during lipid separations. Besides, inorganic membranes made of TiO_2 and silica can be used during processing to minimize the effect of CO_2 on membrane structure.